ORNL/TM-2018/915

Standard Modular Hydropower: Case Study on Modular Facility Design

Adam Witt
Scott DeNeale
Thanos Papanicolaou
Benjamin Abban
Norm Bishop

November 2018

OAK RIDGE NATIONAL LABORATORY
MANAGED BY UT-BATTELLE FOR THE US DEPARTMENT OF ENERGY

ORNL/TM-2018/915

Environmental Sciences Division

STANDARD MODULAR HYDROPOWER: CASE STUDY ON MODULAR FACILITY DESIGN

Adam Witt
Scott DeNeale
Thanos Papanicolaou
Benjamin Abban
Norm Bishop

Date Published: November 2018

Prepared by
OAK RIDGE NATIONAL LABORATORY
Oak Ridge, TN 37831-6283
managed by
UT-BATTELLE, LLC
for the
US DEPARTMENT OF ENERGY
under contract DE-AC05-00OR22725

TABLE OF CONTENTS

LIST OF FIGURES

LIST OF TABLES

ABBREVIATIONS, ACRONYMS, AND INITIALISMS

DOE	Department of Energy
EDF	environmental design framework
ICC	installed capital cost
LCOE	levelized cost of energy
NSD	new stream-reach development
SHP	small hydropower plant
SMH	standard modular hydropower
USGS	US Geological Survey
waterSHED	water allocation tool enabling rapid Small Hydropower Environmental Design

ACKNOWLEDGMENTS

The authors would like to acknowledge and express their appreciation to the following individuals for their review, comments, and support of this report.

Department of Energy Water Power Program
- Marisol Bonnet, Project Engineer
- Tim Welch, Hydropower Program Manager

Oak Ridge National Laboratory
- Brennan Smith, Water Power Program Manager
- Kevin Stewart, Water Resources and Hydraulic Engineer
- Mark Bevelhimer, Aquatic Ecologist
- Chris DeRolph, Geospatial Scientist
- Rebecca Brink, Post-Bachelors Research Associate
- Miles Mobley, Post-Bachelors Research Associate
- Shelaine Curd, Energy-Water Resource Systems Operations Manager
- Deborah Counce, Technical Writer/Editor

University of Tennessee
- Sarah Pierce, Graduate Research Assistant

University of Vermont
- Lindsay Worley, PhD Student

Birmingham-Southern College
- Margot Woolverton, SULI Program

EXECUTIVE SUMMARY

Hydropower is a reliable, cost-effective, and widely deployed method of harnessing the power of river systems for human benefit. The undeveloped technical hydropower resource in the United States consists overwhelmingly of sites with small hydropower potential of less than 10 MW of installed capacity. Most existing hydropower projects and the bulk of proposed projects in the Federal Energy Regulatory Commission development pipeline are also small hydropower projects. However, the rate of development of new small hydropower projects is at a historical low because of the risks, costs, and uncertainty associated with project development. An acute challenge is the identification and mitigation of adverse environmental impacts, such as alterations to streamflow and water quality and the introduction of barriers that threaten geomorphologic processes and the resiliency of ecological communities. Success in new small hydropower development demands that low-cost, innovative approaches be developed to decrease the adverse environmental impacts of construction and operation.

This report outlines a new approach to developing small hydropower projects that emphasizes standardization, modularity, and environmental compatibility as essential elements of a low-cost, low-impact facility design strategy. The approach is formally established through an environmental design framework that prioritizes preservation of essential river processes, including continuity of water, maintenance of designated pathways for aquatic life, recreation as a natural resource service, and sediment connectivity. To sustain the power of the stream, the optimization of hydroelectric generation occurs around these essential processes. The goal of this framework is to transparently prioritize river processes at the outset of project development with the hope of more quickly achieving cooperation and consensus on feasible project designs and operations.

To implement the environmental design framework in a systematic and transparent fashion, we have developed a decision support tool that enables standardized engineering design and simulation of a modular hydropower facility. The “water allocation tool enabling rapid Small Hydropower Environmental Design” (waterSHED) develops preliminary designs and operational rules for aquatic species, recreation, sediment, and water passage modules and for a suite of generation modules. Using a set of hydrologic, biologic, and geomorphologic site inputs, waterSHED establishes reference module designs based on existing technologies, such as vertical slot fish ladders and axial flow turbines. Whereas traditional design paradigms implement a customized approach for every project feature, offering little opportunity for standardization, modularization, advancement of ecological sustainable design, limits economization, and value engineering, waterSHED designs modules using equations that are parametrically linked to site inputs so that modular and facility designs can be established independent of site geometry or configuration. waterSHED approaches site assessment by estimating a modular facility footprint, simulating mean daily facility performance using a user-prescribed flow prioritization to individual modules, and producing a set of visualizations to enable a technical, environmental, social, and economic comparison of design options and performance outputs with clarity and earlier than would be achieved in the typical project development cycle. The tool is meant to assess a critical question facing small hydropower project developers early in the site development process: at a potential site, using a modular approach, how do you allocate flow across modules to meet energy and environmental objectives?

The utility of waterSHED is demonstrated through a case study at a potential new stream-reach development site with characteristics representative of the US small hydropower resource potential. A suite of modeling scenarios is developed, and trade-offs related to flow allocation, generation sizing, and facility footprint are assessed. Major findings show that the addition of passage modules has a minimal impact on annual energy generation but a significant impact on the physical footprint of the facility. It is also clear that cost reductions across modules will be necessary to achieve a levelized cost of electricity that is competitive with other renewable generation sources.

The major contribution of this case study is the establishment of a benchmark engineering design methodology and operations simulation for a reference standard modular hydropower facility. Future work should focus on developing firm cost estimates for individual modules, assessing the feasibility of modules with combined functionality and submersible modules, and applying the tool to different streams and regions to develop a more robust understanding of the feasibility of standard modular hydropower development.

1. INTRODUCTION

More than 1,700 small hydropower plants (SHPs), defined broadly as hydropower plants with <10 MW of installed capacity, currently generate electricity throughout the United States. These facilities provide many benefits, including carbon-free electricity, grid reliability, local jobs, and recreation opportunities. Though SHPs are poised to play an important role in a national renewable energy future, development of greenfield projects, referred to herein as new stream-reach development or NSD, is challenging and controversial in many areas of the world (Kelly-Richards et al. 2017). This is particularly true in mature markets like the United States, where less than 10 NSD SHPs have been installed in the past 15 years because of a combination of economic and environmental factors (Uria-Martinez et al., 2018). The environmental impacts of SHPs are often uncertain, complex, and require difficult and expensive mitigation measures. The economics of SHP development are challenging; installed costs are generally greater than larger projects on a $/kW basis (O'Connor et al. 2015) and less competitive than solar, wind, and natural gas in many markets. To overcome the economic and environmental barriers to new development and to harness renewable power from water resources, a new generation of environmentally compatible, efficient, and low-cost SHPs is needed.

SHP development begins with identification and characterization of hydropower potential. As noted recently in (Garegnani et al. 2018), there are generally four types of hydropower studies that define the energy potential at a given location: theoretical, planning, technical, and financial. Each type provides a progressively resolved estimate of potential capacity based on a series of increasingly granular constraints and variables. Theoretical potential and planning potential studies generally set an upper bound on the resource available for development. For example, a national-scale US assessment used a geospatial approach to establish an upper technical limit on new development based on topography and hydrology (Kao et al. 2014; Pasha et al. 2014). Other Geographic Information System approaches couple hydrologic modeling with digital elevation data sets to identify promising sites for development (Soulis et al. 2016; Rojanamon, Chaisomphob, and Bureekul 2009; Punys et al. 2011; Mosier, Sharp, and Hill 2016; Garegnani et al. 2018). These models tend to identify hydrologic and landscape features of natural systems that are compatible with the geometric features and constraints of conventional hydroelectric systems. In general, most small hydro resource planning studies do not give substantial weight to environmental attributes of potential sites (Punys et al. 2011), and mitigation is often applied retrospectively using a process of trial-and-error (Kemp 2012) or long-term adaptive management. Recent models focus on multiscale environmental impacts and spatial optimization for sustainable design by striking a balance between hydropower design and the conservation of environmentally sensitive areas (McManamay et al. 2015; Jager et al. 2015).

In general, the inclusion of environmental impact mitigation measures and the consideration of low-impact technologies are not addressed early in hydropower planning studies. This is a challenge for hydropower project developers because identification of environmental attributes and their translation into environmental design criteria are more valuable the earlier they are considered in the development process (Bishop et al. 2015). Eco-engineering and sustainable water infrastructure designs are broadly advocated (Poff et al. 2015), but the hydropower industry currently lacks generalized tools and methodologies to develop early feasible engineering designs that consider environmental and energy objectives, particularly for small low-head structures. Thus, there is a significant need for SHP design tools that bridge the gap between planning-level assessments and site-level environmental design.

In this report, we propose a new approach to developing SHPs that emphasizes early development adoption of standardization, modularity, and environmental compatibility as strategies for lower-cost, lower-impact development.

1.1 STANDARD MODULAR HYDROPOWER BACKGROUND

The standard modular hydropower (SMH) project contemplates a new approach to SHP development focused on the principles of early development adoption of standardization, modularity, and environmental compatibility. These principles—outlined in detail in prior works (Witt et al. 2016; Smith et al. 2016)—are hypothesized as enabling pathways towards a low-cost, low-impact hydropower growth strategy.

- **Standardization:** Developing a framework of guidelines, rules, and specifications (i.e., standards) to maximize compatibility, acceptance, interoperability, quality, safety, and repeatability while minimizing environmental disturbance. In a hydropower context, standardization of design, review, regulation, manufacturing, operations, maintenance, and other features is intended to reduce site specificity and project costs.

- **Modularity:** The physical or virtual organization of a hydropower facility into discrete functional units, known as modules. In SMH, the entire facility is envisioned as a modular structure, with generation, passage, and foundation modules assembled to deliver energy and environmental benefits at many different sites.

- **Environmental compatibility:** Siting and developing hydropower facilities with an understanding that streams provide valuable environmental benefits that must be preserved. SMH development must embody an understanding of how coupled stream-hydropower systems can minimize disturbances to landscape features, water quantity, connectivity, geomorphology, water quality, and biota and potentially offer enhancements to water ecosystems.

While previous SMH project reports and studies have focused on developing standard design specifications for generation, passage, and foundation modules, this work provides explicit examples of how environmental design can be incorporated at a systems level into a standard modular facility arrangement.

1.2 ENVIRONMENTAL DESIGN FRAMEWORK

A new environmental design framework (EDF) is proposed for developing SMH concept designs earlier in the project development cycle. The EDF relies on five design categories—water, fish, recreation, sediment, and energy—each with a guiding design principle (Figure 1).

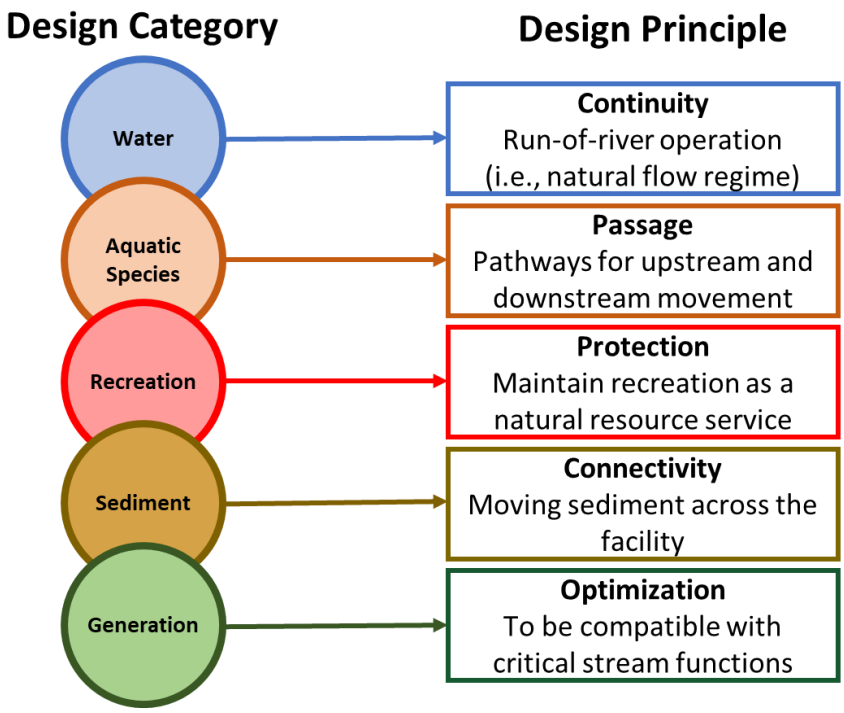

Figure 1. Summary of principles and design targets for environmental design of standard modular hydropower projects.

The EDF strives to incorporate an understanding of hierarchical and interdependent river functionalities at each level of design:

- *Water*. Streamflow is considered the master variable of river ecosystems (Poff et al. 1997). Structures that significantly alter the natural flow regime—the timing, magnitude, frequency, duration, and rate of change of streamflow—can have negative consequences to aquatic communities. The EDF emphasizes water continuity by prescribing a run-of-river operation, where outflows from the facility are maintained equivalent to inflows. Streamflow should also be allocated across a facility to equipment and structures designed to sustain the important functionalities of the river.

- *Aquatic Species*. Hydraulic structures can act as barriers to the movement of fish and other aquatic species, disrupting natural migratory patterns and blocking access to critical habitat. The EDF incorporates aquatic species passage modules as pathways for safe and timely transport across the facility.

- *Recreation.* Some of the most common protection, mitigation, and enhancement measures at existing hydropower facilities are related to recreation management (Schramm, Bevelhimer, and DeRolph 2016). A function of streams is the provision of natural resource services that are often enjoyed by recreationists—rapids for rafting, pools for paddling, and pleasing riverscapes. The EDF considers recreation passage modules to provide safe watered pathways across the facility that will not disrupt rafting or kayaking activity and as a means to ensure recreation is maintained as a natural resource service.

- *Sediment.* Sediment is sourced, transported, and deposited by rivers from headwaters to deltas. To sustain natural sediment transport regimes, we hypothesize that small low-head hydro facilities must not let sediment accumulate behind the structure, and that sediment routing can be accomplished

through dedicated sediment passage modules that open to pass sediment-laden flows when a flow threshold is exceeded. Though considerable uncertainty exists regarding the sediment trapping potential of small run-of-river dams (Csiki and Rhoads 2010), the EDF proposes structural solutions to maintain sediment connectivity to downstream reaches.

- *Generation.* The flow of a stream is allocated among the various functions just described, among others. We hypothesize that harnessing flow for renewable electricity generation while sustaining other critical functions of the stream can be achieved through careful planning and management of flow allocation across a modular hydropower facility. This is the ultimate goal of the EDF.

The EDF is implemented through the water allocation tool enabling rapid Small Hydropower Environmental Design (waterSHED), a holistic open-source decision support tool used to explore tradeoffs in SMH design. The tool is meant to assess a critical question facing SMH developers: *at a potential site, using a modular approach, how do you allocate flow across modules to meet energy and environmental objectives?* This tool addresses the need to prescribe flow and assess the performance of modules that might have competing objectives when operating to achieve their design principles. For example, generation modules require flow to produce hydropower, whereas aquatic species passage modules require flow to pass aquatic species upstream. waterSHED enables a user to rapidly prescribe different design flows for modules, simulate that allocation of flow over time, and assess the trade-offs in energy generation and passage flow desired to meet various environmental performance objectives.

A basic overview of the modeling tool workflow is shown in Figure 2. It consists of four main components for each module: user inputs, design optimization, rule-based simulation, and visualization and analysis.

- **User inputs**: waterSHED enables a systematic categorization of the preliminary inputs necessary to maintain the EDF design principles. These range from mean sediment size to aquatic and fish species of interest to mean daily flow time series. A detailed description of inputs and their utility within waterSHED for each module is provided in Sections 2 and 3 and in the Appendixes.

- **Design optimization**: waterSHED produces optimized but conservative module designs based on user inputs. Designs are conservative in the sense that they are based on proven technologies with design criteria and documented field installations. As a basis for case studies explored in this report, we use a set of pre-existing reference modules and design criteria, described in detail in the appendixes and summarized in Table 1. Basic dimensions, profiles, and design flows are produced for each module, and operational rule curves are established and fed into a performance simulation.

- **Rule-based simulation**: Based on site inputs, module designs, and operational rules, waterSHED performs a simulation of mean daily facility operation over the length of the available flow time series (either historically gaged or synthetically developed), allocating water to the appropriate module.

- **Visualization and analysis**: Model outputs are summarized and visualized to enable a first-order assessment of energy performance, module performance, and the physical footprint of the facility.

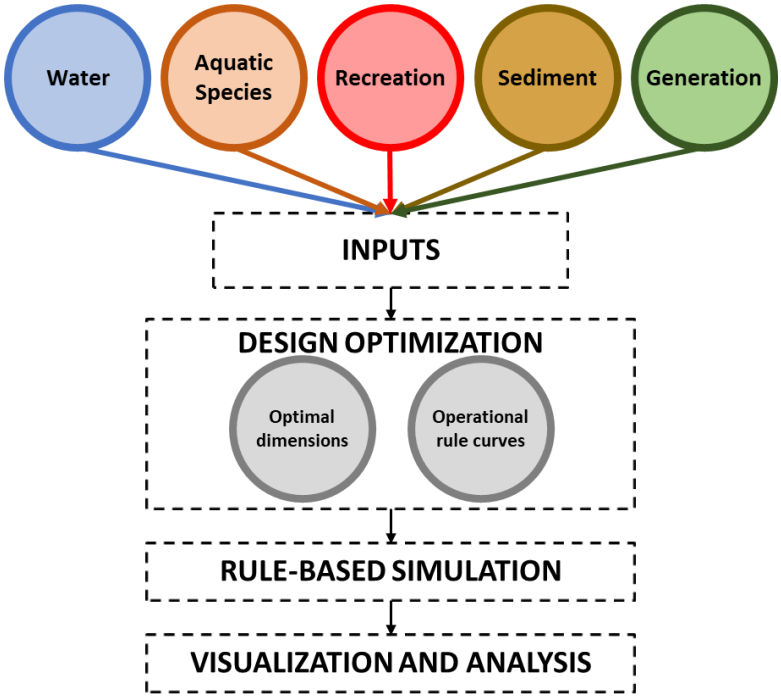

Figure 2. General overview of the four main components of waterSHED structure and functionality: inputs, design optimization, rule-based simulation, and visualization and analysis.

Implementation of waterSHED as discussed in this report enables a systems-level, first-order prediction of module footprint, operation, and performance. A set of reference modules are used as a design basis for the individual generation and passage modules[1] that comprise the modular facility (Table 1). We use conventional, proven technologies as reference modules for several reasons: design criteria are available, most of the technologies have been validated at the laboratory and field scales, and several technologies are in a modular form and lend themselves to replicability across multiple sites. To ease the presentation of case study results, detailed descriptions of reference modules are provided in the appendixes. We are intentionally conservative in the approach to defining reference modules and operations, relying on design criteria for proven individual technologies that when assembled as a modular facility might not represent the most optimized or efficient design. Furthermore, the tool does not prescribe an optimal modular arrangement with respect to the engineered positions of modules in a given stream-reach location. Future work that considers physical river characteristics, biological characteristics, morphology, and other important factors will take this factor into consideration. Our hope is that future innovation on individual modules and modular arrangements will reduce project footprints, lead to more cost-effective facility arrangements and construction technique, streamline and standardize project operational strategies, and enhance environmental performance.

Table 1. Description of reference modules.

Module	Reference description
Sediment passage	Vertical lift sluice gate
Aquatic species passage	Vertical slot fishway
Recreation passage	Canoe chute drop structure
Generation	Axial flow Kaplan turbine (fixed blade variable speed, or adjustable blade)
Spill	Adjustable overshot gate

[1] Though foundation modules are integral to the SMH concept, they are not currently incorporated into the EDF.

1.3 OBJECTIVE OF CASE STUDY

In this report, we present a case study for SMH development through application of waterSHED. The objective is to implement the EDF through waterSHED at a physical location to (1) promote early adoption of best practices in environmental design, (2) develop preliminary concept modular arrangements, (3) establish module operational rules, (4) simulate performance, and (5) understand how modular facilities will operate over a 30-year lifetime. We estimate the target installed capital cost of different modular arrangements based on a range of potential levelized cost of energy (LCOE) thresholds and discuss the implications based on conventional approaches to development. The case study is meant to be first of many iterations to establish acceptable, integrated design and simulations tools for SMH development.

1.4 STRUCTURE OF REPORT

The remainder of the report is organized as follows:

- Section 2 provides a methodology for developing modular facility reference designs and specifying cost targets for development.
- Sections 3 applies methodologies outlined in Section 2 as a case study.
- Section 4 summarizes the report and provides conclusions based on the case study.
- Appendixes A–F provide engineering details for individual module reference designs.

2. METHOD TO DEVELOP AND ANALYZE SMH REFERENCE DESIGNS

A five-step approach is developed for establishing and analyzing the SMH reference design:

- Hydrologic assessment to develop flow and stage estimates and establish site geometry
- Sediment, aquatic species, and recreation assessment
- Reference module development
- Rule-based performance simulation
- Levelized cost of energy and project cost target assessment

2.1 HYDROLOGIC ASSESSMENT

2.1.1 Streamgage Data

For preliminary SMH site assessment, hydrologic analysis can be performed using streamflow gages near the location of interest. US Geological Survey (USGS) streamgages offer broad coverage across the United States and typically provide several years' worth of instantaneous stage-discharge data, often recorded every 15 minutes. Longer-term mean daily discharge data are typically available, with Granato et al. (2017) reporting more than 7,000 gages (roughly 35% of the 20,438 streamgages analyzed) across the United States with 30+ complete years of mean daily streamflow data (Figure 3). Additional monthly, annual, and other streamflow statistics are also provided through the USGS National Water Information System web interface.[2]

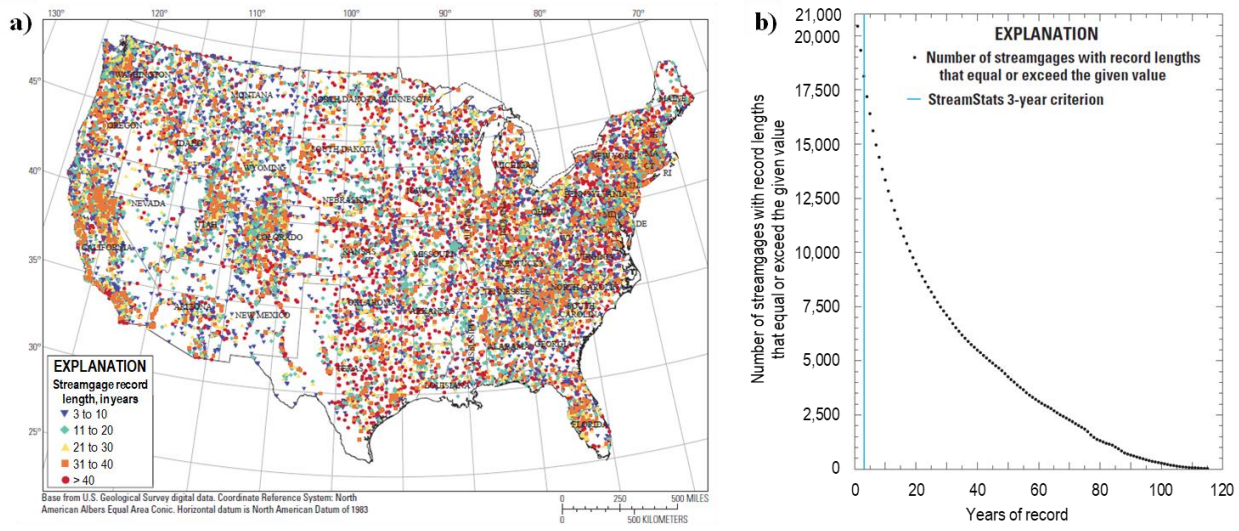

Figure 3. USGS streamgage record length distribution. (Modified from Granato et al. 2017.)

For locations in which the historical streamgage data are too short, not available, or cannot be reasonably inferred using nearby gage data, synthetic streamflow models are often generated (U.S. Army Corps of Engineers 1967). Typical synthetic streamflow applications for ungaged streams may use parametric methods, in which streamflow characteristics are assumed to follow a known distribution with parameters

[2] https://waterdata.usgs.gov/nwis/sw

fit based on historical record, or non-parametric methods such as block bootstrapping, k-nearest neighbor, and kernel density methods. These methods are not discussed in detail in this report.

2.1.2 Flow Duration Curve

Using time-series streamflow data, a flow duration curve can be developed to quantify the frequency of historical flow observations. The flow duration curve shows that probability that a certain streamflow will be exceeded a given percentage of time. For example, the streamflow associated with a 90% exceedance has been exceeded for 90% of the time over the period of record. A sufficiently long historical record of streamflow data, gathered from a USGS stream gage or generated synthetically, should be used in developing a flow duration curve. For instance, Zhang et al. (2013) recommend a minimum of 6 complete years of flow data for preliminary analysis, while the US Army Corps of Engineers suggests 20 to 30 years should be used (USACE, 1992). Since the introduction of engineered systems (e.g., dams) can alter flow characteristics, care should be taken to ensure the data used to develop a flow duration curve are representative of present conditions and reflect a consistent stream environment. An example flow duration curve developed using mean daily flow data is provided in Figure 4.

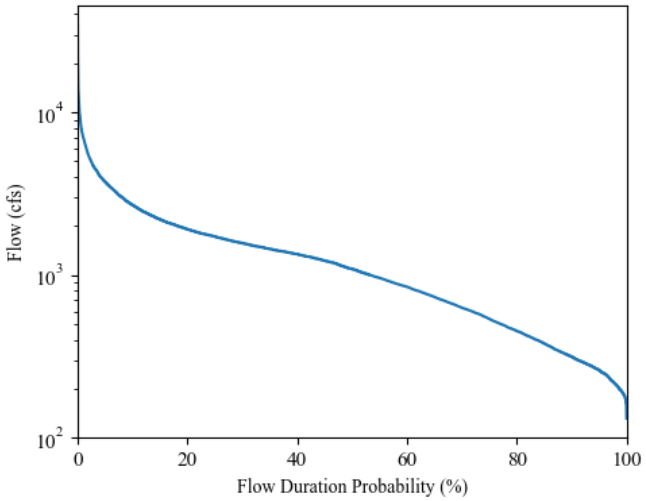

Figure 4. Example flow duration curve based on mean daily flow.

Care should be taken to ensure all of the selected gage data are recorded along the same stream of interest and that the data are representative of the site. In cases where the best available gage and the proposed site are separated by moderate-to-large distances, or where the contributing drainage areas are notably different, adjustments to the flow duration curve might be warranted. For instance, Gulliver et al. (1980) recommend using the following formula (based on work by Leopold et al. 1964) to estimate flow of i percent exceedance at a site located away from a USGS gage:

$$Q_i(\text{at site}) = \left[\frac{A_d(\text{site})}{A_d(\text{USGS gage})}\right]^{0.75} \times Q_i(\text{USGS gage}) \ .$$

To assist in drainage area estimation, USGS StreamStats[3] can be used. Using a mapped interface, the user can click on a stream location of interest and delineate the upstream basin. Flow duration statistics, among other information, can be generated for some locations.

[3] https://water.usgs.gov/osw/streamstats/index.html

2.1.3 Flow Depth Determination

Because an SMH reference design requires knowledge of the streambed elevation to inform module height criteria, information on flow depth is also desired; but it might not be readily available. Ideally, stream bathymetry data would be available to specify streambed features; however, given a lack of data, approximations could be made. For instance, based on the stage-discharge curve, it might be reasonable to assume (for approximation) that gage height and flow depth are equivalent or that the elevation associated with the minimum flow observation is representative of the streambed elevation; however, this could be highly site specific. For the purposes of this study, to estimate streambed elevation, gage height was assumed to be equal to flow depth. A more detailed method to estimate flow depth based on sediment characteristics is described in Appendix C.

2.1.4 Stage-Discharge Curve

Instantaneous USGS streamgage data typically include both flow and depth, or stage, records. Water surface elevations are recorded as gage height, which is defined as "the height of water in the stream above a reference point."[4] Using gage height data, a stage-discharge curve can be developed. To develop a reliable stage-discharge curve, data should be collected throughout a period when flows range from very low to very high so the full stage-discharge relationship can be fully represented. Given enough information, a fitted curve (e.g., second order polynomial or power curve) could be used to represent the relationship (Figure 5). For this study, the predevelopment stage-discharge curve was used to inform the tailwater surface elevation response to flow changes.

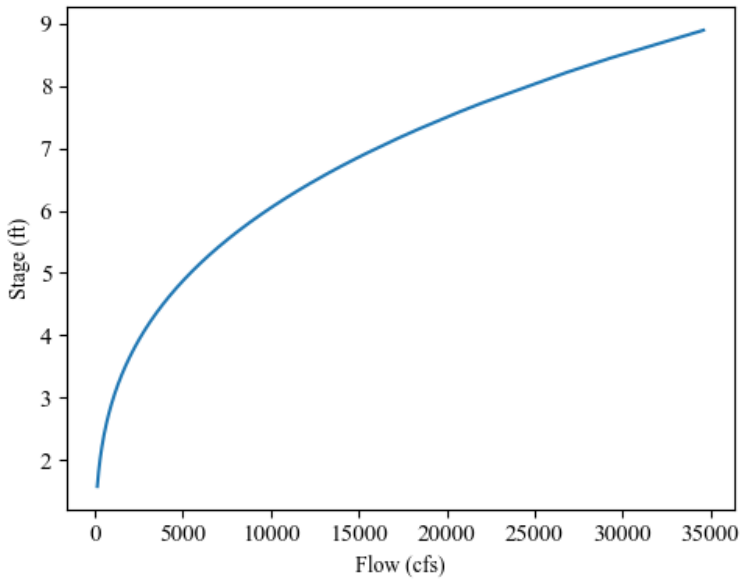

Figure 5. Example stage-discharge curve.

2.1.5 Gross Head Duration Curve

Similar to a flow duration curve, a gross head duration curve (Figure 6) can be developed to estimate the probability of a given head available for generation under varying flow conditions. The gross head

[4] https://help.waterdata.usgs.gov/tutorials/surface-water-data/how-do-i-interpret-gage-height-and-streamflow-values

duration is the probability of exceedance—that is, that a gross head, or difference between headwater and tailwater water surface elevation, is exceeded for any given flow value.

The tailwater rating curve is assumed to follow the predevelopment stage-discharge curve with only minor modification to account for any difference in normal water surface elevation between the site and the USGS gage location. This approach assumes that the tailwater flow regime of the proposed SMH development is unaffected by the new structures.

In contrast, the headwater rating curve can be approximated in two ways: (1) by using a single constant headwater elevation, or (2) by computing headwater depth above the invert of the facility using a weir equation and assuming a single uniform weir of constant crest elevation. The top width of the weir is calculated based on cross-sectional geometry to ensure impoundment across the stream. Flow would be transported through or over the various generation or passage modules, with structural overtopping occurring only under high-flow conditions (or not occurring at all, depending on the design). This approach does not consider drawdown below the crest resulting from subsurface flow (e.g., flow through a generation module or submerged gate). To construct a headwater rating curve, the depth of flow over the weir is computed based on the broad-crested weir equation (Tracy 1967):

$$Q = CLH^{1.5} ,$$

where
Q is discharge (cfs),
C is weir coefficient (2.6 to 3.4 for US customary units, 1.44 to 1.88 for metric units),
L is weir length perpendicular to flow (ft),
H is weir flow depth (ft).

When there is a lack of field measurements, the approach outlined herein provides a rough first-order approximation of the gross head available for power generation.

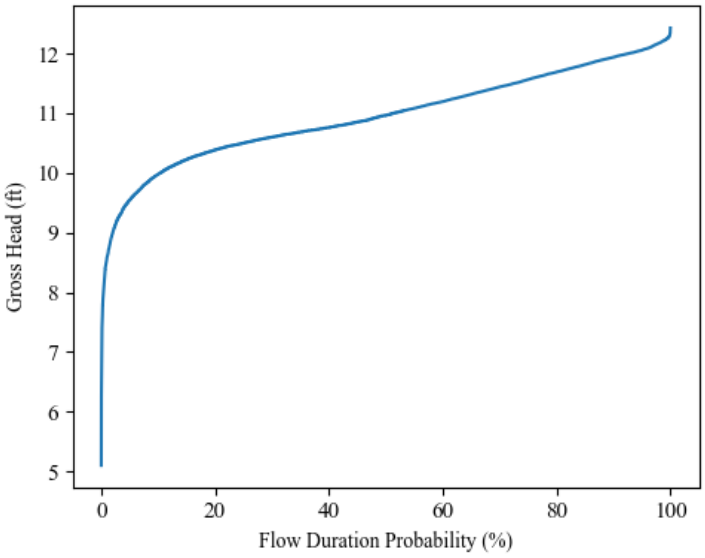

Figure 6. Example gross head duration curve assuming a constant headwater elevation.

2.1.6 Flood Frequency Analysis

An SMH facility must safely pass flood flows. The reference design assumes water passage modules must pass flows in excess of the non-overflow capacity, i.e., all flows greater than the maximum flow passable with a combination of generation and passage modules. Water passage modules are designed and sized to safely pass a 10-year flood without overtopping, which is consistent with New York State's service spillway design flood requirement for low-hazard dams with heights of less than 40 ft, as specified in *Guidelines for Design of Dams* (NYSDEC 1989). The reference facility is assumed to be overtopped by flows exceeding the 10-year flood.

The 10-year flood flow is estimated by fitting USGS annual peak streamflow gage measurements to a log-Pearson Type III frequency distribution using USGS PeakFQ software (Figure 7), where the annual probability of exceedance of 10% is equivalent to a 10-year flood flow.

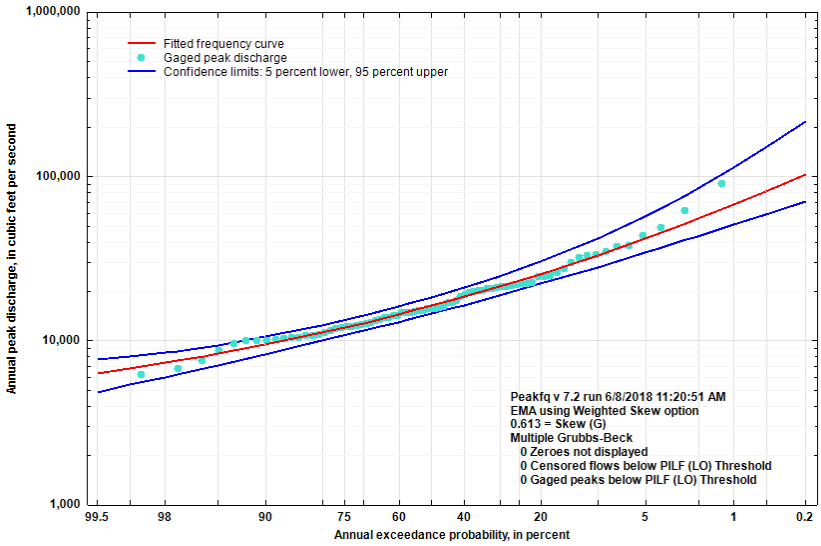

Figure 7. Example log-Pearson Type III frequency distribution produced with PeakFQ.

2.1.7 Site Geometry

The reach-scale mean bed slope is estimated using the NHDPlusV2 data set. At a site level, natural stream channels are typically trapezoidal in shape, with bank slopes changing over time through erosive and geomorphological processes. For SMH development, information on a proposed location's elevation profile is needed to assess the size and location of the facility. Optimally, a facility would be constructed at a location with an adequate geotechnical foundation (outside the scope of this study) that the volume of excavation and structural materials could be minimized. For this study, Geocontext-Profiler,[5] a freely available online tool for creating topographical land profiles, was used to extract cross-sectional data. The resulting data were checked against Google Earth[6] to ensure consistency. Although the elevation profiles do not account for underwater features, a normal trapezoidal bathymetry was assumed at a depth observed when the flow is equivalent to Q_{80} on the stage-discharge curve. The full submerged and above-ground profiles are used in this study to estimate SMH facility geometry, including the bottom and top width and side slope requirements (Figure 8).

[5] http://www.geocontext.org/publ/2010/04/profiler/en/
[6] https://www.google.com/earth/

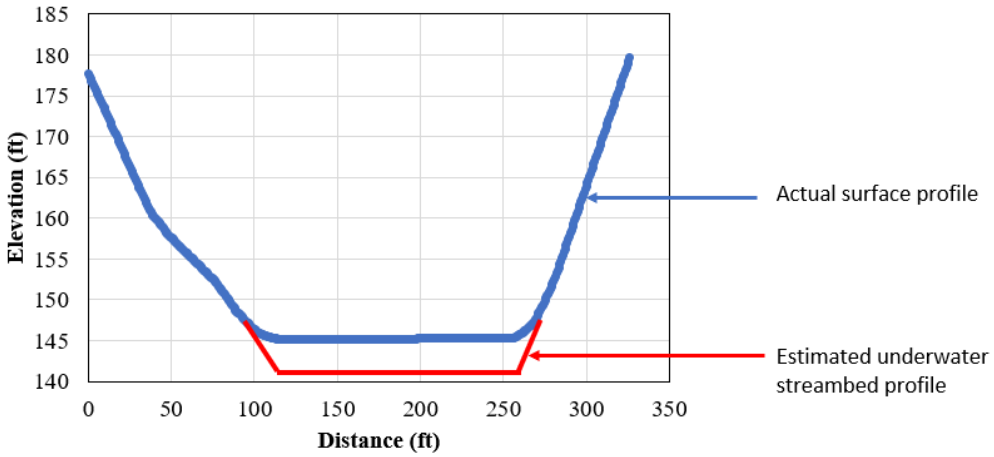

Figure 8. Example site cross-section and elevation profile estimate.

2.2 AQUATIC SPECIES, RECREATION, AND SEDIMENT ASSESSMENT

The EDF is designed to take a minimum amount of aquatic species, recreation, and sediment input data and produce preliminary passage module concept designs. It is not intended to decide whether a passage module is needed at a site, but to provide a concept design should the user determine the module is needed. Design inputs and sampling methods are introduced briefly in this section: more detail is found in Section 3.1 and in Appendixes A – C.

2.2.1 Aquatic species

The upstream and downstream movement patterns of aquatic life in rivers and streams depends on the species, life stage, the size, location, and characteristics of the river, and type of migration, e.g., anadromous or potadromous (Katopodis, 1992). Many aquatic species passage designs are sized for specific species: to pass flows that occur during migratory periods, to provide resting pools based on species behavior, and to limit maximum flow velocities to accommodate species swimming performance. Streams should be assessed for the type of species present using online guides from local Department of Natural Resources or Fish and Wildlife Service websites, or from national databases like FishTraits[7].

2.2.2 Recreation

Rivers and streams throughout the US are used for water-based recreation. Passage of small recreational craft, including kayaks and rafts, across a hydropower facility is an essential component of SMH design and a relatively new and untested concept for the hydropower industry. Preliminary assessments of streams and rivers for likelihood of water-based recreation should consider the proximity of urban developments, and the proximity of whitewater runs[8] or water trails[9] from national inventories.

2.2.3 Sediment

Site assessments should consider all sources of sediment that contribute to fluxes at the stream-reach of interest. The fluxes are the combined net contributions of eroded material from hillslopes and floodplains, as well as from channel beds and banks. Incoming terrestrial soil, typically finer material, is

[7] http://www.fishtraits.info/
[8] https://www.americanwhitewater.org/content/River/view/
[9] https://www.river-management.org/national-rivers-database

transported by the stream mostly as suspended load, whereas instream, coarser sediment may be transported as bed load or suspended load depending on flow conditions. A full balance of sediment inflows and outflows at the dam can only be achieved when both fine and coarse fractions are transported successfully beyond the dam. To achieve this balance, a designer must consider the particle-size distributions of the riverbed.

At the preliminary assessment phase, the median diameter of coarse sediment particles is the primary variable used to size sediment passage modules and set operational rules. Standard methods for obtaining particle-size distributions are generally labor intensive and require access to the site or site-specific information. These include volumetric, grid, areal, transect, and photographic methods (Diplas et al., 2008), of which the most common is the grid method established by Wolman, where 100 sediment particles are selected and measured from a small area of a stream by a technician pacing at regular intervals, picking and measuring a sediment particle under their toe. For a preliminary desktop study, data sources that aggregate site specific measurements obtained over many years can be used rather than site sampling methods. The EPA National Aquatic Resource Surveys (NARS) database[10] provides channel and sediment size characteristics at over 1,900 sites in the U.S, covering some 1.2 million river miles across the country. Information from this database may be complemented with data from the USGS Fluvial Sediment and Ancillary (FSA) database[11], which contains data for fewer sampling locations. Detailed water quality studies with channel and sediment size data may exist for watersheds – these can be found by searching for reports for the watershed within which the SMH site is located.

2.3 REFERENCE SMH FACILITY DESIGN

To convey the concept of a modular facility design, a schematic of an existing nonpowered modular hydraulic structure is shown in Figure 9. The image is of a small low-head dam in Lincoln, Nebraska, recently retrofitted with modular recreation and fish passage solutions. The existing structure consists of modular gates that function for both sediment and water passage. The SMH concept is envisioned to broadly mimic this type of modular arrangement, with the addition of generation modules to produce hydropower and foundation modules to anchor all modules into the streambed.

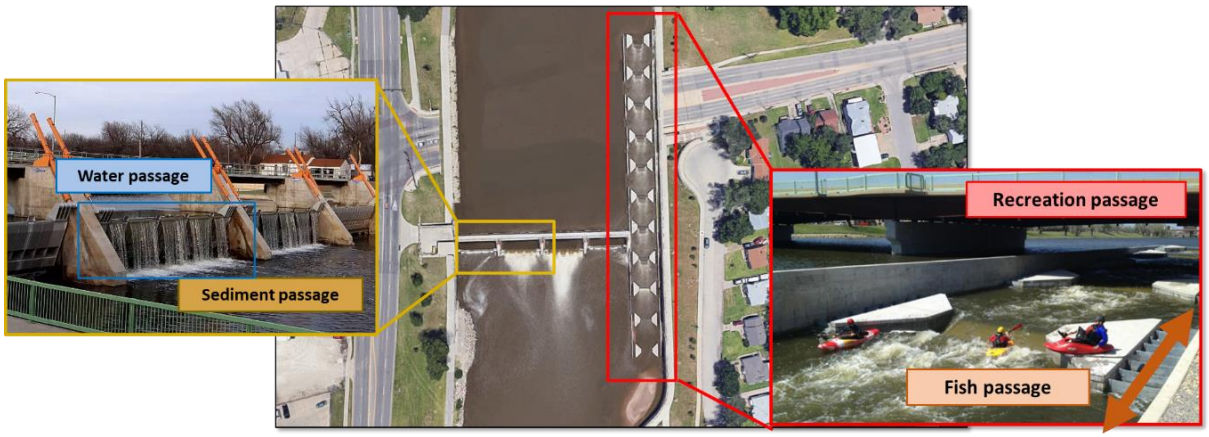

Figure 9. Example modular design of a low-head hydraulic structure.

[10] https://www.epa.gov/national-aquatic-resource-surveys
[11] https://water.usgs.gov/osw/sediment/

The waterSHED tool designs and simulates the performance of an SMH facility similar in nature to the reference facility (Figure 10). In general, the tool sizes modules individually and parametrically based on inputs and assembles them together as an integrated facility for performance simulation purposes.

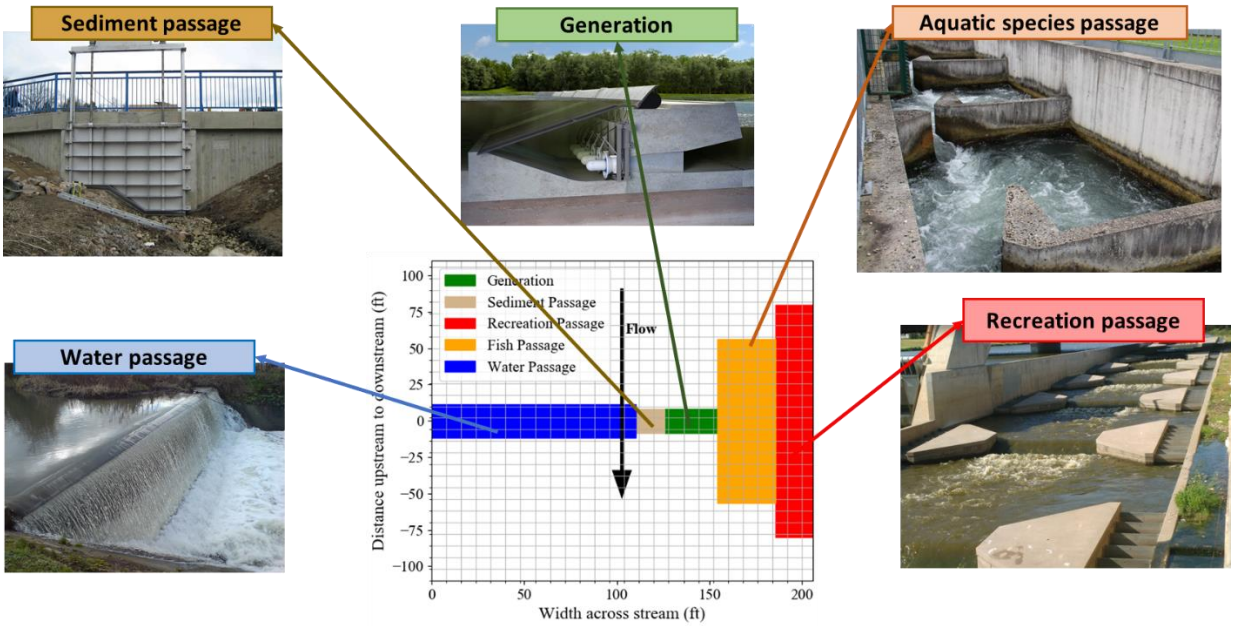

Figure 10. Example top view of an SMH facility footprint and individual reference modules as produced and designed in waterSHED.

The reference SMH facility is developed assuming passage and generation modules are supported by a set of center, left, and right foundation modules (Figure 11). A maximum excavation depth (user input, default of 5 ft) below the channel bottom and side abutments is assumed to volumetrically size the foundation modules.

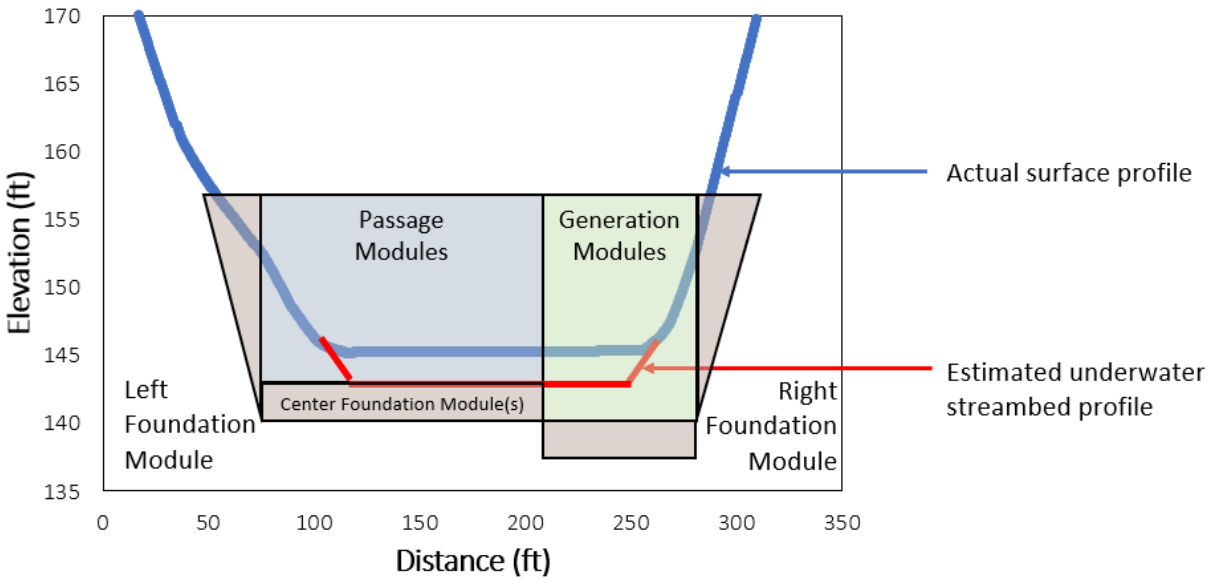

Figure 11. Example front view of an SMH facility (view is from downstream to upstream). In this example, the generation modules are set locally deeper to depict a minimum submergence.

A more detailed modeling framework describing the waterSHED workflow and reference facility design and operation shows the relationships among inputs, design optimization, and rule-based simulation (Figure 12). Beginning with an estimate of mean daily discharge and stage (as determined following steps in Section 3.1), waterSHED guides users through a series of decisions regarding the inclusion of passage modules. When a module is selected, an optimized reference design is established based on known reference module relationships that parameterize dimensions and design flows to input variables. An operational rule curve for each module is generated that specifies when modules are to be passing flow. For example, an upstream aquatic species passage module might be operational only during a key migration period, or a sediment passage module might be operational only when a certain flow threshold is exceeded. Custom operational rules can serve as input variables if the default rule curve is not desired. Following the selection and design optimization of each passage module, the generation design flow and number of generating units are selected. An optimal turbine dispatch curve is calculated based on the design flows of all modules. The remaining flow not passing through a module is spilled over a water passage module.

Detailed information about the critical inputs, optimized design procedure, and rule curve specification for each reference module is found in Appendixes A–F. An example of the basic inputs, key decision variables, sizing procedure, and operational rule specifications for fish, recreation, sediment, and generation modules gives an idea of how each module is established (Figure 13).

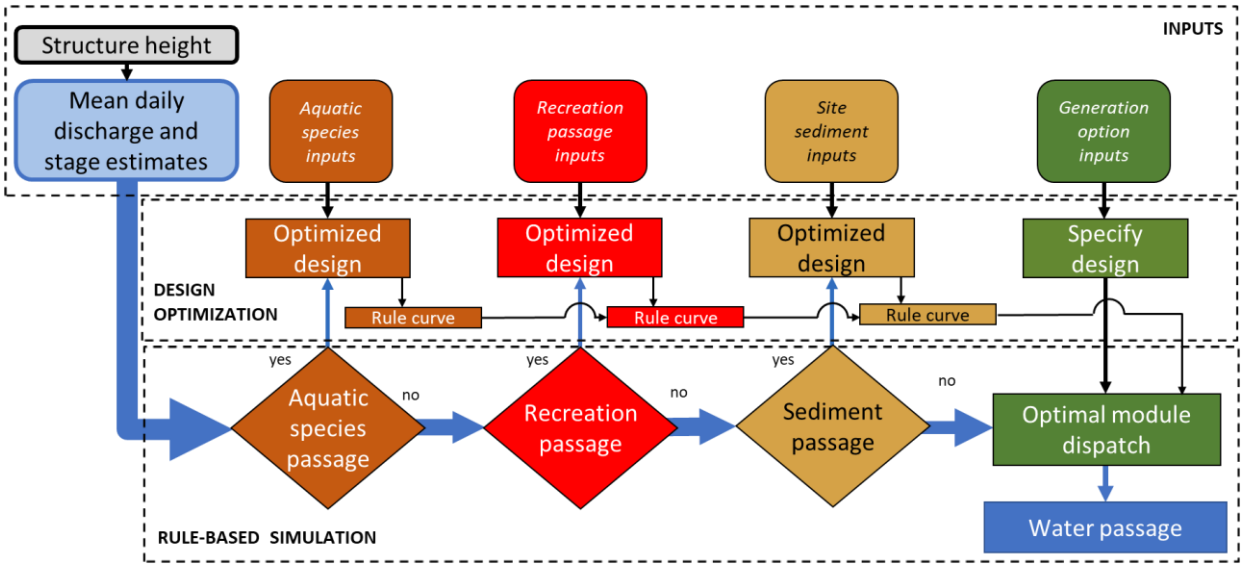

Figure 12. Main modeling workflow for waterSHED.

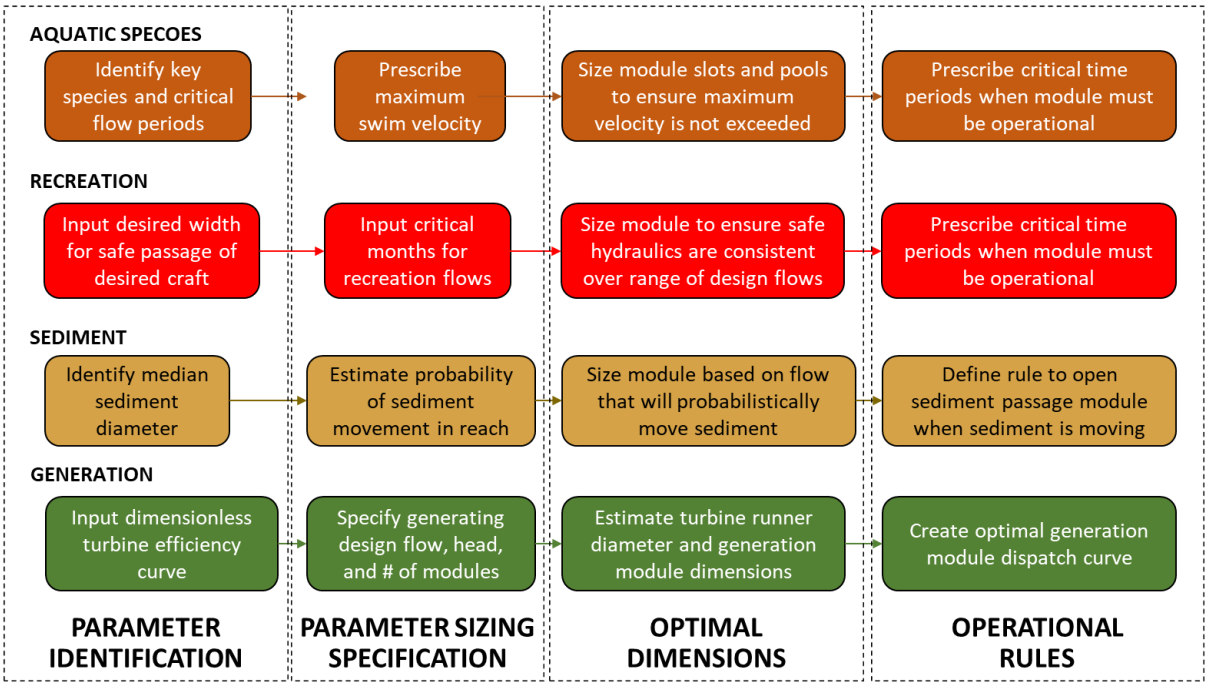

Figure 13. Simplified workflow of module design and operation specification.

2.3.1 Caveats to reference design

The reference design consists of generation and passage module dimensions and operations. It does not account for several more detailed but critical aspects of small hydropower engineering design, including design adjustments for local geotechnical characteristics, generation module orientation with respect to the river, submergence and location of generation module intakes, optimum aquatic species attraction flow design, optimum arrangement of modules with respect to one another, protection of abutments during overtopping by flows greater than the 10-year flood, location of substation, and watertight design of submersible equipment. The assumption that all modules and module components across a stream need to have the capacity to be overtopped from the 10-year to the 100-year flood is a specific design assumption that requires more detailed cost and engineering analysis. While important, these details are not considered in this preliminary design tool, and will be the subject of future research.

2.4 RULE-BASED PERFORMANCE SIMULATION

A rule-based performance simulation is conducted that allocates mean daily flow through all generation and passage modules simultaneously, if operational (as prescribed by rule curves per Figure 12), and estimates hydroelectric output based on generation module characteristics (Figure 14). A predetermined priority allocation of flow is established as follows:

- Aquatic species passage module passes minimum flow up to its design flow.
- Recreation passage module passes additional flow up to its design flow.

- Sediment passage modules passes additional flow up to its design flow if the mean daily flow exceeds a predetermined flow threshold.

- Generation modules use the remaining available flow up to the maximum design flow to generate electricity.

- Water passage modules spill the remaining flow.

For every day of the flow time series, the simulation allocates mean daily flow across modules based on rule curves, flow thresholds, and optimized dispatch. At the end of the simulation, a mean annual hydrograph is generated to visualize the flow distribution in an average year (Figure 15).

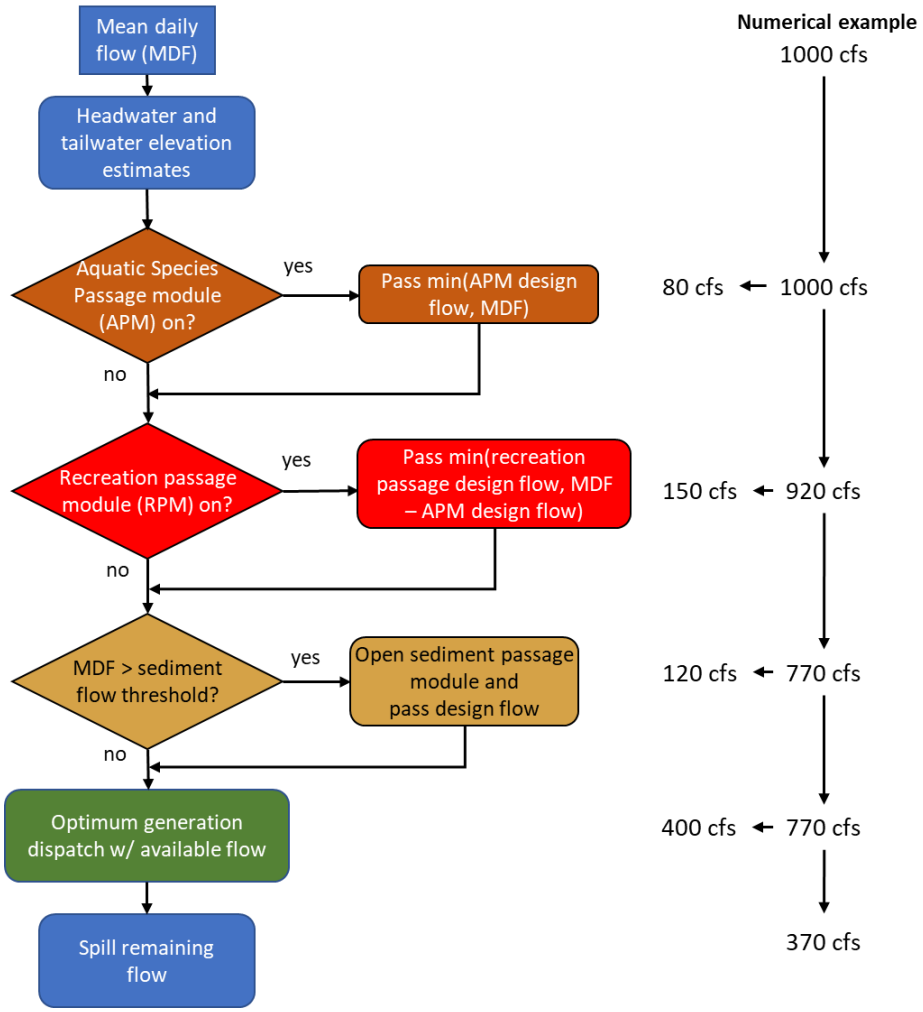

Figure 14. Simplified workflow of rule-based flow allocation.

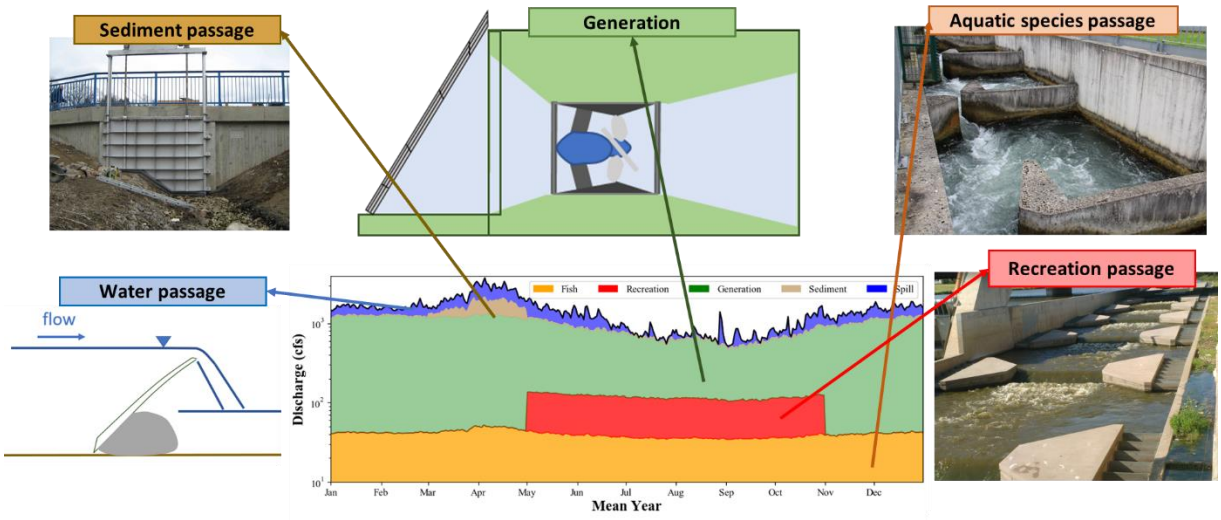

Figure 15. Example mean daily flow averaged over 30 years of operation at a reference site. For each day, the mean daily flow is allocated across modules. Each filled section of the plot represents the flow that passes through the specific module(s).

Although this simulation approach relies on simple operational rules to enable a standard trade-off assessment of modular designs, the method of defining and assembling essential components of a hydrograph to achieve a desirable flow allocation that meets energy and environmental benefits might not yield optimal results because of the inherent complexity in ecosystem function (Acreman et al. 2014). Nevertheless, the simplifying assumptions made to enable a trade-off assessment are crucial as a first step in establishing standard methods of small hydropower environmental design.

2.5 ICC LCOE AND PROJECT ECONOMIC ASSESSMENT

To assess project economics, we set LCOE targets and back-calculate the required installed capital costs (ICC) to meet those targets. This approach allows us to better understand the relationship among modular facility arrangements, generation performance, and project costs.

LCOE represents the net present value of the unit cost of energy over the lifetime of the project, assuming a single capital structure, cost of capital, and operational and cost assumptions. In general, a simplified LCOE is computed as the sum of ICC (in dollars) and discounted annual expenses divided by the energy output over the lifetime of the project, computed as

$$LCOE = \frac{ICC + \sum_{i=1}^{n} \frac{O\&M_{i,a}}{(1+r)^i}}{\sum_{i=1}^{n} \frac{E_{i,a}}{(1+r)^i}},$$

where $O\&M_{i,a}$ = annual operation and maintenance (O&M) expenses in year i, $E_{i,a}$ = annual energy output in year i, r = the real discount rate.

In this report, we set ICC as a dependent variable and reformulate the equation as

$$ICC = LCOE * \sum_{i=1}^{n} \frac{E_{i,a}}{(1+r)^i} - \sum_{i=1}^{n} \frac{O\&M_{i,a}}{(1+r)^i}.$$

Unless otherwise specified, LCOE is computed using the assumptions outlined in Table 2, which reflect common assumptions associated with hydropower development. In particular, the annual O&M rate of $80/kW/year is near the low end of the reported expenditures for small hydropower plants, which ranges from $80 - $120/kW/year (Uria-Martinez et al. 2018). The value used here reflects a future with mature SMH facilities deployed at scale.

Table 2. Default economic assumptions for LCOE estimate.

Category	Variable	Value
Discount rate	*r*	10%
Project life	*n*	30 years
Annual fixed operations and maintenance costs	*O&M*	$80/kW/year

A user can prescribe a capital cost percentage to each module or group of modules to better understand how expected modular development costs are allocated across categories. For example, a developer with a desired LCOE of $0.12/kWh must meet an ICC target of $1.86 million ($2,964/kW) for a given modular arrangement with 627 kW of installed capacity. Based on the module cost distribution shown in Figure 16, the total capital cost of all generation modules should not exceed $978/kW, or $614K. The cost distribution can be altered by users to reflect fixed costs unique to a particular site, such as increased provisions for a substation, transmission lines, or other electrical infrastructure needs.

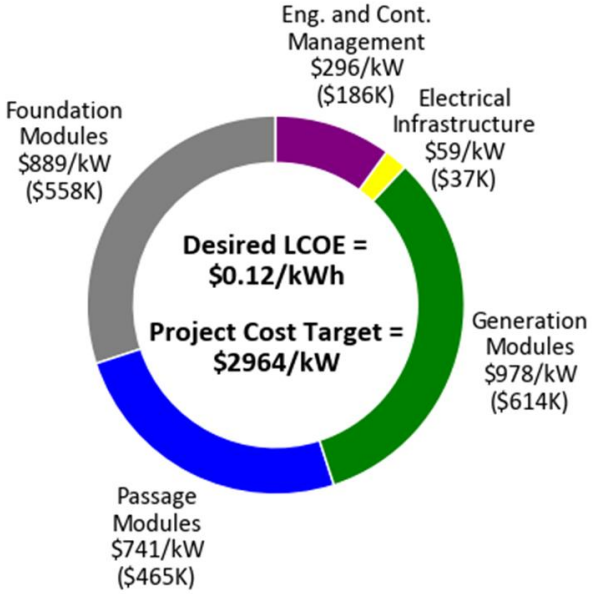

Estimated Cost Distribution	%	$	$/kW
Foundation Modules	30	558,000	889
Passage Modules	25	465,000	741
Generation Modules	33	614,000	978
Electrical Infrastructure	2	37,000	59
Development/Licensing	10	186,000	296
Total	100	1,860,000	2,964

Figure 16. Example of how desired LCOE is translated into a project and module cost target.

3. CASE STUDY

A stream-reach on the Deerfield River in Massachusetts was chosen for the case study. Based on the NSD resource assessment, the stream-reach has approximately 12 ft of gross hydraulic head, a 30% flow exceedance of 1,400 cfs, and a potential installed capacity of 1.2 MW if the project is developed with a normal surface elevation in the forebay that remains below the 100 year floodplain. The stream-reach is not located within 8,000 m of critical habitat, as designated by the US Fish and Wildlife Service, and a virtual hydropower facility modeled at the site estimated a residence time of less than 1 hour at the site based on stream-reach slope and plant hydraulic head, indicating run-of-river would be a feasible mode of operation. Additional characteristics of the site compared with the bulk of NSD potential sites are shown in Figure 17.

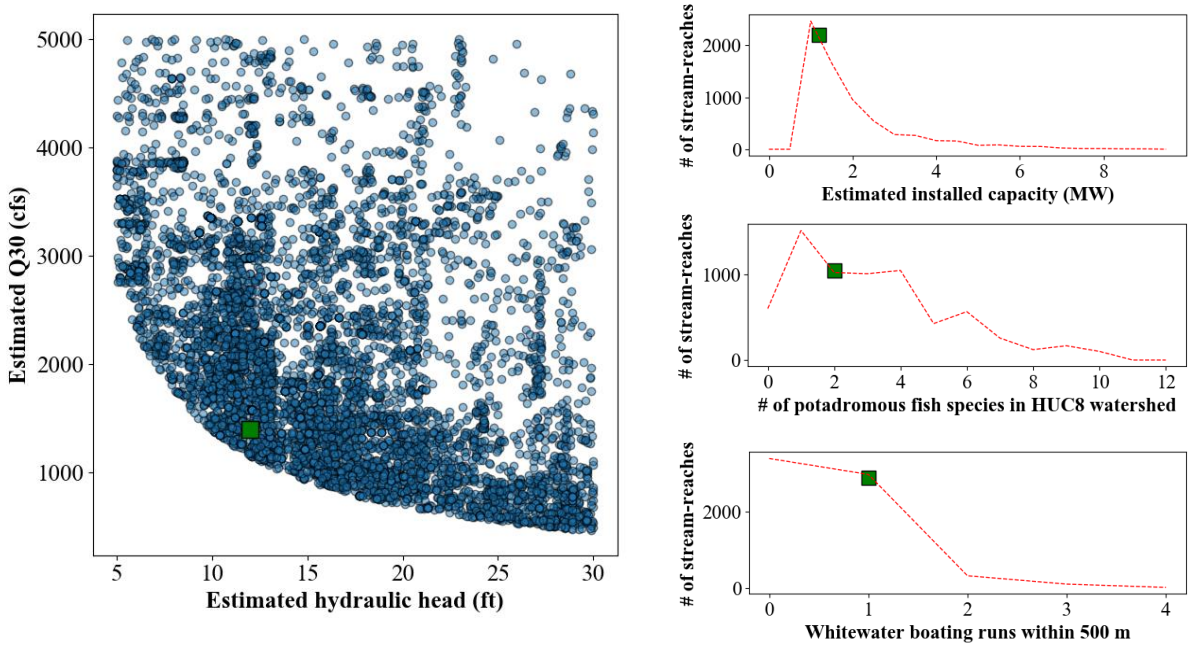

Figure 17. Characteristics of the reference site (green square) compared with the characteristics of all NSD sites with less than 30 ft of head, 5,000 cfs of potential generation flow, and 10 MW of capacity. Left: estimated hydraulic head and Q30. Right: frequency distribution of estimated installed capacity(top); number of potadromous fish species in the HUC8 watershed (middle); and number of whitewater boating runs near the potential site (bottom).

3.1 SITE INPUTS

3.1.1 Hydrologic Estimates and Inputs

Flow data were obtained from USGS gage 01170000, located less than 1 mile upstream from the potential site. The raw data were averaged to produce a mean daily flow from 1980 to 2017 (Figure 18). In general, the site has higher mean flow during the spring and low flow in the late summer and early fall. The flow duration curve shows a range of flow exceedance, with common design flow variables that range from 261 cfs (Q_{95}) to 1570 cfs (Q_{30}).

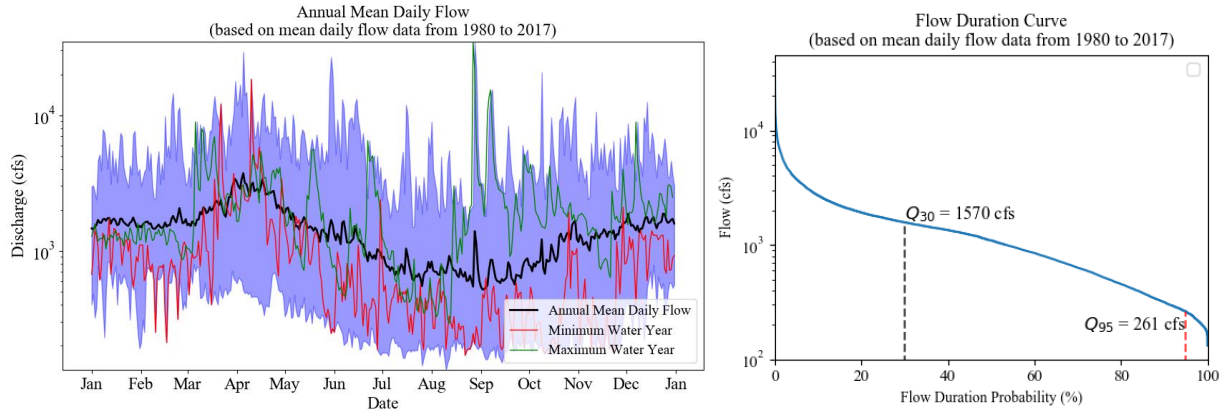

Figure 18. Hydrologic input data for case study 1. Left: annual mean daily flow from 1980 to 2017. The solid black line indicates mean values, the green line indicates daily values for the maximum water year, the red line indicates values for the minimum water year, and the blue filled area represents the bounded minimum and maximum observed mean daily flows. Right: flow duration curve.

To obtain a tailwater estimate, stage information from the gage was fitted to a power law curve and a function was produced for predicting stage as a function of discharge. The headwater of the SMH site was assumed constant at 14 ft above the riverbed to ensure the normal surface elevation remains below the 100-year floodplain. Using the tailwater equation and the flow exceedance values, a gross head duration curve was estimated (Figure 19).

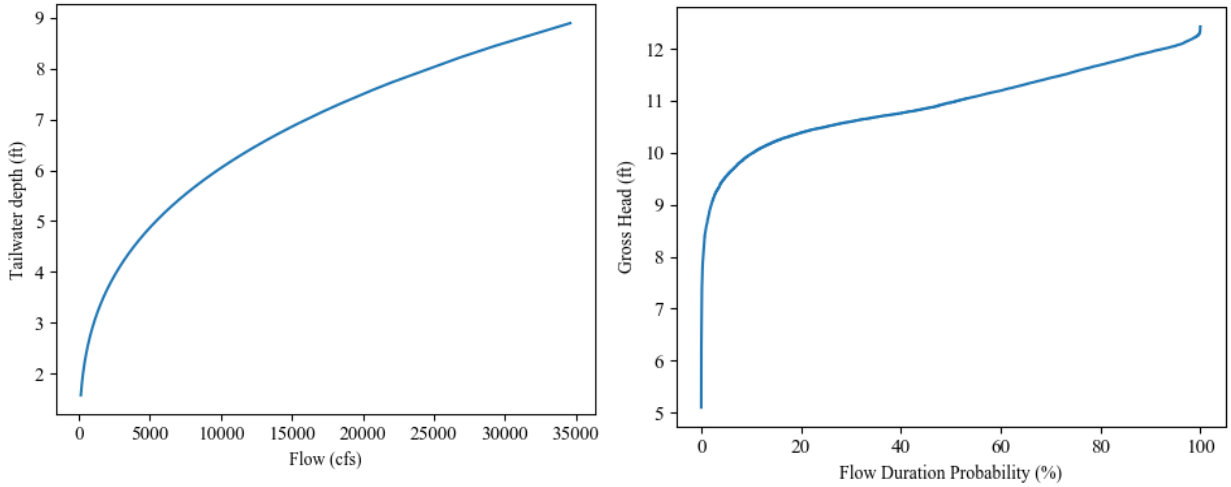

Figure 19. Left: tailwater rating curve. Right: Gross head duration curve.

The 10-year flood flow is estimated by fitting USGS annual peak streamflow gage measurements to a log-Pearson Type III frequency distribution using USGS PeakFQ software. For this site, the 10-year flood is estimated at approximately 33,000 cfs and the 100-year flood at approximately 90,000 cfs.

3.1.2 Site Geometry Inputs

A topographical cross-section is obtained[12] and analyzed to determine preliminary SMH facility dimensions (

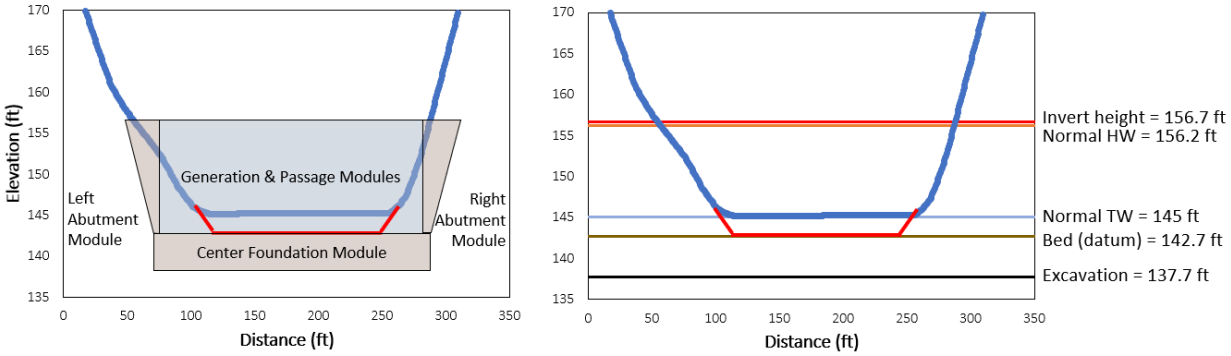

Figure 20). The water surface elevation is approximately 145 ft (above sea level); and assuming a normal trapezoidal bathymetry with a channel bottom located at a depth equivalent to Q_{80} on the stage-discharge curve, 2.3 ft, we set the datum at 142.7 ft. Measurements indicate a stream width of approximately 160 ft at normal flow. Assuming a 14 ft invert height above the channel bottom, the top width of the facility—the overall top width of generation and passage modules—is approximately 205 ft. A channel bottom excavation depth of 5 ft is assumed along with a center foundation module 5 ft deep and 170 ft wide. Left and right side slopes of 1:5.55 and 1:1.75, respectively, are measured and used as inputs to left and right foundation modules, along with an assumption of 5 ft of excavation depth required at side slopes. Key distances, slopes, and foundation module inputs are summarized in Table 3.

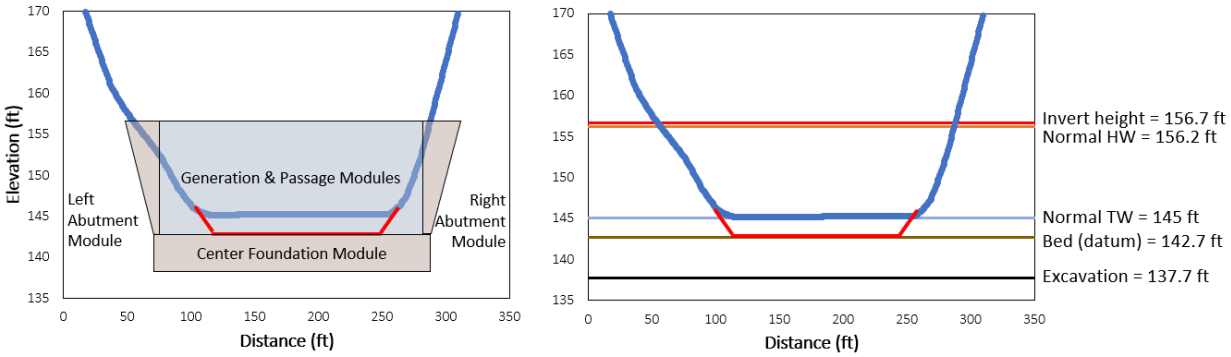

Figure 20. Elevation profile with modules in place (view is downstream to upstream).

Table 3. Site topographical and geometric inputs.

Parameter	Value	Source
River slope	0.001223	NHDPlusV2
Stream width	160 ft	Google
SMH facility top width	205 ft	Estimate
Estimated center excavation depth	5 ft	Estimate

[12] http://www.geocontext.org/publ/2010/04/profiler/en/

3.1.3 Generation and Passage Module Input Variables

A review of publicly available literature and state resources was carried out to establish a first-order estimate of basic module input variables (summary provided in Table 4). In general, input variables are unique to the stream-reach and region (e.g., primary species), or they are selected based on the characteristics of a unique, site-specific variable (e.g., a maximum aquatic species passage module velocity of 5.25 ft/s is recommended for a given primary species).

Table 4. waterSHED generation and passage module input variables.

Category	Value	Source/comments
Aquatic species		
Primary species	Various	US Fish and Wildlife Service 2018. See also Section 3.1.3.1
Key migratory months for sizing design flow	Mar–Jun	Walburg and Nichols 1967
Max velocity in module	5.25 ft/s	Turek, Haro, and Towler 2016
Opening width	1.3 ft	Brownell et al. 2012
Minimum tailwater depth	2.1 ft	Tailwater stage at Q_{95} during aquatic species flows
Maximum tailwater depth	4.9 ft	Tailwater stage at Q_5 during aquatic species flows
Recreation		
Primary craft	Whitewater	Executive Office of Environmental Affairs 2004
Recreation months	Apr–Nov	www.zoaroutdoor.com/schedule.htm
Pool length	20 ft	Estimate based on standard whitewater raft length of 14 ft
Drop width	10 ft	
Pool width	18 ft	
Minimum tailwater depth	1.9 ft	Tailwater stage at Q_{95} during recreation flows
Maximum tailwater depth	2.6 ft	Tailwater stage at Q_{50} during recreation flows
Sediment		
Median grain size	24.6 mm	Mitchell 2009
Target sediment passage months	Mar-Apr	Analysis of annual hydrograph
Sediment entrainment probability	50%	See Section 3.1.3.3
Generation		
Average net head to generation modules	10.4 ft	95% of gross head at 50% flow exceedance
Minimum generation design flow	455 cfs	20% flow exceedance
Maximum generation design flow	1920 cfs	80% flow exceedance
Number of generation modules	2 – 4	
Minimum tailwater depth	2.1 ft	Tailwater stage at Q_{95}
Water		
10-year flood flow	33,000 cfs	USGS peak streamflow for the nation analysis
100-year flood flow	89,800 cfs	USGS peak streamflow for the nation analysis

3.1.3.1 Aquatic species

The US Fish and Wildlife Service maintains online information regarding migratory species conservation on the Connecticut River, of which the Deerfield River is a major tributary (US Fish and Wildlife Service 2018). They identify alewife, American shad, blueback herring, sea lamprey, and striped bass as migratory species of interest with a known range on the Connecticut River. In addition, the state of Massachusetts identifies the Deerfield River watershed as a region that attracts sport fishers, and the state stocks the river with trout and salmon (Commonwealth of Massachusetts 2018).

For our model, we assume an aquatic species passage module is required to pass a variety of species. To establish conservative but specific preliminary module design and operational flow rules, we identify the maximum burst velocity of all migratory species and use the lowest velocity, 5.25 ft/s, as an aquatic species passage module input (Table 5). We selected March through June, the high flow season and a key migratory run time for American shad (Walburg and Nichols 1967), for sizing aquatic species passage flows to ensure the module is operational over a wide range. The minimum and maximum aquatic species passage flows—flows during which the module is designed to be operational—are 352 cfs and 5,120 cfs, respectively (Figure 21). Minimum and maximum tailwater depths associated with these flows are 2.1 ft and 4.9 ft, respectively.

Table 5. Target species and maximum suggested velocities for fishways. (Turek, Haro, and Towler 2016)

Species	Maximum velocity (ft/s)
Alewife	6
American shad	8.25
Blueback herring	6
Sea lamprey	6
Striped bass	5.25

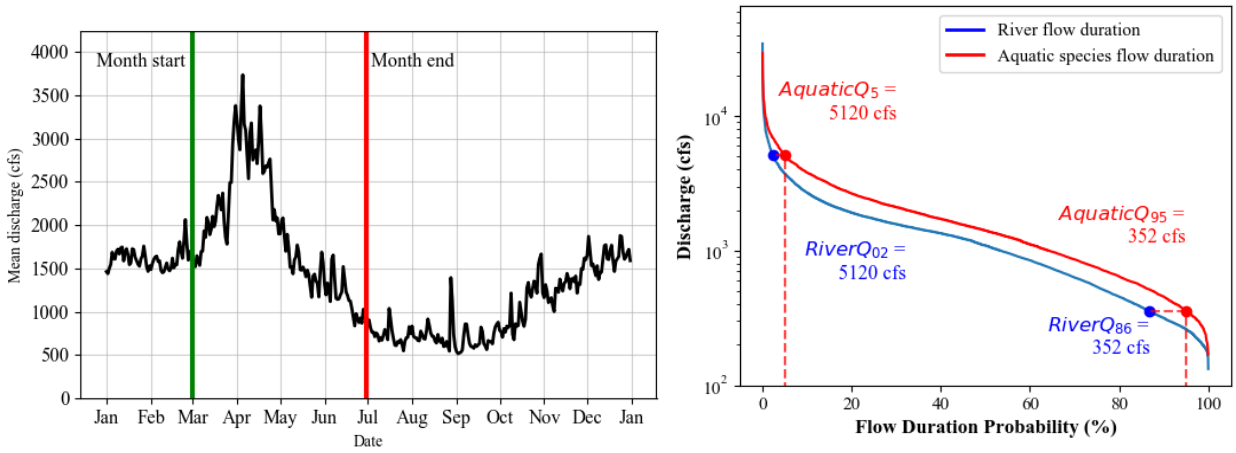

Figure 21. Assessment of mean daily flow to identify (left) specific segment of the mean annual hydrograph used to establish aquatic species passage design flows and (right) flow duration associated with aquatic species passage design flows.

3.1.3.2 Recreation

The Deerfield River is heavily used for recreation, most notably for whitewater rafting because of its high gradient and scheduled flow releases from existing hydropower facilities (Executive Office of

Environmental Affairs 2004). An online release schedule shows that whitewater recreation generally occurs from April through October[13]; thus, we used flows in these months to determine the range of river flows during which a recreation passage module must operate. We also sized the module to pass a 14 ft whitewater raft, with a pool length of 20 ft, drop width of 10 ft, and pool width of 18 ft. The minimum and maximum recreation passage flows—flows during which the recreation passage module is designed to be operational—are 234 cfs and 702 cfs, respectively (Figure 22). Minimum and maximum tailwater depths associated with these flows are 1.9 ft and 2.6 ft, respectively.

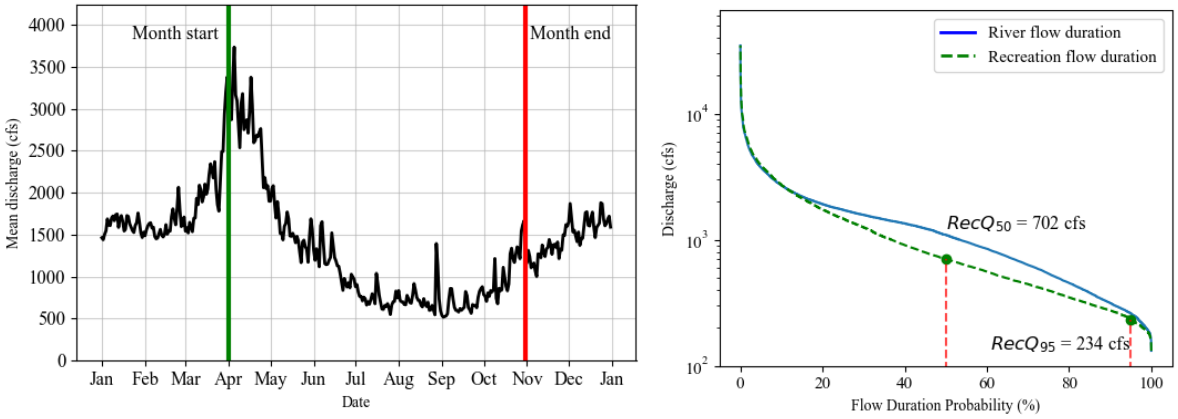

Figure 22. Assessment of *mean* daily flow to identify (left) specific segment of the mean annual hydrograph used to establish recreation passage design flows, and (right) flow duration associated with recreation passage design flows.

3.1.3.3 Sediment

An online search was conducted for documents containing information about the sediment distribution and, more specifically, sites close enough to the study site that the measurements would be relevant.

The median particle size for the site was calculated using data from the report *Deerfield River Watershed 2005 Benthic Macroinvertebrate Assessment* (Mitchell 2009) prepared by the Massachusetts Watershed Planning Program. This report includes data collected at 15 sites throughout the Deerfield watershed, one of which, LDR01, was approximately 1 mile downstream of the study site (Figure 23).

This site reported the river sediment composition to be 50% boulder, 30% cobble, 15% gravel, and 5% sand. The average diameter size for each sediment class—2.125 mm for boulders, 157 mm for cobble, 32.5 mm for gravel, and 1.031 mm for sand—was used to calculate the median particle size for the study site. Excluding the boulder and cobble size fractions, which will not be entrained in the flow conditions present at this site, the median particle size was calculated to be 24.63 mm. Note that the Deerfield River has 11 existing conventional hydropower dams altering its hydrology and sediment fluxes (Commonwealth of Massachusetts 2018).

The sediment passage module is assumed operational when the probability of sediment entrainment surpasses a pre-determined threshold during pre-specified sediment passage months. We assume a bankfull event is capable of mobilizing most sediment in the stream, and that this is associated with a 50% probability of entrainment. Thus, we set P = 50% in the sediment passage model (see Appendix C), which results in a critical flow depth of 5.4 ft and a critical flow discharge of 6,774 cfs (Figure 24). When inflow exceeds the critical flow discharge during sediment passage months, the sediment passage module

[13] http://www.zoaroutdoor.com/schedule.htm

is opened to pass sediment. We assume suspended sediment entrained into the flow is passed through the sustained flow of other passage and generation modules and that bedload is being transported through the sediment passage module. We assume a high passage efficiency as the bed load is transferred through the sluice gate opening along a bottom slope aligned with the upstream-to-downstream channel bottom.

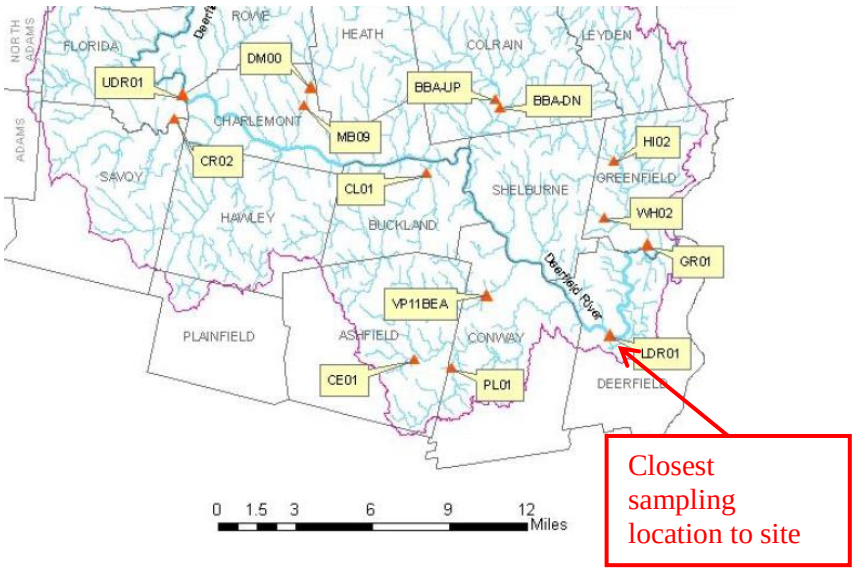

Figure 23. Sediment sampling locations from Mitchell 2009.

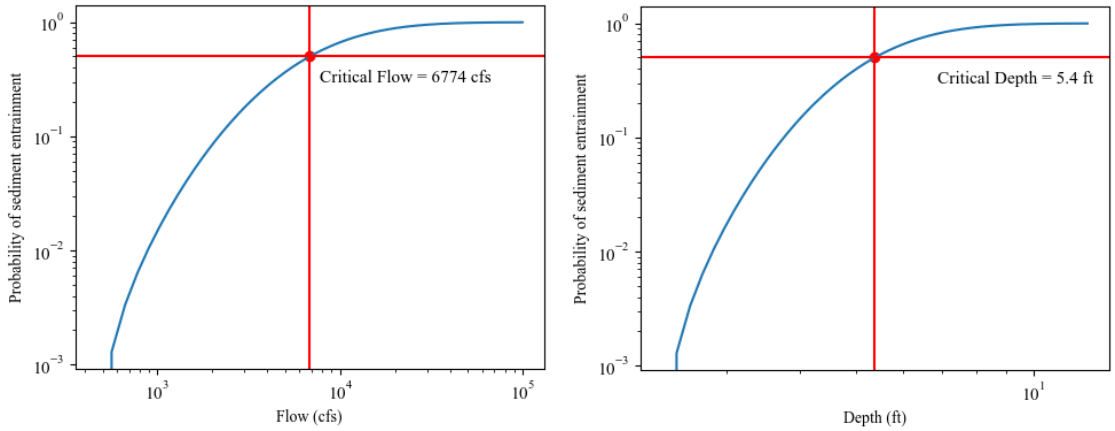

Figure 24. Critical flow (left) and depth (right) associated with a 50% probability of sediment entrainment.

3.1.3.4 Generation

A suite of generation modules of varying capacity is modeled to enable trade-off analysis of facility footprint, generation capacity, and operational flexibility. Input variables include number of generation modules (two to four are selected for this case study); plant design flow between a 20% flow exceedance (1920 cfs) and an 80% flow exceedance (455 cfs); and average net head, estimated as 95% of the gross

head associated with a 50% exceedance flow, or 10.4 ft. The minimum tailwater to submerge the turbine outlet is estimated as the stage at a 95% flow exceedance, or 2.1 ft. See Appendix D for specific details about generation module sizing and specification of additional operational parameters.

3.1.3.5 Water

Water passage modules are sized to pass a 10-year flood estimate of 33,000 cfs, computed from USGS gage 01170000 and PeakFQ software. The facility is assumed to be safely overtopped for flows between the 10-year and 100-year floods. The top of the water passage module crest is estimated as 14 ft, equivalent to the normal operating elevation plus 0.5 ft. The maximum width available for water passage modules is set as the SMH facility top width, 205 ft, minus the width of passage and generation modules.

3.2 SMH FACILITY DESIGN SPECIFICATION

3.2.1 Generation and Passage Module Output Variables

After waterSHED completes a design optimization step, major dimensions and operational characteristics are prescribed for each module. These are summarized in Table 6, and basic module designs are visualized in the following subsections.

Table 6. waterSHED generation and passage module output variables.

Category	Value
Aquatic species	
Module design flow	34.5 cfs
Normal module flow depth	4.7 ft
Module pool length	13 ft
Module pool width	10.4 ft
Number of pools	16
Total module length	208 ft
Recreation	
Module design flow range	23–79 cfs
Number of drops	7
Total module length	175 ft
Sediment	
Module width	12 ft
Module depth	4.7 ft
Module design flow threshold	11,068 cfs
Generation	
Module array length and width, runner diameter, rotational speed	Variable, see Section 3.2.1.4
Module installed capacity	Variable, see Section 3.2.1.4
Water	
Module length, width, and profile	Variable, see Section 3.2.1.5

3.2.1.1 Aquatic species

A total of 16 pools across a slope of 0.055 are required to ensure a maximum velocity of 5.25 ft/s (minimum burst speed for species of interest in Table 5) is not exceeded for the given aquatic species

passage module design flow (Figure 25). The design flow of 34.5 cfs ensures maximum velocities and energy dissipation functions in each slot and pool, respectively, are not exceeded. To minimize the upstream-to-downstream footprint and ensure the downstream entrance is near the base of the SMH facility, the aquatic species passage modules can include turning pools at predetermined intervals. The number and location of turning pools can be adapted to individual sites and user preferences. We selected one turning pool, which reduced the overall aquatic species passage module length to 104 ft but increased the width to 20 ft (Figure 26).

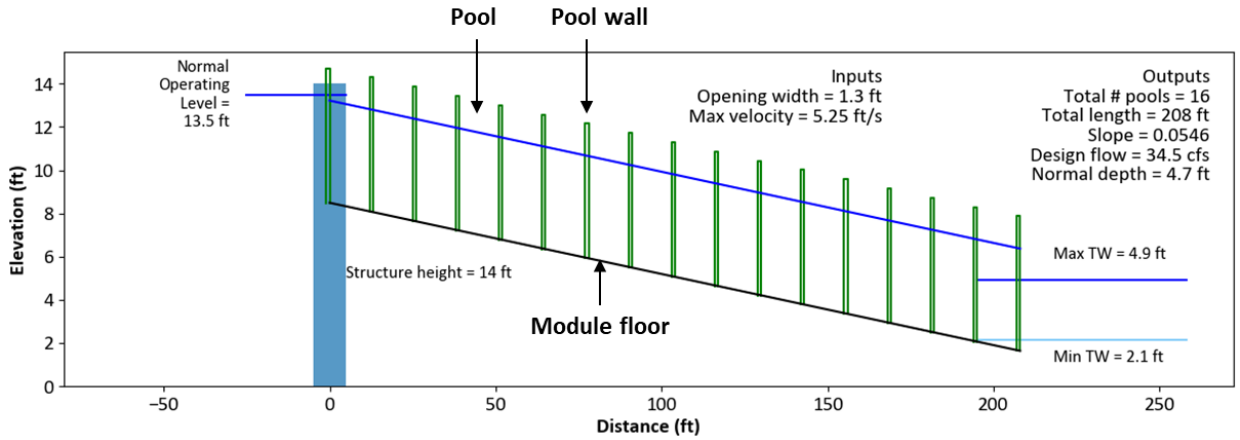

Figure 25. Aquatic species passage module side view (without a turning pool). Note the axes are not to scale.

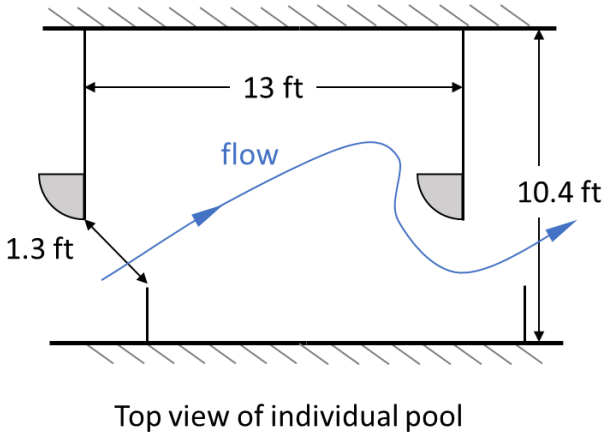

Figure 26. Aquatic species passage module top view of single pool.

While a slope of 1:10 is generally recommended for vertical slot fishways (Katopodis 1992), the maximum velocity of 5.25 ft/s is the limiting factor in prescribing aquatic species passage module slope, as it sets the maximum drop height per pool and number of pools. The resulting aquatic species passage module slope of 0.0546 is below the suggested maximum slope and more closely aligned with the suggested slope of 1:30 for nature-like fishways designed for striped bass outlined in (Turek, Haro, and Towler 2016).

3.2.1.2 Recreation

The recreation passage module consists of seven total drops across 175 ft of length, giving an average slope of approximately 0.07 (Figure 27). Each drop is approximately 1.5–1.6 ft above the next

downstream drop and is designed to create an undular wave regime in the receiving pool that is safe and favorable for recreation throughout the design flow of 23 to 79 cfs in a tailwater range of 1.9 to 2.6 ft.

The recreation passage module is required to be in operation only during pre-specified seasons and only during hours of the day when water recreation is allowed or likely to occur (i.e., during daylight hours). Thus, we restricted the recreation passage module to operate only 12 hours a day and only during April through October. This is accounted for in the simulation loop, which splits each mean day into 24 equal segments and allocates flow to the recreation module during half of them.

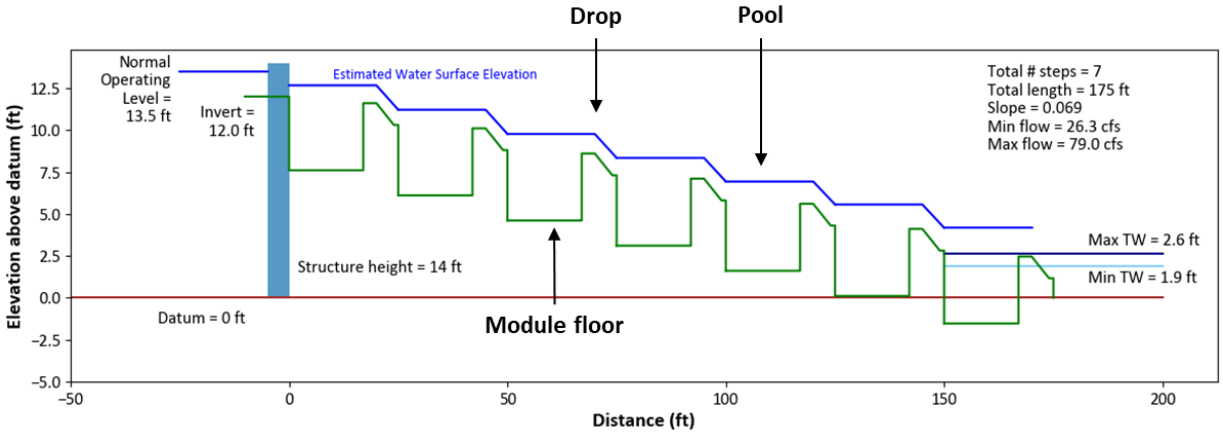

Figure 27. waterSHED output of recreation passage module side view.

3.2.1.3 Sediment

The critical flow depth and critical flow discharge associated with a 50% probability that the median sediment grain size is entrained into the flow, 5.4 ft and 6,774 cfs, respectively, are used to size the sediment passage module. When this flow discharge is exceeded during user-determined time periods, the sediment module is opened to create a low-level outlet capable of passing sediment downstream (Figure 28). Using these inputs, waterSHED estimates a sediment sluice gate with a width of 8 ft and a maximum opening depth of 10.5 ft would be enough to pass 20% of the critical flow discharge at the critical depth (Figure 29).

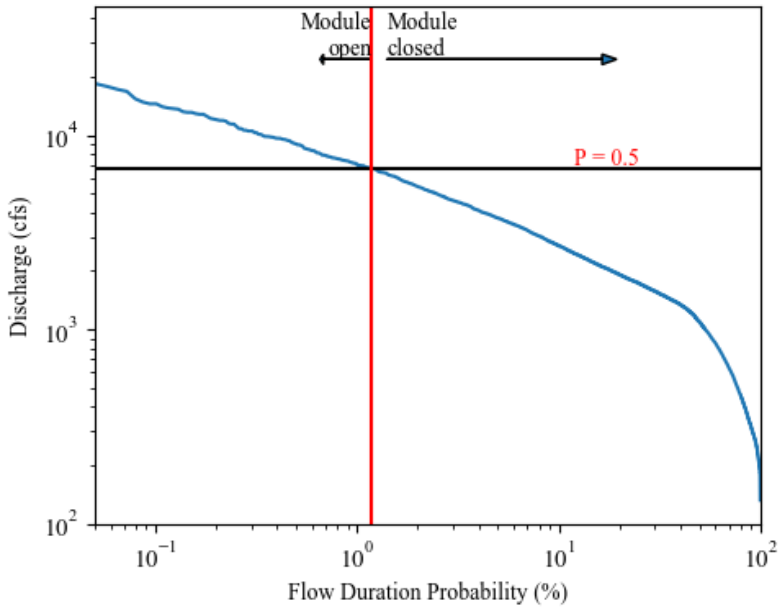

Figure 28. Sediment passage module operation is plotted on the flow duration curve to show when the module is open, or passing flow, and closed.

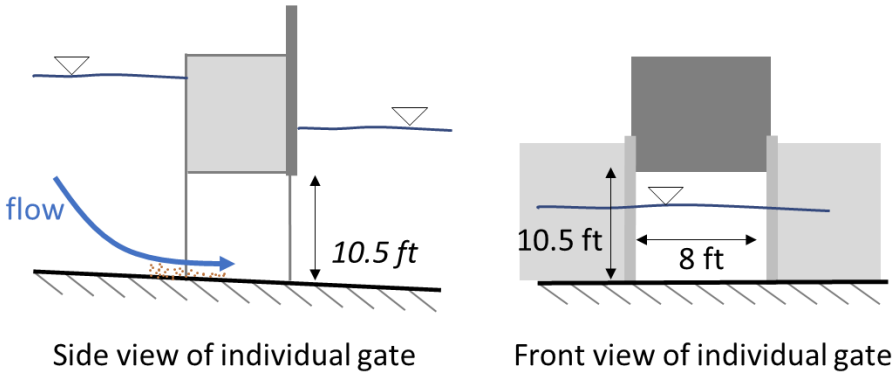

Figure 29. Side view (left) and front view (right, view is downstream to upstream) of an open sediment passage module.

3.2.1.4 Generation

An optimal plant efficiency curve is developed and used to determine optimal plant dispatch (Figure 30). Generation module dimensions and operating characteristics are shown in Table 7 and Figure 31. Note that excavation depth is not optimized for a specific design and location and may in fact be significantly less than the values shown, based on turbine arrangement and site conditions.

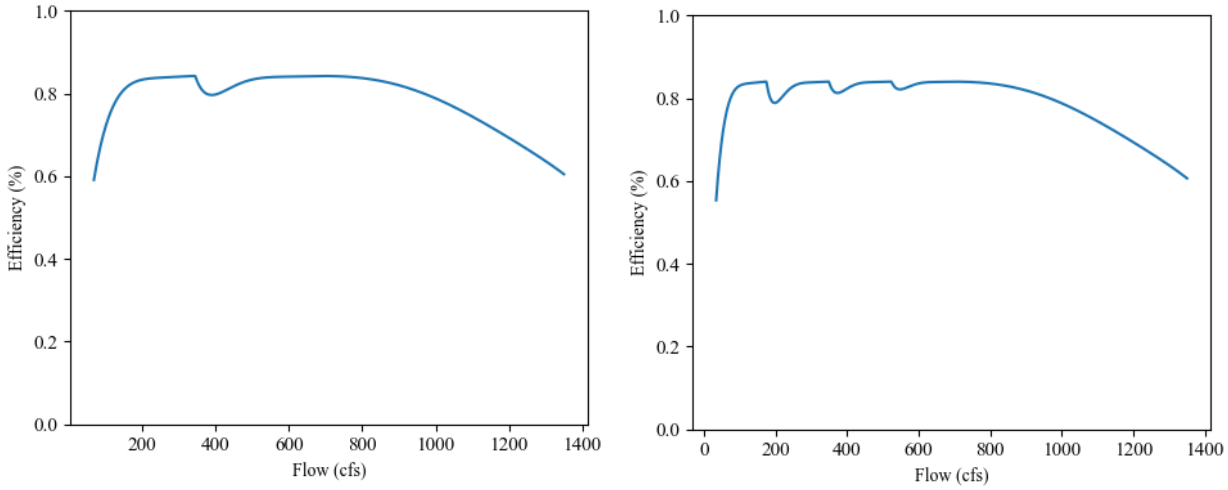

Figure 30. Plant efficiency curve for two generation modules (left) and four generation modules (right) using the same plant design flow.

Table 7. waterSHED design outputs for generation modules. Image for highlighted row is shown in Figure 31.

Number of generation modules	Plant design flow (cfs)	Module design flow (cfs)	Turbine rotational speed (rpm)	Turbine outer diameter (ft)	Turbine installed capacity (kW)	Plant installed capacity (kW)	Module excavation depth (ft)	Module array width (ft)	Module array length (ft)
2	1920	960	163	7.4	714	1428	12.9	45	52
2	1350	675	192	6.3	502	1003	10.7	38	44
2	849	425	236	5.1	315	630	8.3	31	36
2	455	228	319	3.8	168	337	5.7	23	27

Table 7. waterSHED design outputs for generation modules (continued).

Number of generation modules	Plant design flow (cfs)	Module design flow (cfs)	Turbine rotational speed (rpm)	Turbine outer diameter (ft)	Turbine installed capacity (kW)	Plant installed capacity (kW)	Module excavation depth (ft)	Module array width (ft)	Module array length (ft)
3	1920	640	197	6.2	475	1426	10.4	55	43
3	1350	450	232	5.2	339	1001	8.6	47	37
3	849	283	288	4.2	210	629	6.5	38	30
3	455	152	385	3.2	112	336	4.4	29	22
4	1920	480	225	5.4	356	1425	8.9	65	38
4	1350	338	265	4.6	250	1000	7.3	56	32
4	849	212	329	3.7	157	628	5.5	45	26
4	455	114	440	2.8	84	335	3.7	34	20

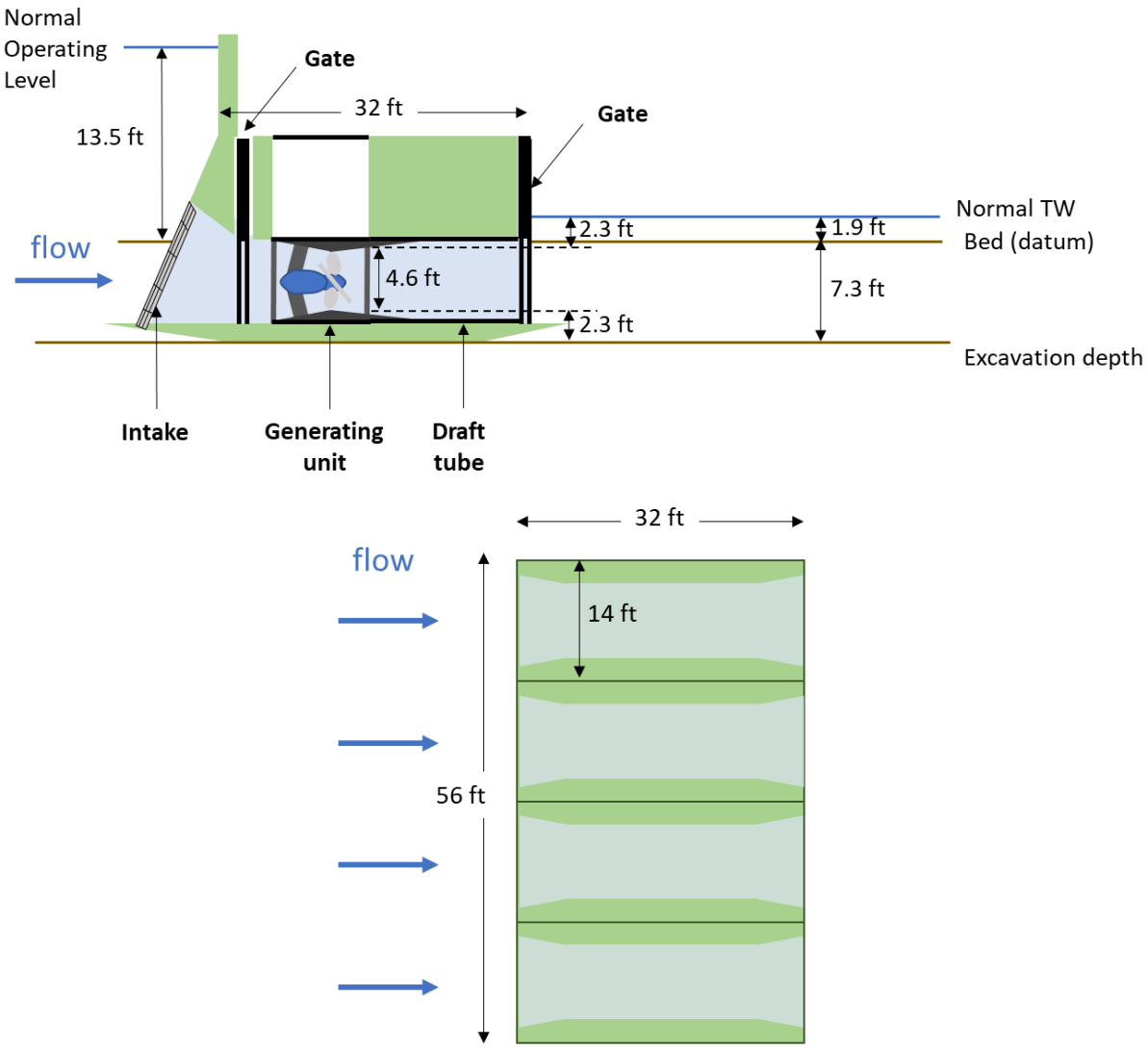

Figure 31. Generation module basic dimensions based on highlighted row from Table 7. Side view of a single module (top) and top view of an array of modules (bottom).

3.2.1.5 Water

Water passage module profiles and lengths are sized based on a 10-year flood flow estimate of 33,000 cfs. The length and width of water passage modules are dependent on the combination of generation and passage modules deployed in the stream. If the width of the water passage modules required to pass a flood flow is greater than the available width in the stream— i.e., the width of the stream minus the width of generation and passage modules—the design is flagged as not suitable. If the required water passage module width is less than the available width, the design width is specified as the available width. Using the same design output as highlighted in Table 7, an example module arrangement is shown in Figure 32. The width of the water passage modules, 120 ft in this example, is suitable to pass the design flood and is the width of the stream minus the width of the generation, fish, recreation, and sediment passage modules.

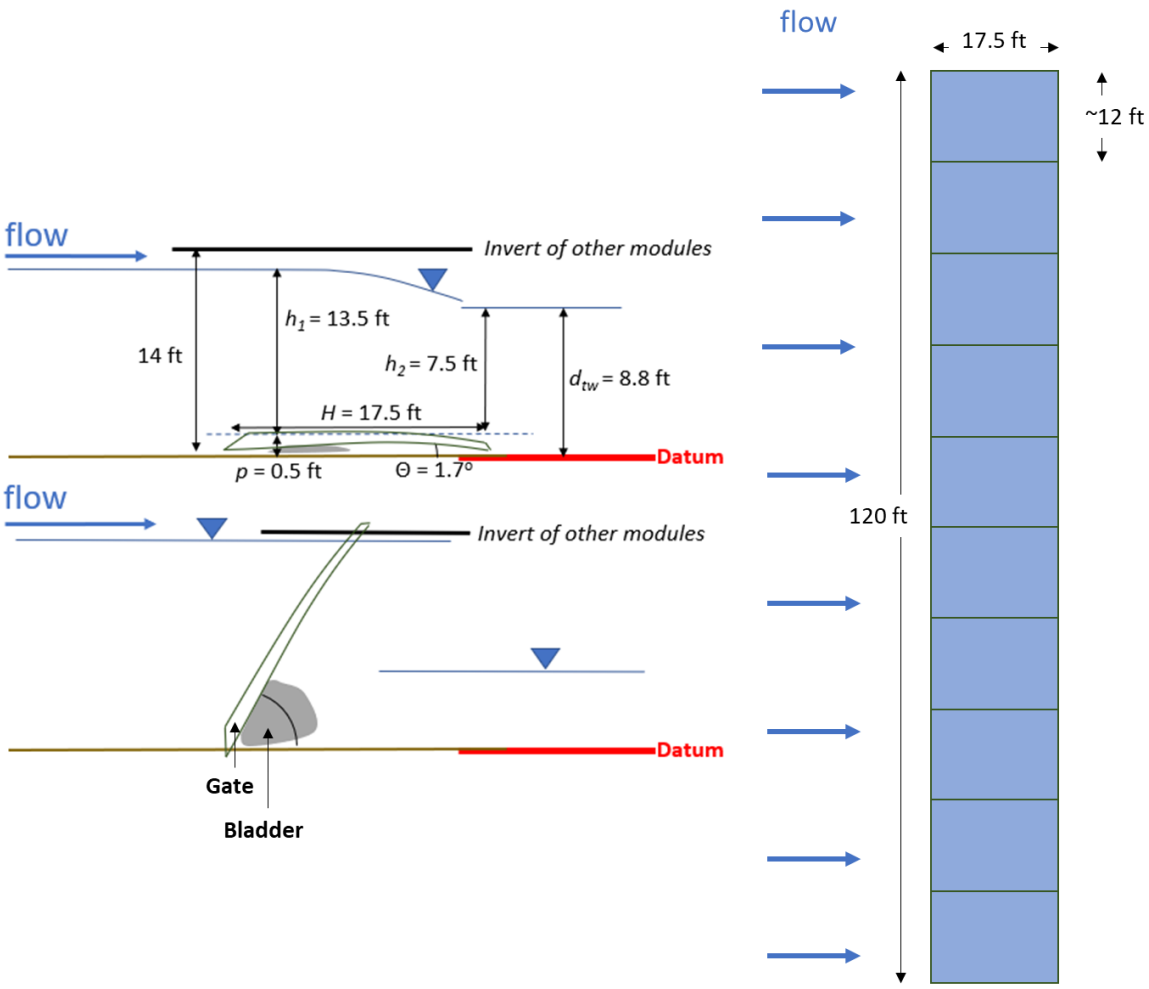

Figure 32. Water passage module basic dimensions. Side view of a single module in the down position (top left) and raised position (bottom left) and top view of an array of modules (right).

3.2.2 Modeling scenarios

To explore how annual energy output profiles and generation flexibility vary based on decisions to incorporate modules and allocate more or less flow to modules, we established a set of four modular arrangement modeling scenarios (Table 8). The first scenario (S1) is a facility with generation and water passage modules only. Aquatic species, sediment, and recreation passage modules are added, respectively, for scenarios 2–4 (S2, S3, S4).

Table 8. Modeling scenarios.

	Generation	Water passage	Aquatic species passage	Sediment passage	Recreation passage
Scenario 1	X	X			
Scenario 2	X	X	X		
Scenario 3	X	X	X	X	
Scenario 4	X	X	X	X	X

3.2.3 Facility footprint

Virtual SMH facilities are generated based on four modeling scenarios. Once the dimensions of each passage module are recorded, waterSHED plots a top-down view of the modular facility. As an example, four potential configurations associated with a generation design flow of 1350 cfs distributed across four generation modules are shown in Figure 33. The generation modules have the same installed capacity across scenarios, and the addition of each passage module causes an overall increase in the footprint of the facility. If the required width of the water passage modules is greater than the width available in the stream after the generation and passage modules are sized and placed, a message is printed on the plot estimating the additional width of passage modules needed to pass the design flood. As discussed in Section 1, module placement and layout are not optimized for any particular scenario.

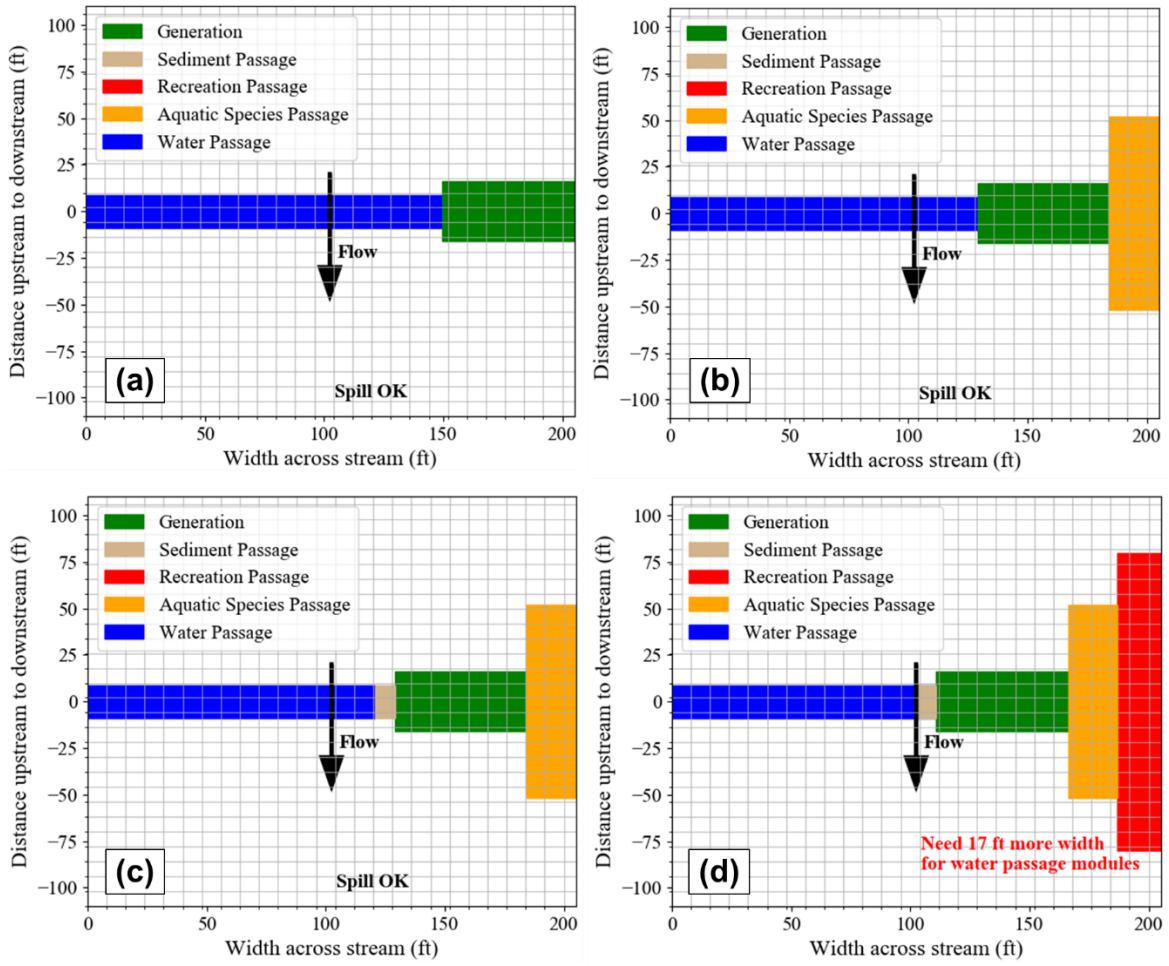

Figure 33. Top view of SMH facility arrangements for four modeling scenarios. (a) S1: water passage and generation; (b) S2: water and aquatic species passage, generation; (c) S3: water, aquatic species, and sediment passage, generation; and (d) S4: water, aquatic species, sediment, and recreation passage, generation.

3.3 RESULTS

To showcase the results in a straightforward way, we provide detailed model outputs for S4 with three generation modules sized to Q_{40}. On a mean annual basis, the temporal variation of generation and

passage module operation reflects the design and operational rules established in the model (Figure 34, top). The aquatic species passage module is operational year-round; the recreation passage module is passing flows for 12 hours a day during recreation season from April through November; the sediment passage module is operational during the high flow season, from March through May; generation modules use the balance of flow to produce electricity; and spill modules are used to safely pass excess flow that cannot be passed through other modules. The recreation module flow output is half of the design flow as a result of averaging—the module is open 12 hours a day and closed 12 hours a day to accommodate a theoretical recreation schedule. Also shown is the operation from a single year, where the day-to-day change in module operations is observed more clearly (Figure 34, bottom). In this case, the sediment passage module is opened twice when flood flows are present, the water passage modules operate sporadically throughout the year but mostly during the high flow months of April and June, and the generation modules are capable of handling the intermittency of flows throughout the rest of the year.

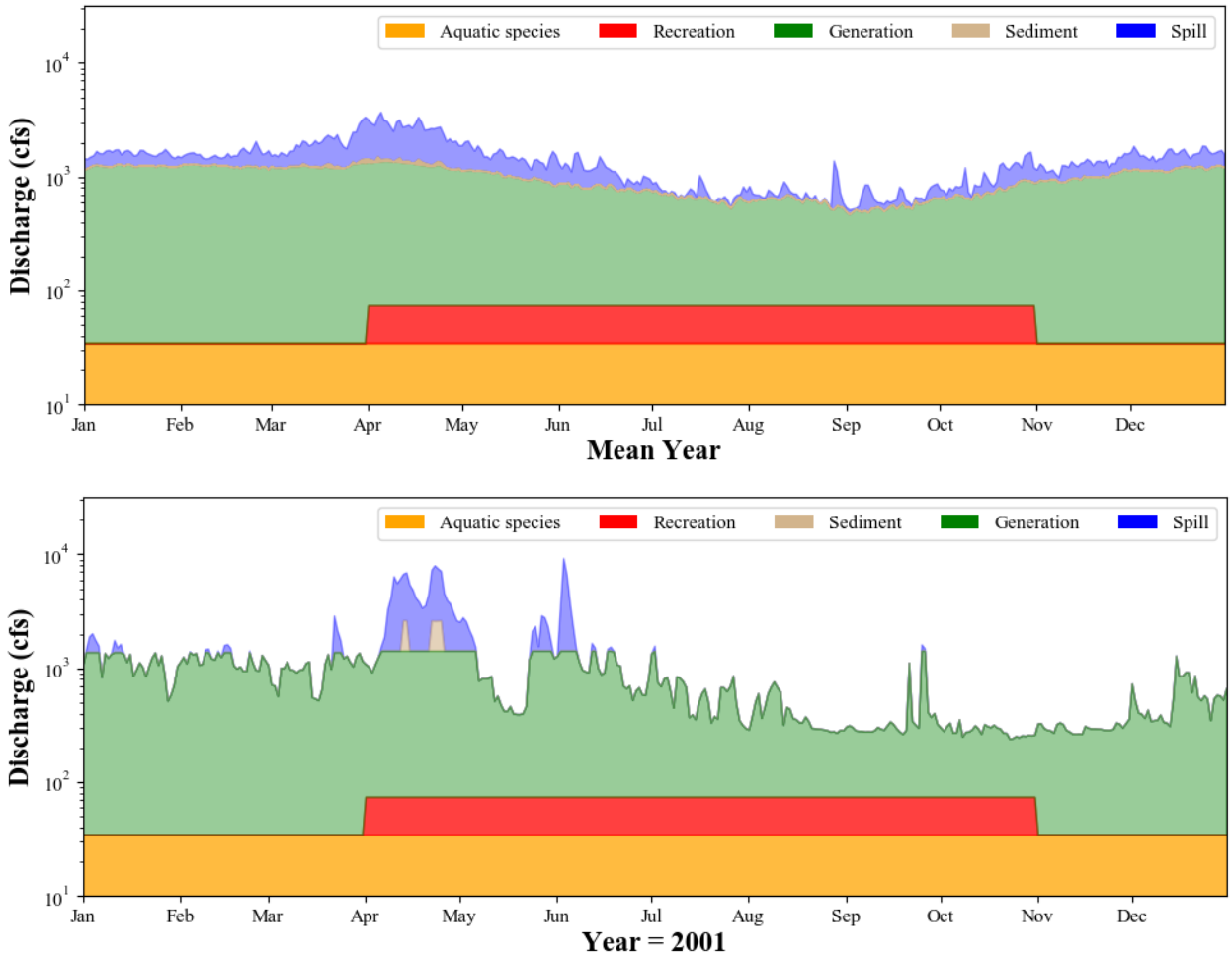

Figure 34. Flow allocation across modules for S4 with three generation modules sized to Q_{40}. Top: mean of all years (1980–2017). Bottom: single year.

Generation modules are operating at peak capacity from December through May, when flows are highest (Figure 35). During low flow months (July through October) and minimum water years (red line) there is often only one generation module in operation. During high water years, all three modules could be in operation, highlighting the variability of a potential site and the need to efficiently optimize generation module sizing. The passage of sediment flows does not have a significant influence on modeled

operations, as the flood pulse generally seen in the spring is routed through a sediment passage module with sufficient flow to continue generation.

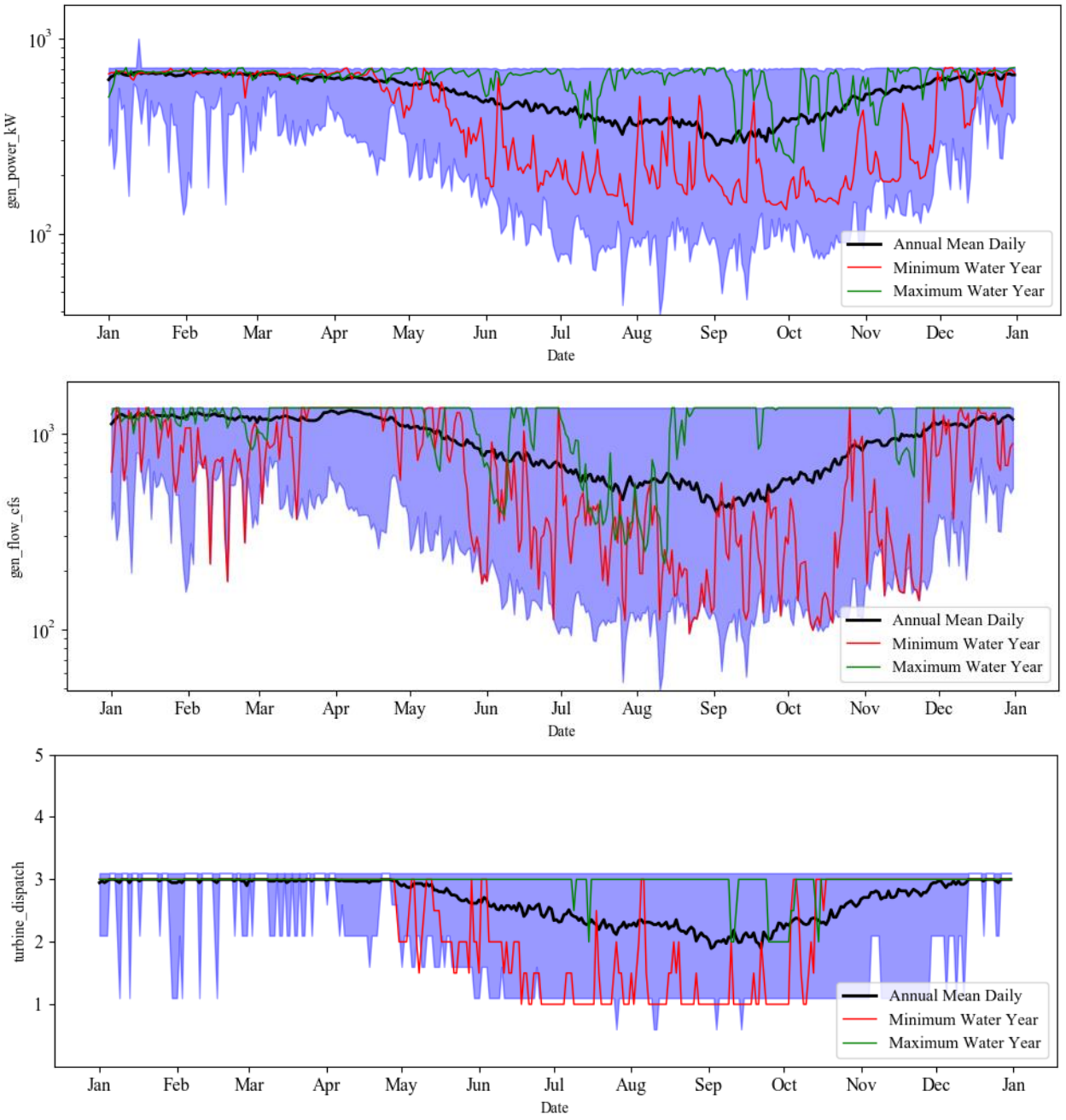

Figure 35. Generation module performance for S4 with three generation modules sized to Q_{40}. Top: mean daily generation in kilowatts. Middle: mean generation flow in cfs. Bottom: mean turbine dispatch.

Aquatic species and recreation passage modules operate at a pre-determined design flow regardless of river discharge. Sediment passage module operation shows some variation aligned with seasonal flood flows (Figure 36). The sediment passage module on average is operational throughout the specified operational period; however, in minimum flow years, the module might be operational only for a single day if river discharge stayed below the assumed sediment transport threshold. There may not be

significant sediment deposition during low flow years, as the local (i.e., site-level) bed shear stress may not be strong enough to move bedload. Having the sediment passage module operation tied to high flow events is appropriate because of the timing of expected high-river-flow bedload. If so desired, a user could adjust the sediment module to operate during all high flow events throughout an entire year, rather than during pre-determined months.

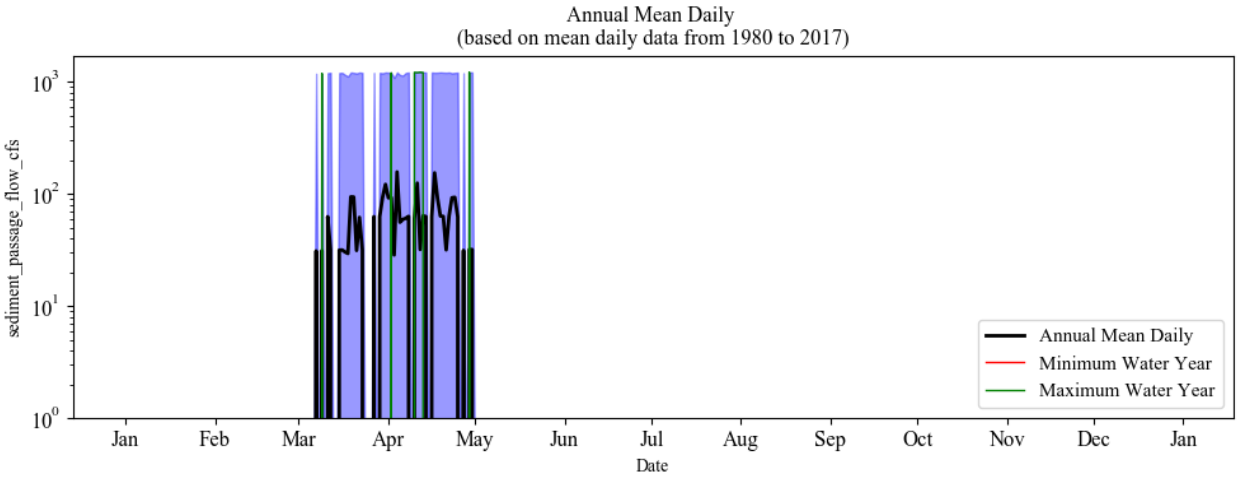

Figure 36. Sediment passage module mean daily flow for S4 with three generation modules sized to Q_{40}.

Mean water passage flow may vary substantially throughout the year, from roughly 1,000 cfs in spring to nearly 0 cfs in summer months (Figure 37). In low water years, the water passage modules may not be used for months at a time, while in high flow years, they may be operated continuously for several months at a time.

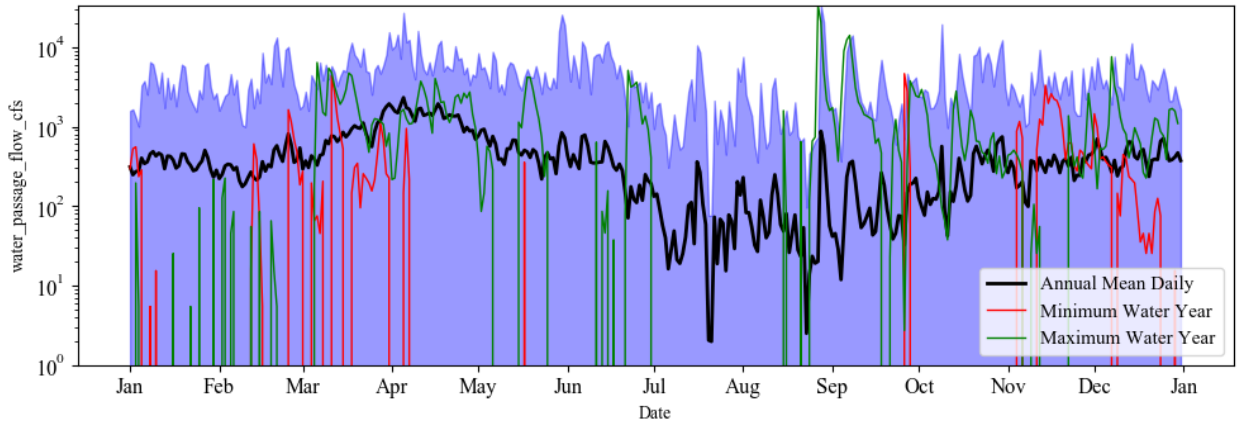

Figure 37. Water passage module mean daily flow for S4 with three generation modules sized to Q_{40}.

3.4 SCENARIO TRADE-OFF ANALYSIS

For each scenario, we assess a suite of modeling options in which flow priority is given to aquatic species passage flow, recreation passage flow, generation, sediment passage flow, and then water (spill) passage. We change generation design flows using a flow exceedance varying from Q_{20} to Q_{80} in increments of

Q_{20}; and for each design flow, we model two, three, and four generation modules, each sized based on the specified design flow. This enables a detailed look at different energy generation and modular arrangement strategies that might provide differing levels of operational flexibility. Aquatic species, recreation, and sediment passage modules are all maintained at the same size, though a user can change design flows and establish alternative passage scenarios by altering inputs for passage reference modules.

The annual energy output of each modeling scenario and design option is compared with the overall ground footprint (in square feet) of all modules combined (Figure 38). The biggest driver of annual generation change is the design flow of generation modules—as the design flow is decreased, significant drops in MWh are observed that are due to the change in installed plant capacity. For the Q_{20} option, the impact on annual energy output as additional modules are added is a reduction of 5% from S1 with no passage modules, to S4 with all passage modules. For smaller generation flows, energy generation is minimally affected by the addition of passage modules because the flow available in the river is sufficient to pass through all modules nearly all of the time. However, the footprint still grows significantly. The plant footprint serves as a proxy for the total surface area of the foundation modules required to support the facility. In general, the plant footprint decreases as generation design flow is decreased, primarily because of the smaller-diameter turbines. The footprint increases approximately threefold when the scenario changes from S1 with no passage modules, to S4 with all passage modules. The biggest addition is the recreation module, which requires large pools to receive boaters. When all modules are modeled, only SMH plant arrangements that use generation flows sized to a Q_{80} flow exceedance are feasible within the given stream width, as noted by the empty markers for nearly all S4 options.

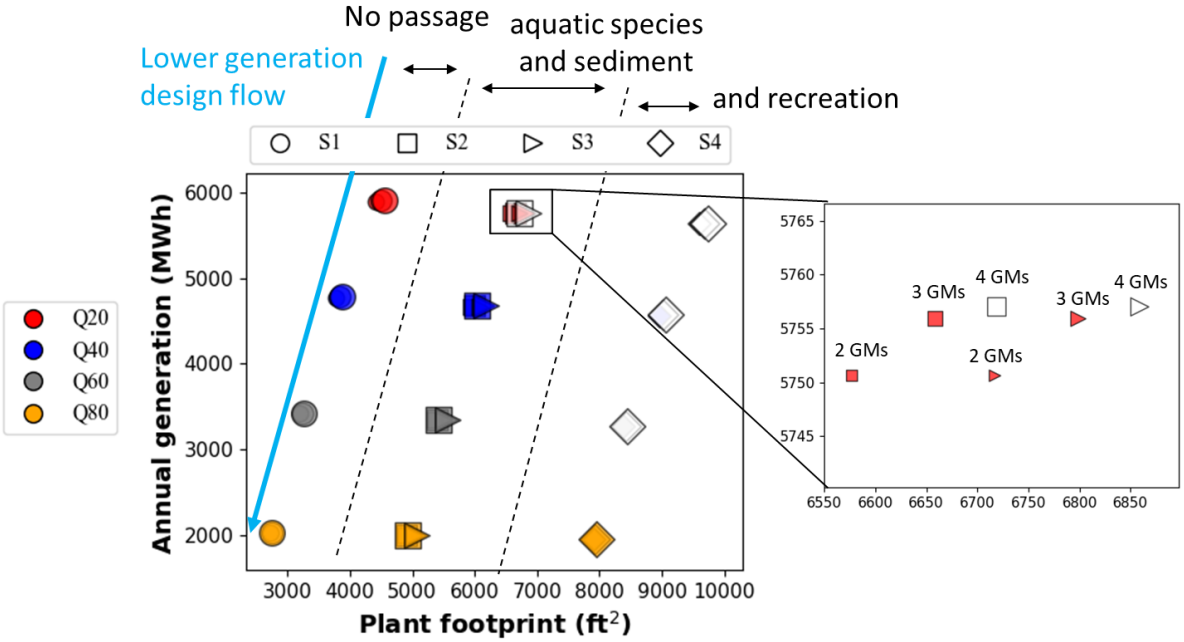

Figure 38. Comparison of mean annual energy generation and plant footprint for four modeling scenarios. Moving right to left, the plant footprint is increased by the addition of passage modules. Moving from top to bottom, generation design flow is decreased, leading to lower mean energy output. Markers are sized relative to the number of turbines for each scenario (2 turbines = smaller, 4 turbines = larger). Empty markers indicate the effective length of the water passage modules was not sufficient to pass the design flood.

A comparison of installed generation capacity and capacity factor for each scenario and option shows that generation design flow (proportional to installed generation capacity) has a more significant effect on capacity factor than either the number of turbines or the modular arrangement (Figure 39). Smaller

installed capacities sized for a Q_{80} flow exceedance show modeled capacity factors near 70%, with an approximate 3% reduction when all aquatic species, recreation, and sediment passage modules are modeled. Larger installed generation capacities sized for a Q_{20} flow exceedance have modeled capacity factors in the range of 47%, with a 2% reduction when all passage modules are included. The addition of more generation modules decreases the installed capacity slightly, but it adds an additional 0.2% of capacity factor.

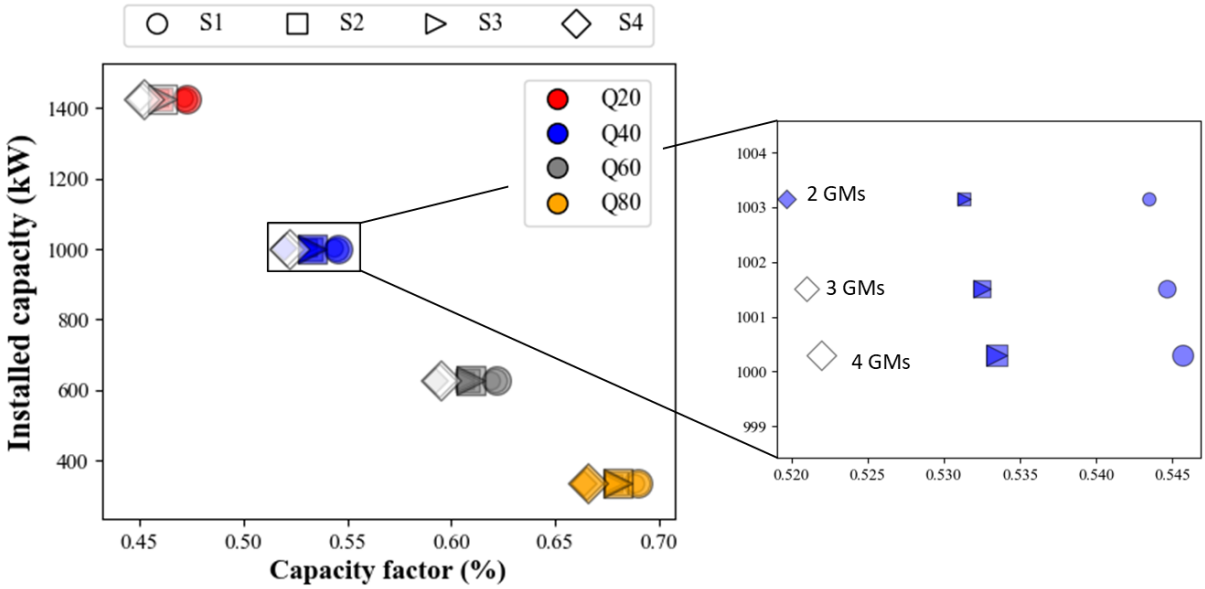

Figure 39. Comparison of mean annual capacity factor and installed capacity for four modeling scenarios. For symbol description, see Figure 38.

The plant generation exceedance probability for all scenarios differs based mainly on generation design flow, which is proportional to installed generation capacity (Figure 40). As generation design flow is increased, more power is available more of the time; but this becomes evident only below specific exceedance points. For example, generation modules sized for Q_{80} flow exceedance are generating at near full capacity roughly 85% of the time, as indicated by the departure of the yellow line from the general trend of all lines when the exceedance probability = 85%. That departure occurs at 70% for generation modules sized based on a Q_{60} flow exceedance, meaning those generation modules are operating at or near full capacity only 70% of the time. The 95% power exceedance, a common value for estimating firm capacity, varies only from 160 to 230 kW across all modeling scenarios, despite the plant installed capacity range from 330 to 1425 kW. This difference appears to be independent of modular arrangement, meaning the addition of flow through aquatic species, recreation, and sediment passage modules does not impact firm capacity nearly as much as the difference in generation module capacity as determined by the flow exceedance.

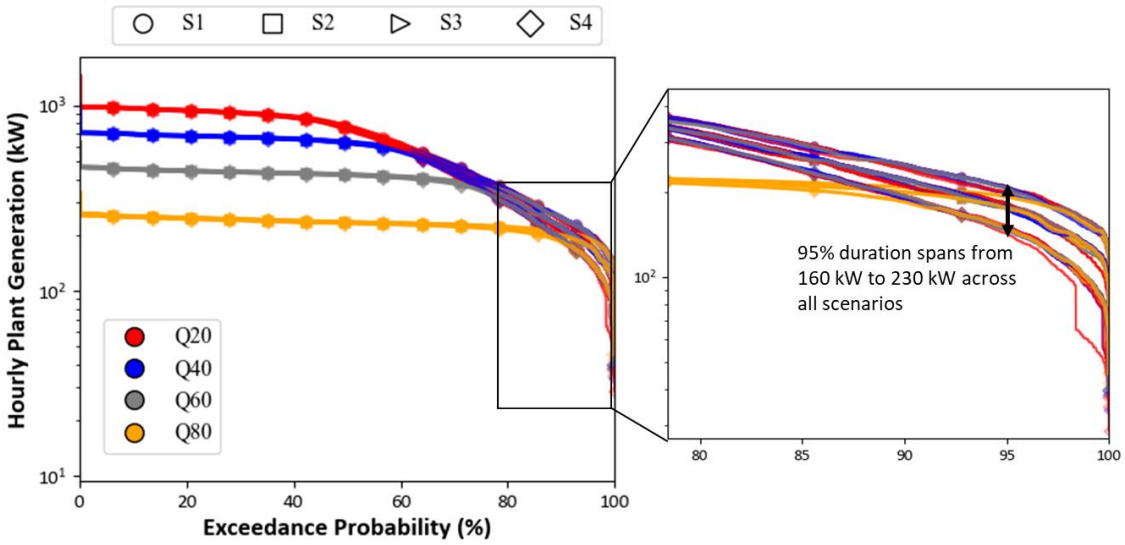

Figure 40. Plant generation exceedance curve for four modeling scenarios. For symbol description, see Figure 38.

3.5 ICC AND LCOE ANALYSIS

To set project ICC targets across modeling scenarios, the method and assumptions outlined in Section 2.5 are used to generate maximum ICCs based on a desired LCOE target that ranges from $0.04/kWh to $0.30/kWh (Figure 41). A project must have an ICC of the plotted value or less to achieve the given LCOE target given. A linear increase in maximum ICC is observed as the LCOE target increases, with the slope of the relationship increasing as project flow is decreased. For a given LCOE target, smaller-capacity projects tend to have higher allowable maximum ICCs—they generate less in terms of annual MWh but tend to have higher capacity factors, producing more kilowatt-hours across which project costs can be spread.

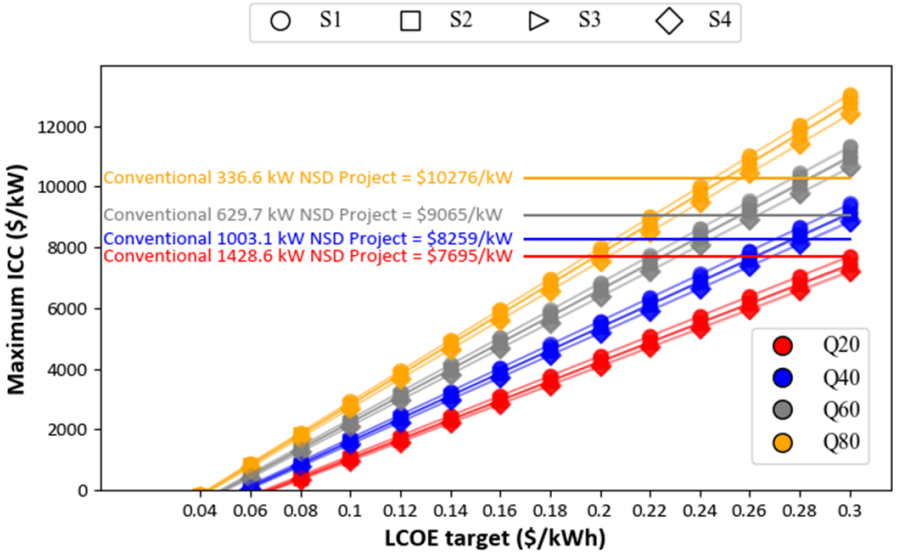

Figure 41. Maximum initial capital costs as a function of LCOE. For symbol description see Figure 38. Conventional project costs are estimated using the equation $9076016 \times P^{0.8} H^{-0.04}$, where P is installed capacity in megawatts and H is head in feet (O'Connor et al. 2015) for new low-head hydropower projects.

Some intuition can be gained by analyzing the line where conventional low-head project costs intersect with modeled project cost targets. This point indicates the LCOE at which conventional projects would need to deploy today and provides a cost baseline against which SMH plants must show some reduction to achieve deployment. In general, smaller-capacity projects can support higher ICCs at a lower relative LCOE than higher-capacity projects. For example, an LCOE of roughly $0.25/kWh could support SMH plants with generation modules sized using the Q_{80} flow exceedance across all modeled scenarios. However, scenarios with generation modules sized using a Q_{20} flow exceedance would require capital cost reductions of roughly $2,000/kW, from $7,695/kW for conventional projects to roughly $4,600/kW. To achieve an LCOE of $0.08/kWh, SMH projects in this case study would need to deploy at $2,000/kW for smaller-capacity projects and $500/kW for larger-capacity projects, representing cost reductions of 80% and 95%, respectively, compared with conventional projects.

To understand specifically where cost estimates benchmark against conventional values, we estimated a hypothetical cost distribution across module categories based on the known cost distribution for conventional projects with less than 67 ft of head (O'Connor et al. 2015) (Figure 42).

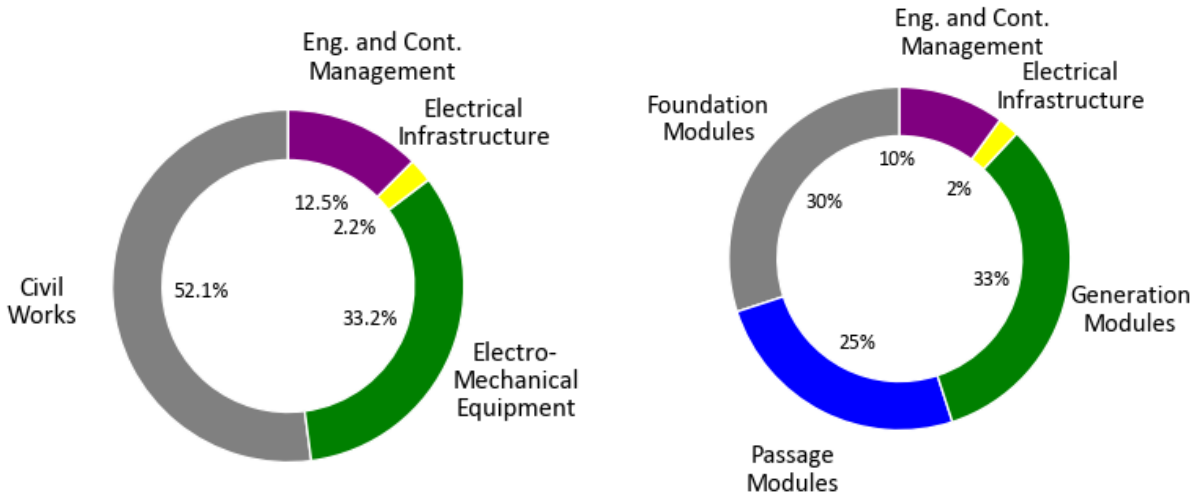

Figure 42. Estimated cost distribution between conventional low-head new stream-reach development projects (left) and standard modular hydropower projects (right).

We applied this cost distribution across scenario 4 (all passage modules) with three generation modules for a range of design flows, from the Q_{20} flow exceedance to the Q_{80} flow exceedance. We used a target LCOE of $0.14/kWh and estimated maximum project initial capital costs of between $2,209/kW and $4,626/kW. This economic scenario is meant to strike a balance between the $7,000/kW target for low-head NSD projects, as modeled in the *Hydropower Vision Report* (DOE 2016), and the unsubsidized LCOE of $0.04/kWh – $0.05/kWh of new renewable generation resources estimated to enter into service over the next 3 years (EIA 2018). In all cases, maximum cost targets per module category change with installed capacity (Figure 43). For the largest project, 1426 kW (Figure 43, top left), when the maximum ICC of $3,150,000 ($2,209/kW) is distributed across major module categories, an estimated $935,000 ($945/kW) is available for foundation modules; $552,000 ($787/kW) for sediment, recreation, and aquatic species passage modules; and $729,000 ($1,040/kW) for three generation modules. For the smallest project, 336 kW (Figure 43, bottom right), when the maximum ICC of $1,500,000 ($4,626/kW) is distributed across major module categories, an estimated $466,000 ($1,387/kW) is available for foundation modules; $388,000 ($1,156/kW) for sediment, recreation, and aquatic species passage modules; and $512,000 ($1,526/kW) for three generation modules.

Figure 43. Estimated cost distribution across scenario 4 models with three generation modules sized to varying flow exceedance values: Q_{20} (top left), Q_{40} (top right), Q_{60} (bottom left), Q_{80} (bottom right).

To provide one example of how these specific project cost distributions compare with conventional technologies, maximum individual generation module costs are compared with actual electromechanical (turbine, generator, and regulator) costs for small, low-head Kaplan turbines established by Ogayar and Vidal (2009) (Figure 44). Actual costs (blue line) decrease as design flow and installed capacity increase, while the modeled allowable maximum cost increases as design flow increases (black line). The point of intersection between the blue and black lines represents the point at which modeled generation module costs are equivalent to actual costs of electromechanical equipment at the same head and capacity. This point is dependent on the LCOE target. For example, a project with an LCOE target of $0.18/kWh intersects with the blue line at S4 Q_{60}. This indicates that under scenario 4, with a plant sized to the Q_{60} flow exceedance, the modeled cost of three generation modules is roughly equivalent to the actual

electromechanical costs of three similarly sized turbines. Conversely, the maximum generation module costs for projects with an LCOE target of $0.10/kWh are below the actual costs regardless of generation capacity; and SMH projects that seek to deploy at $0.10/kWh require electromechanical cost reductions compared with conventional technology.

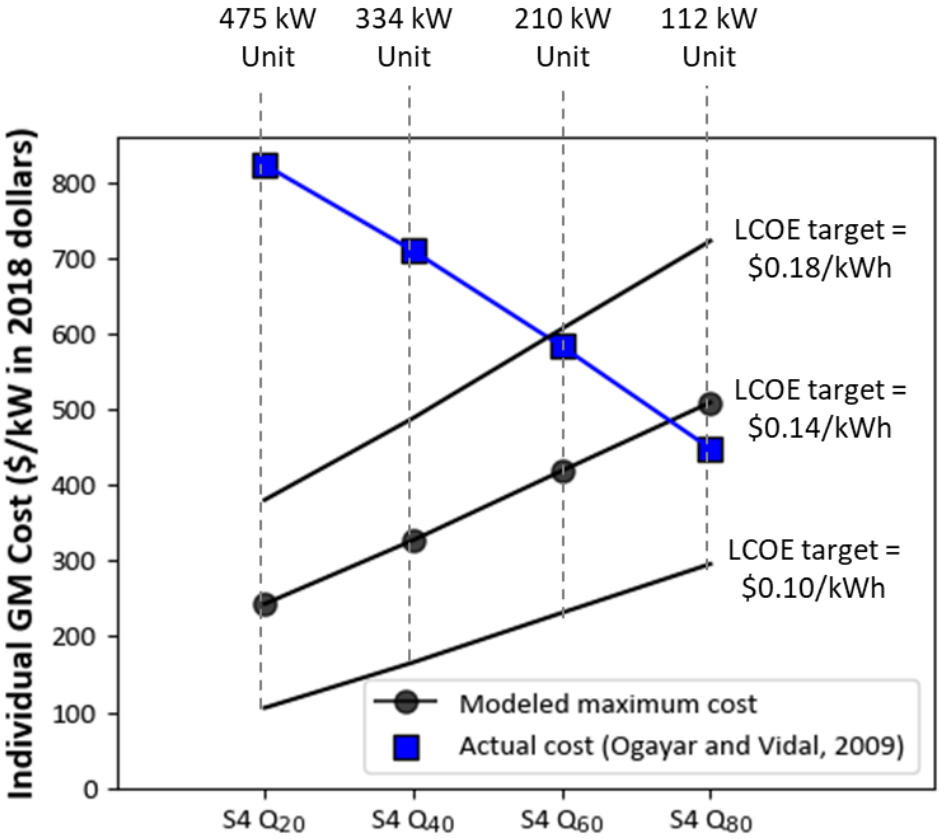

Figure 44. Estimated individual generation modules costs across scenario 4 models with three generation modules sized to varying flow exceedance values, compared with estimated costs of electromechanical equipment developed by Ogayar and Vidal (2009). The capacity of an individual generating unit is included above the dashed lines.

Generation modules are envisioned as encompassing intakes, draft tubes, and structural support cost elements that are in addition to the turbine, generator, and regulator included in the actual costs shown in Figure 44. It is clear that electromechanical cost reductions are necessary to achieve SMH generation module cost targets.

4. CONCLUSIONS

This report outlines a new environmental design framework for standard modular hydropower development that combines module design, systems design, performance modeling, and economic assessment. Based on a limited set of site inputs, the water allocation tool enabling rapid small hydropower environmental design (waterSHED) cycles through several modular design options and simulates a historical record of hydropower and aquatic species, recreation, and sediment passage performance. Importantly, this work establishes the following:

- A common SMH system modeling methodology and transparent development framework.
- A modeling capability that takes a series of technical and environmental site inputs, develops a feasible preliminary engineering design for individual modules, integrates them into a whole facility layout, assesses a range of design and operational decisions, and simulates rule-based performance.
- A baseline approach to assess SMH development using current technology, to be improved upon in future iterations and through technology design innovation.

The waterSHED model was demonstrated as a case study on a potential low-head hydropower site. Several scenarios were developed to assess different module configurations and generation design flows. Major findings include the following:

- Using a limited set of site inputs, aquatic species, recreation, and sediment passage modules, along with generation modules, can be designed with feasible dimensions, design flows, and operational rules.
- The addition of passage modules reduces annual energy generation by a maximum of 5% for facilities with generation modules sized based on the Q_{20} flow exceedance, and negligibly for facilities with generation modules sized based on the Q_{80} flow exceedance.
- The addition of passage modules has a significant impact on facility footprint—in nearly all cases, the facility footprint is tripled from the base case with only generation modules and water passage modules, to the most inclusive case with generation modules and all passage modules.
- Variation in generation design flow has the largest impact on annual energy generation across scenarios.
- Projects with lower installed capacities (i.e., lower design flows) have higher capacity factors and can support higher installed capital costs. However, they produce less energy and have lower revenue potential.
- Compared with conventional technologies and facility development, significant cost reductions across all modules are needed to achieve LCOE targets of less than $0.14/kWh.

Application of the waterSHED model as a case study highlighted several opportunities for future SMH research. Specifically:

- Module functionalities should be combined to decrease module footprint and lower overall facility costs. Promising combinations include modules that serve to pass recreational craft and aquatic species, and modules that can pass water and bedload sediment.
- Additional module design specifications should be added to see how innovative designs compare with reference designs in both physical footprint and flow allocations.
- The lengths of water passage modules required to pass flood flows will vary substantially by site, and additional sites should be examined to determine optimal cost-effective arrangements.
- Detailed cost estimates of modules should be developed to enable a true initial capital cost analysis of various module arrangements.
- The model should be applied across different regions to assess variation in results.

5. REFERENCES

Acreman, Mike, Angela H. Arthington, Matthew J. Colloff, Carol Couch, Neville D. Crossman, Fiona Dyer, Ian Overton, Carmel A. Pollino, Michael J. Stewardson, and William Young. 2014. "Environmental flows for natural, hybrid, and novel riverine ecosystems in a changing world." *Frontiers in Ecology and the Environment* 12(8), 466–73. https://doi.org/10.1890/130134.

Bishop, Norm Jr., Deborah Linke, Carl Vansant, Chuck Alsberg, Jay Anders, Ali Grovue, Sarah Hill-Nelson, et al. 2015. *New Pathways for Hydropower: Getting Hydropower Built—What Does It Take?* ORNL/TM-2015/48, Oak Ridge National Laboratory.

Bosch, N. 2008. The influence of impoundments on riverine nutrient transport: An evaluation using the Soil and Water Assessment Tool. *Journal of Hydrology* 355(1–4), 131–147.

Brownlie, W. R. 1983. "Flow depth in sand-bed channels." *J. Hydraul. Div. ASCE* 109(7), 959–990.

Brownell, P, A. Haro, S. McDermott, A. Blott, and F. Rohde. 2012. "Diadromous Fish Passage: A Primer on Technology, Planning, and Design for the Atlantic and Gulf Coasts." National Oceanic and Atmospheric Administration, National Marine Fisheries Service.

Brune, Gunnar M. 1953. "Trap efficiency of reservoirs." *Eos, Transactions American Geophysical Union* 34(3), 407–418. https://doi.org/10.1029/TR034i003p00407.

Caisley, Marjorie E., Fabian A. Bombardelli, and Marcelo H. Garcia. 1999. *Hydraulic Model Study of a Canoe Chute for Low-Head Dams in Illinoi*s. Hydraulic Engineering Study 63, UILU-ENG-9-2012. Illinois Department of Water Resources.

Chang, H. H. 1998. *Fluvial Processes in River Engineering.* Krieger Publishing Company

Choi, S. U., and S. Kwak. 2000. "Probabilistic analysis of incipient motion of sediment particles." *Proceedings of the 8th International Symposium on Stochastic Hydraulics*, Beijing, China, July 25–28, 2000, pp. 317–324.

Commonwealth of Massachusetts. 2018. "Deerfield River Watershed." Available at https://www.mass.gov/service-details/deerfield-river-watershed.

Csiki, Shane, and Bruce L. Rhoads. 2010. "Hydraulic and geomorphological effects of run-of-river dams." *Progress in Physical Geography* 34 (6), 755–80.

Diplas, P., Kuhnle, R., Gray, J., Glysson, D., Edwards, T. 2008. Sediment transport measurements. *Sedimentation Engineering: Theories, Measurements, Modeling, and Practice. ASCE Manuals and Reports on Engineering Practice*, *110*, 165-252.

DOE (Department of Energy). 2016. *Hydropower Vision: A New Chapter for America's First Renewable Energy Source*, Water Power Technologies Office.

EIA (Energy Information Administration). 2018. "Levelized Cost and Levelized Avoided Cost of New Generation Resources in the Annual Energy Outlook 2018." Available at https://www.eia.gov/outlooks/aeo/pdf/electricity_generation.pdf.

Einstein, H. A., and N. Barbarossa. 1952. “River channel roughness,” *Transactions ASCE* 117, 1121–1146.

Elhakeem, Mohamed, A. N. Thanos Papanicolaou, and Achilleas G. Tsakiris. 2017. “A probabilistic model for sediment entrainment: The role of bed irregularity.” *International Journal of Sediment Research* 32(2), 137–48.

ESHA (European Small Hydropower Association). 2004. *Guide on How to Develop a Small Hydropower Plant*. Thematic Network on Small Hydropower. http://citeseerx.ist.psu.edu/viewdoc/download?doi=10.1.1.172.1731&rep=rep1&type=pdf.

Executive Office of Environmental Affairs. 2004. *Deerfield River Watershed 5-Year Watershed Action Plan 2004–2008*. Commonwealth of Massachusetts Executive Office of Environmental Affairs. Boston, MA. https://www.mass.gov/files/documents/2016/08/rw/wap-deerfield-2004.pdf.

FERC (Federal Energy Regulatory Commission). 2012. *Environmental Assessment for Hydropower License: Gartina Falls Hydropower Project*. FERC Online eLibrary. https://elibrary.ferc.gov/idmws/file_list.asp?document_id=14072983

FERC (Federal Energy Regulatory Commission). 2014. *Environmental Assessment for Original Hydropower License: Calligan Creek Hydroelectric Project*. FERC Online eLibrary. https://elibrary.ferc.gov/idmws/file_list.asp?document_id=14279488

FERC (Federal Energy Regulatory Commission). 2014. *Draft Environmental Assessment for Original Hydropower License: Hancock Creek Hydroelectric Project*. FERC Online eLibrary. https://elibrary.ferc.gov/idmws/file_list.asp?document_id=14279495

Garegnani, Giulia, Sandro Sacchelli, Jessica Balest, and Pietro Zambelli. 2018. “GIS-based approach for assessing the energy potential and the financial feasibility of run-off-river hydro-power in Alpine valleys.” *Applied Energy* 216, 709–23.

Granato, G. E., K. G. Ries III, and P. A. Steeves. 2017. Compilation of Streamflow Statistics Calculated from Daily Mean Streamflow Data Collected during Water Years 1901–2015 for Selected U.S. Geological Survey Streamgages. US Geological Survey, Reston, VA.

Gulliver, J., Garver, R., Arndt, R., Bowers, C. 1980. Preliminary analysis of hydropower production feasibility at twenty-one existing dam sites in the state of Minnesota. Project Report No. 196, St. Anthony Falls Hydraulic Laboratory.

Jager, Henriëtte I., Rebecca A. Efroymson, Jeff J. Opperman, and Michael R. Kelly. 2015. “Spatial design principles for sustainable hydropower development in river Basins.” *Renewable and Sustainable Energy Reviews* 45, 808–16.

Kao, Shih Chieh, Ryan McManamay, Kevin Stewart, Nicole Samu, Boualem Hadjerioua, Scott DeNeale, Dilruba Yeasmin, M. Fayzul Pasha, Abdoul Oubeidiilah, and Brennan Smith. 2014. *New Stream-Reach Development: A Comprehensive Assessment of Hydropower Energy Potential in the United States*. US Department of Energy, Wind and Water Power Technologies Office. http://nhaap.ornl.gov/sites/default/files/ORNL_NSD_FY14_Final_Report.pdf

Katopodis, Chris. 1992. *Introduction to Fishway Design*. Freshwater Institute, Central and Arctic Region, Department of Fisheries and Oceans.

Kelly-Richards, Sarah, Noah Silber-Coats, Arica Crootof, David Tecklin, and Carl Bauer. 2017. "Governing the transition to renewable energy: a review of impacts and policy issues in the small hydropower boom." *Energy Policy* 101, 251–64.

Kemp, Paul S. 2012. "Bridging the gap between fish behaviour, performance and hydrodynamics: An ecohydraulics approach to fish passage research." *River Research and Applications* 28(4), 403–406.

Kössler. 2018. "Kaplan Turbines." Available at http://www.koessler.com/en/kaplan-turbines.

Leopold, L. B., M. G. Wolman, and J. P. Miller. 1964. *Fluvial Processes in Geomorphology*, W. H. Freeman and Co., San Francisco, CA.

McManamay, Ryan A., Nicole Samu, Shih-Chieh Kao, Mark S. Bevelhimer, and Shelaine C. Hetrick. 2015. "A multi-scale spatial approach to address environmental effects of small hydropower development." *Environmental Management* 55(1), 217–43. https://doi.org/10.1007/s00267-014-0371-2.

Mitchell, Peter. 2009. *Deerfield River Watershed 2005 Benthic Macroinvertebrate Assessment*. TM-33-7, Commonwealth of Massachusetts, Executive Office of Energy and Environmental Affairs. http://www.mass.gov/eea/docs/dep/water/resources/wqreports/cn-223-3tm-2005-deerfieldbiomonitoring.pdf.

Morris, Gregory L., and Jiahua Fan. 1998. *Reservoir Sedimentation Handbook: Design and Management of Dams, Reservoirs, and Watersheds for Sustainable Use*. McGraw Hill Professional.

Mosier, Thomas M., Kendra V. Sharp, and David F. Hill. 2016. "The Hydropower Potential Assessment Tool (HPAT): Evaluation of run-of-river resource potential for any global land area and application to Falls Creek, Oregon, USA." *Renewable Energy* 97, 492–503. https://doi.org/10.1016/j.renene.2016.06.002.

NYSDEC (New York State Department of Environmental Conservation). 1989. *Guidelines for Design of Dams*. Division of Water, Albany, New York.

O'Connor, Patrick, Katherine Zhang, Scott T. Deneale, Dol Raj Chalise, and Emma Centurion. 2015. *Hydropower Baseline Cost Modeling*. ORNL/TM-2015/14, Oak Ridge National Laboratory.

Ogayar, B., and P. G. Vidal. 2009. "Cost determination of the electro-mechanical equipment of a small hydro-power plant." *Renewable Energy* 34(1), 6–13.

Papanicolaou, A. N., P. Diplas, N. Evaggelopoulos, and S. Fotopoulos (2002), "A stochastic incipient motion criterion for spheres under various packing conditions," *Journal of Hydraulic Engineering*, 128(4), 369–380.

Papanicolaou, A. N. and B. Abban (2016), "Channel Erosion and Sediment Transport. " Chapter 65 in *Handbook of Applied Hydrology*, 2nd Edition. Ed. V.P. Singh. McGraw Hill. ISBN:9780071835107.

Pasha, M. Fayzul K., Dilruba Yeasmin, Shih-Chieh Kao, Boualem Hadjerioua, Yaxing Wei, and Brennan T. Smith. 2014. "Stream-reach identification for new run-of-river hydropower development through a merit matrix–based geospatial algorithm." *Journal of Water Resources Planning and Management* 140(8), 04014016. https://doi.org/10.1061/(ASCE)WR.1943-5452.0000429.

Pearson, A. J. and J. Pizzuto. 2015. “Bedload transport over run-of-river dams, Delaware, U.S.A.” *Geomorphology*, 248, 382–395.

Poff, N. LeRoy, Casey M. Brown, Theodore E. Grantham, John H. Matthews, Margaret A. Palmer, Caitlin M. Spence, Robert L. Wilby, et al. 2015. “Sustainable water management under future uncertainty with eco-engineering decision scaling.” *Nature Climate Change* 6, 25–34. https://doi.org/10.1038/nclimate2765.

Poff, N Leroy, J. David Allan, Mark B. Bain, James R. Karr, Karen L. Prestegaard, Brian D. Richter, Richard E. Sparks, and Julie C. Stromberg. 1997. “The natural flow regime: A paradigm for river conservation and restoration.” *BioScience* 4 (11), 769–84. https://doi.org/10.2307/1313099.

Pugh, Clifford. 1979. *Standardized Intakes and Outlets for Low-Head Hydropower Developments*. DOE 79-01/PAP-453. US Bureau of Reclamation.

Punys, Petras, Antanas Dumbrauskas, Algis Kvaraciejus, and Gitana Vyciene. 2011. “Tools for small hydropower plant resource planning and development: A review of technology and applications.” *Energies* 4(9), 1258–77. https://doi.org/10.3390/en4091258.

Rajaratnam, Nallamuthu, Gary Van der Vinne, and Christos Katopodis. 1986. “Hydraulics of vertical slot fishways.” *Journal of Hydraulic Engineering* 112 (10): 909–27.

Rickenmann, D., and A. Recking. 2011. “Evaluation of flow resistance in gravel-bed rivers through a large field data set.” *Water Resour. Res.* 47, W07538. doi:10.1029/2010WR009793.

Rojanamon, Pannathat, Taweep Chaisomphob, and Thawilwadee Bureekul. 2009. “Application of geographical information system to site selection of small run-of-river hydropower project by considering engineering/economic/environmental criteria and social impact.” *Renewable and Sustainable Energy Reviews* 13(9), 2336–2348. https://doi.org/10.1016/j.rser.2009.07.003.

Schramm, Michael P., Mark S. Bevelhimer, and Chris R. DeRolph. 2016. “A synthesis of environmental and recreational mitigation requirements at hydropower projects in the United States.” *Environmental Science and Policy* 61, 87–96. https://doi.org/10.1016/j.envsci.2016.03.019.

Smith, Brennan T., Adam Witt, Kevin Stewart, Kyutae Lee, Scott T Deneale, and Mark S. Bevelhimer. 2016. *A Multi-Year Plan for Research, Development, and Prototype Testing of Standard Modular Hydropower Technology*, ORNL/TM-2016/102, Oak Ridge National Laboratory.

Soulis, Konstantinos X., Dimitris Manolakos, John Anagnostopoulos, and Dimitris Papantonis. 2016. “Development of a geo-information system embedding a spatially distributed hydrological model for the preliminary assessment of the hydropower potential of historical hydro sites in poorly gauged areas.” *Renewable Energy* 92, 222–232. https://doi.org/10.1016/j.renene.2016.02.013.

Towler, Brett, Kevin Mulligan, and A Haro. 2015. “Derivation and application of the energy dissipation factor in the design of fishways.” *Ecological Engineering* 83, 208–217.

Tracy, H. J. 1967. “Discharge characteristics of broad-crested weirs,” Geological Survey Circular 397, US Geological Survey, Washington, D.C.

Turek, James, Alexander J. Haro, and Brett Towler. 2016. *Federal Interagency Nature-like Fishway Passage Design Guidelines for Atlantic Coast Diadromous Fishes*. NOAA National Marine

Fisheries Service, Narragansett, RI.

Uría-Martínez, R., P. O'Connor, and M. Johnson. 2018. *2017 Hydropower Market Report*, DOE/EE-1737. US Department of Energy, Water Power Technologies Office, Washington DC.

U.S. Army Corps of Engineers. 1967. *Streamflow Synthesis for Ungaged Rivers*. U.S. Army Corps of Engineers, Institute for Water Resources, Davis, CA, 30.

U.S. Army Corps of Engineers. 1992. *Engineering Design: Hydrologic Engineering for Hydropower.* ER-1110-2-1463. U.S. Army Corps of Engineers, Washington, D.C.

USBR (US Bureau of Reclamation). 2001. *Water Measurement Manual*. US Bureau of Reclamation, Washington DC, 317.

US Fish and Wildlife Service. 2018. "Species Conservation." Connecticut River Fish and Wildlife Conservation Office website. https://www.fws.gov/r5crc/species.html.

Wahlin, B. T., and J. A. Replogle. 1994. *Flow Measurement Using an Overshot Gate*. UMA Engineering for the Bureau of Reclamation, US Department of Interior.

Walburg, Charles H., and Paul R. Nichols. 1967. "Biology and Management of the American Shad and Status of the Fisheries, Atlantic Coast of the United States, 1960." Aquatic Commons. Available at http://aquaticcommons.org/7934/.

Wetzel, M. A., D. S. Wahrendorf, and P. C. von der Ohe (2012), "Sediment pollution in the Elbe estuary and its potential toxicity at different trophic levels." *Science of the Total Environment* 449(C), 199–207.

Wild, Thomas B., Daniel P. Loucks, George W. Annandale, and Prakash Kaini. 2016. "Maintaining sediment flows through hydropower dams in the Mekong River Basin." *Journal of Water Resources Planning and Management* 142(1), 05015004. https://doi.org/10.1061/(ASCE)WR.1943-5452.0000560.

Witt, Adam, Brennan T. Smith, Achilleas Tsakiris, Thanos Papanicolaou, Kyutae Lee, Kevin M. Stewart, Scott T Deneale, et al. 2016. *Exemplary Design Envelope Specification for Standard Modular Hydropower Technology*, ORNL/TM-2016/298/R1. https://hydropower.ornl.gov/smh/docs/ORNL-SMH-Exemplary-Design-Envelope-Specification.pdf.

Zhang, Q. F., R. Uria-Martinez, and B. Saulsbury. 2013. Technical and Economic Feasibility Assessment of Small Hydropower Development in the Deschutes River Basin, ORNL/TM-2013/221, Oak Ridge National Laboratory.

APPENDIX A. REFERENCE AQUATIC SPECIES PASSAGE MODULE DESIGN

The reference aquatic species passage module is developed as a vertical slot fishway following empirical and expert design guidance available in the literature (Katopodis 1992; Rajaratnam et al., 1986; Brownell et al. 2012). In a vertical slot fishway, a rectangular channel with a sloping floor is partitioned into a number of pools. Water flows through vertical slots on one side of the channel from one pool into the next. Water flowing through the slot forms a jet, the energy of which is dissipated by the next downstream pool.

Geometrically similar scaled hydraulic models have been used to establish dimensionless discharge rating curves and characteristic velocity profiles of vertical slot fishways for a range of flow depths and passage slopes. These fishways are commonly employed throughout the United States to pass migratory and resident fish species. Vertical slot fishway design no. 18 is commonly recommended and was used as a basis for the aquatic species passage module (Katopodis 1992; Figure A-1). The limiting variables informing vertical slot fish passage design are species-specific morphometry and swimming performance. The maximum burst swim speed, or the maximum velocity that can be sustained for less than 20 seconds by a species of interest, is used to set the maximum drop height between structures as

$$h_{drop} = \frac{{u_m}^2}{2g}, \tag{A-1}$$

where u_m = maximum velocity in each slot = maximum burst swim speed of the target species, g = acceleration due to gravity. Additional input design variables are described in Table A-1.

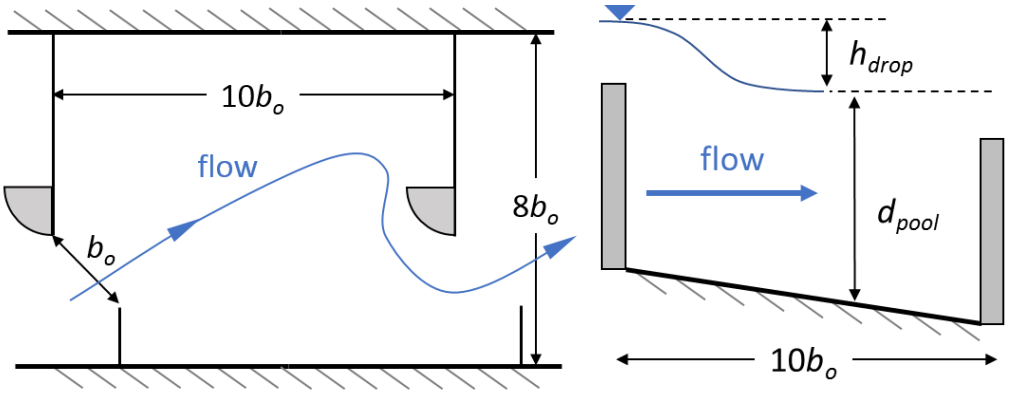

Figure A-1. Top view (left) and side view (right) of single vertical slot pool (not to scale).

Table A-1. Aquatic species passage module input design variables.

Variable	Value	Units	Description
u_m	variable	ft/s	Maximum burst speed of target species/maximum velocity through slot
b_o	variable	ft	Fixed width of the slot opening
APM_{Qstart}			Start month for sizing aquatic species passage design flows
APM_{Qend}			End month for sizing aquatic species passage design flows

A.1 AQUATIC SPECIES PASSAGE DESIGN FLOWS

We first distinguish between passage design flows and module design flows. The former is the range of river discharge expected during a user-specified time period and used to set lower and upper flow limits on when an aquatic species passage module should be operational. The latter is the actual design flows to be passed through the module, which are discussed in Section A.2. According to Brownell et al. (2012), a low aquatic species passage flow is exceeded 95% of the time during the spawning migration period for target species normally present in the river basin and at the passage site, while a high passage flow is exceeded 5% of the time during the same period.

As a basis for setting aquatic species passage design flow limits, a flow duration curve is constructed using only mean daily discharge that occurs during spawning or migration months. For example, a mean annual hydrograph is shown in Figure A-2 highlighting starting and ending months of migration for an arbitrary species. Using only mean daily flows during these months over the length of the entire time series, a flow duration curve is generated and compared with the flow duration curve using flows from all months (Figure A-3). A minimum aquatic species passage design flow is selected as Q_{95} on the aquatic species passage flow duration curve (95% mean daily flow exceedance), while the maximum aquatic species passage design flow is selected as Q_5 on the aquatic species passage flow duration curve (5% mean daily flow exceedance).

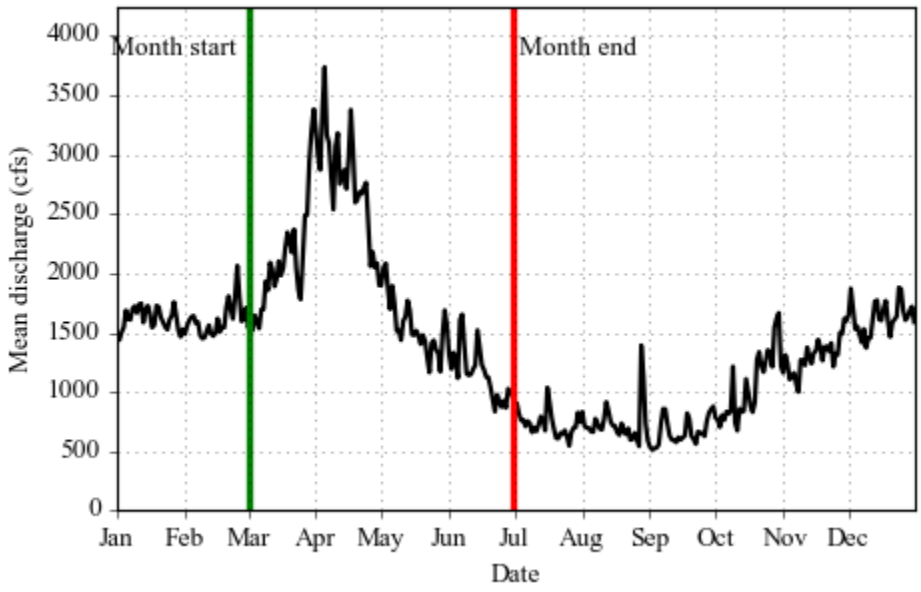

Figure A-2. Mean daily discharge for a hypothetical location, with the start and end months of critical aquatic species migration or movement identified.

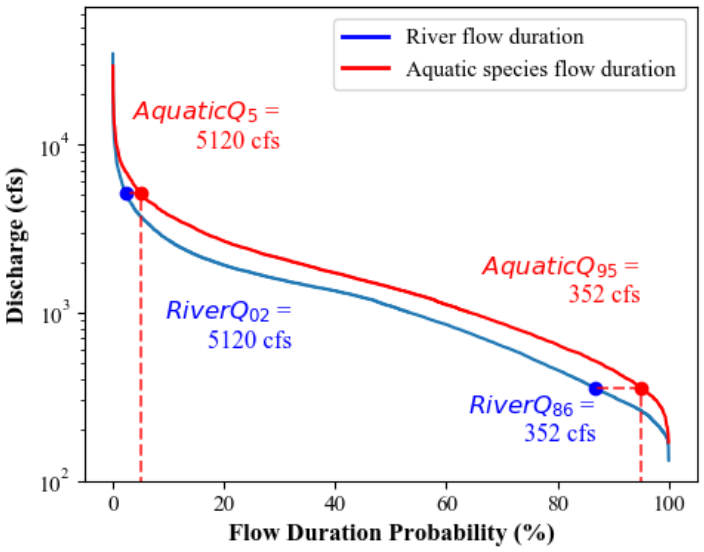

Figure A-3. Flow duration curve for all river flows and for flows that occur during a hypothetical aquatic species passage season of March through July. The high flows that occur during this season are responsible for an aquatic species passage flow duration curve that is higher than the river discharge flow duration curve.

Within the model, an aquatic species passage module must be operational when $Q < AquaticQ_5$, where Q is the instantaneous discharge in the river.

A.2 AQUATIC SPECIES PASSAGE MODULE DESIGN CALCULATIONS

The total number of pools required to meet maximum velocity requirements is estimated by dividing the total head drop between upstream and downstream invert elevations, H_{drop}, by the maximum drop height per pool, h_{drop}. The downstream invert elevation is computed assuming a 0.5 ft submergence below the tailwater depth associated with a Q_{95} flow exceedance. The upstream invert elevation is computed assuming a 1.5 ft submergence below the normal operating water level. For example, assuming a downstream invert elevation of 150 ft, an upstream invert elevation of 160 ft, and a maximum drop per pool of 0.6 ft, the number of pools required is

$$H_{drop} = 160\ ft - 150\ ft = 10\ ft, N_{pools} = \frac{H_{drop}}{h_{drop}} = \frac{10\ ft}{0.6\ ft} = 17\ . \quad \text{(A-2)}$$

The main physical dimensions of each pool are determined based on the fixed width of the slot opening, b_o. In Atlantic Coast rivers, vertical slot fishways have been effective with a slot opening of between 10 and 18 in. for a variety of American shad, Atlantic salmon, and other riverine fish species (Brownell et al. 2012). The standard sizing criterion reported in Katopodis (1992) is used to establish the pool length and width as

$$L_{pool} = 10b_o, W_{pool} = 8b_o\ . \quad \text{(A-3)}$$

The overall length of the aquatic species passage module is taken as $N_{pools}L_{pool}$, and total slope S_o is estimated as $H_{drop}/(N_{pools}L_{pool})$.

Once a user specifies a slot opening, the minimum operating depth in each pool is computed using the relationship of Katopodis (1992) as

$$d_{pool} = 3.64 b_o \, . \tag{A-4}$$

The dimensionless flow varies linearly with relative depth of flow through each slot as

$$Q^* = 3.71 \frac{d_{pool}}{b_o} . \tag{A-5}$$

Using the dimensionless flow equation in Katopodis (1992), the aquatic species passage module design flow is established as

$$Q_{apm} = Q^* \left(g b_o {S_o}^5 \right)^{0.5} . \tag{A-6}$$

To ensure turbulence in pools is kept to a minimum, the energy dissipation function for aquatic species passage pools is constrained based on guidance from Towler, Mulligan, and Haro (2015). The First, the energy dissipation function is computed as

$$EDF = \frac{\gamma Q_{apm} h_{drop}}{L_{pool} W_{pool} d_{min}}, \tag{A-7}$$

where $\boldsymbol{\gamma}$ is the specific weight of water. If the EDF >4, it is considered too large for the design and the user is prompted to increase the pool volume by slightly increasing the opening width. The design procedure is repeated starting from Equation A-3 until a suitable EDF is achieved within the desired constraints of the user.

A.3 RESULTS AND DISCUSSION

By incorporating the preceding steps into a generalized computer model, the variable inputs from Table A-1 can be rapidly assessed for a variety of potential target species. Figure A-4 provides an example of model outputs for a structure height of 14 ft, maximum velocity of 6 ft/s, and slot opening width of 1.5 ft.

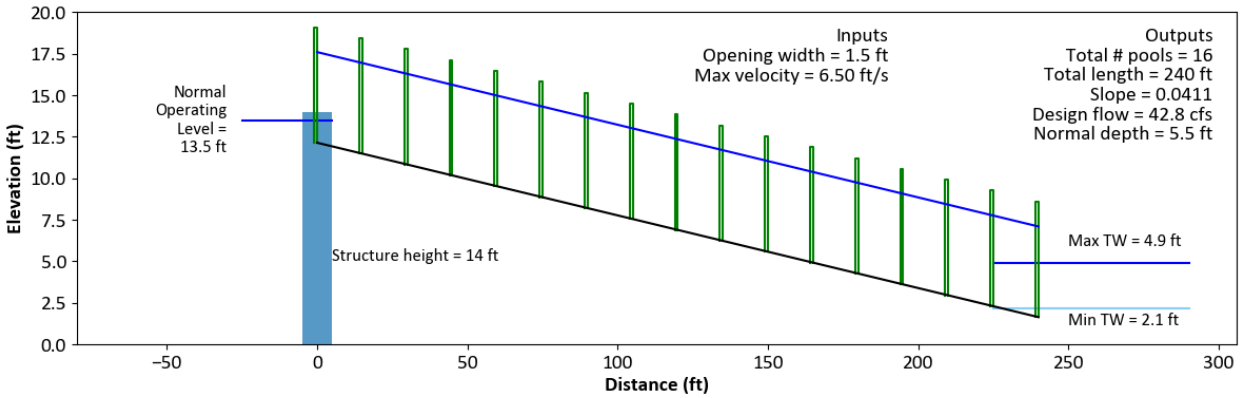

Figure A-4. Generalized reference aquatic species passage module design tool output.

An assessment of several common slot opening widths and maximum velocities shows potential trade-offs in overall module footprint, velocity, and design flow (Figure A-5). For the given structure height of 14 ft, a corresponding aquatic species passage module could vary in length from 130 ft to 355 ft

depending on the combination of desired maximum velocity and slot opening width. The design flow increases as slot opening width increases. This increase is accompanied by a lengthening of the aquatic species passage module, which must decrease in slope to maintain a given maximum velocity with an increase in flow. For a given slot opening width, the overall aquatic species passage module length can be shortened by increasing the design flow, and in turn increasing the maximum velocity. This shortening occurs more quickly at small relative design flows. For example, for b_o = 0.8 ft, an increase in design flow from 10 to 14 cfs decreases the module length from 190 to 110 ft (20 ft/cfs); while for b_o = 1.5 ft, an increase in design flow from 36 to 52 cfs decreases the module length from 360 to 150 ft (13 ft/cfs). Also, maintaining a constant maximum velocity while increasing the slot opening width will result in a more rapid lengthening of the aquatic species passage module at lower relative velocities. An increase in slot opening width from 1.1 to 1.5 ft will require 70 ft of additional length to maintain a maximum velocity of 5.25 ft/s, but only 20 ft of additional length to maintain a maximum velocity of 7.75 ft/s.

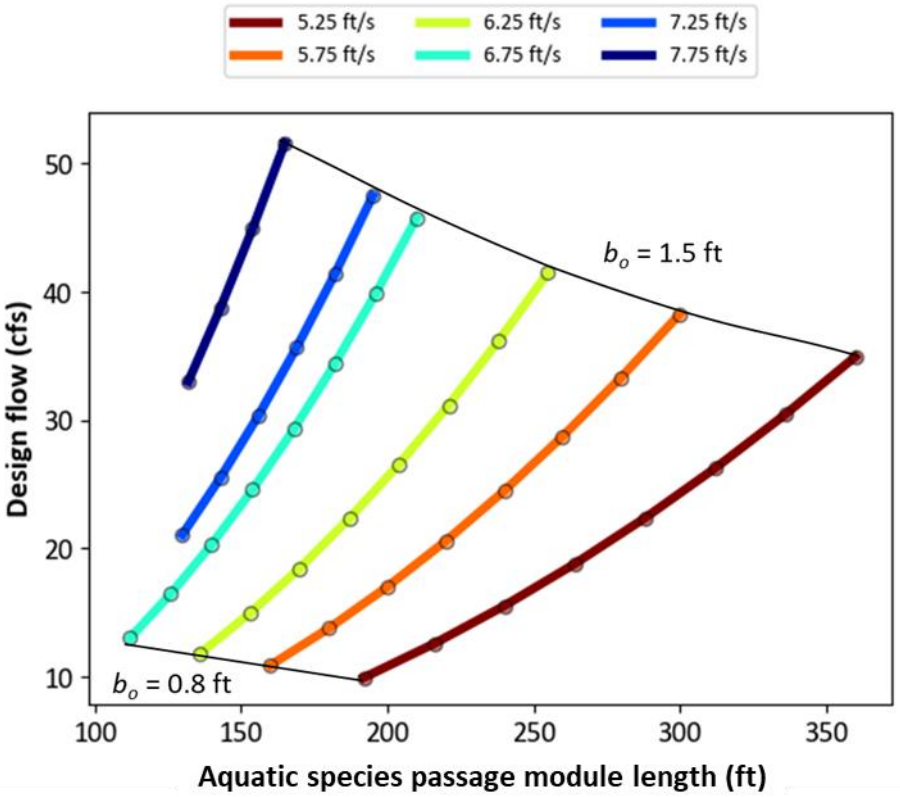

Figure A-5. Design flow of an aquatic species passage module as a function of aquatic species passage module length for a variety of desired maximum velocities (colored lines) and opening widths (scatter points), assuming a normal operating level of 13.5 ft and a 14 ft tall structure

These design trade-offs present clear implications for small hydro project development economics. A greater design flow allocated toward aquatic species passage increases the length of the passage module and in theory should increase the aquatic species passage efficiency up to a point. However, the total module length and overall footprint are significantly increased (for this given reference design).

A.4 REFERENCES

Brownell, P, A. Haro, S. McDermott, A. Blott, and F. Rohde. 2012. "Diadromous Fish Passage: A Primer on Technology, Planning, and Design for the Atlantic and Gulf Coasts." National Oceanic and

Atmospheric Administration, National Marine Fisheries Service.

Katopodis, Chris. 1992. *Introduction to Fishway Design*. Freshwater Institute, Central and Arctic Region, Department of Fisheries and Oceans.

Rajaratnam, Nallamuthu, Gary Van der Vinne, and Christos Katopodis. 1986. “Hydraulics of vertical slot fishways.” *Journal of Hydraulic Engineering* 112 (10): 909–27.

Towler, Brett, Kevin Mulligan, and A Haro. 2015. “Derivation and application of the energy dissipation factor in the design of fishways.” *Ecological Engineering* 83, 208–217.

APPENDIX B. REFERENCE RECREATION PASSAGE MODULE DESIGN

The recreation passage module is developed using design guidelines for canoe and kayak chutes at low-head dams (Caisley, Bombardelli, and Garcia 1999). The design guidelines, established through physical-scale hydraulic model studies and numerical models, offer empirical relationships for acceptable drop structure dimensions based on tailwater levels and minimum and maximum design flows. The guidelines ensure that favorable recreation hydraulics are maintained immediately downstream of each drop between minimum and maximum design flows. Drop dimensions are constrained to (1) ensure an undulating wave flow regime at the foot of the drop and (2) prevent the formation of a recirculating hydraulic jump that poses a safety risk to boaters.

To cost effectively establish a recreation passage module concept design, we develop an optimization procedure to maximize the height of each drop, which in turn minimizes the total length—and, in theory, the cost—of the boat chute for given input design flow conditions. The optimization procedure relies on a mix of variable user inputs and recommended model constants (Table B-1; Figures B-1 and B-2).

Table B-1. Recreation passage module input design variables.

Variable	Value	Units	Description
h_s	variable	ft	Upstream height of the drop structure
H_s	variable	ft	Head of the upstream pool above h_s
h_a	$h_s - 1.3$	ft	Downstream height of the drop structure
H_a	variable	ft	Smallest depth of water over downstream height h_a
h_d	>4	ft	Depth of the tailwater downstream of a drop
l_{drop}	8	ft	Length of the drop structure in the middle (2 ft horizontal, 4 ft sloped, 2 ft horizontal)
l_{pool}	>20	ft	Length of the recovery pool between drops
b_{drop}	10–40	ft	Width of the narrow part of the drop structure
b_{pool}	20–80	ft	Width of the pools
$Q_{rec,min}$	variable	ft^3/s	Minimum viable design flow
$Q_{rec,max}$	variable	ft^3/s	Maximum viable design flow

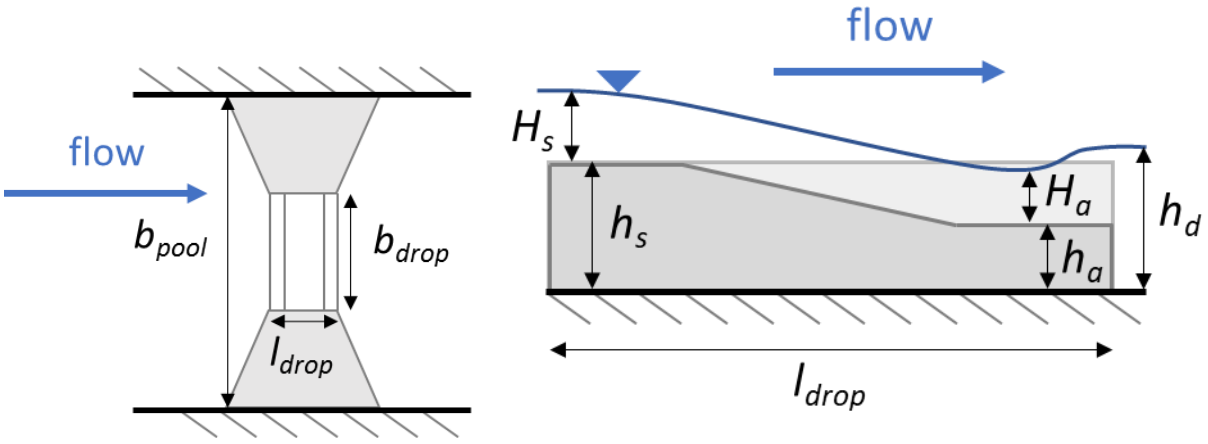

Figure B-1. Top view (left) and side view (right) of single drop structure (not to scale).

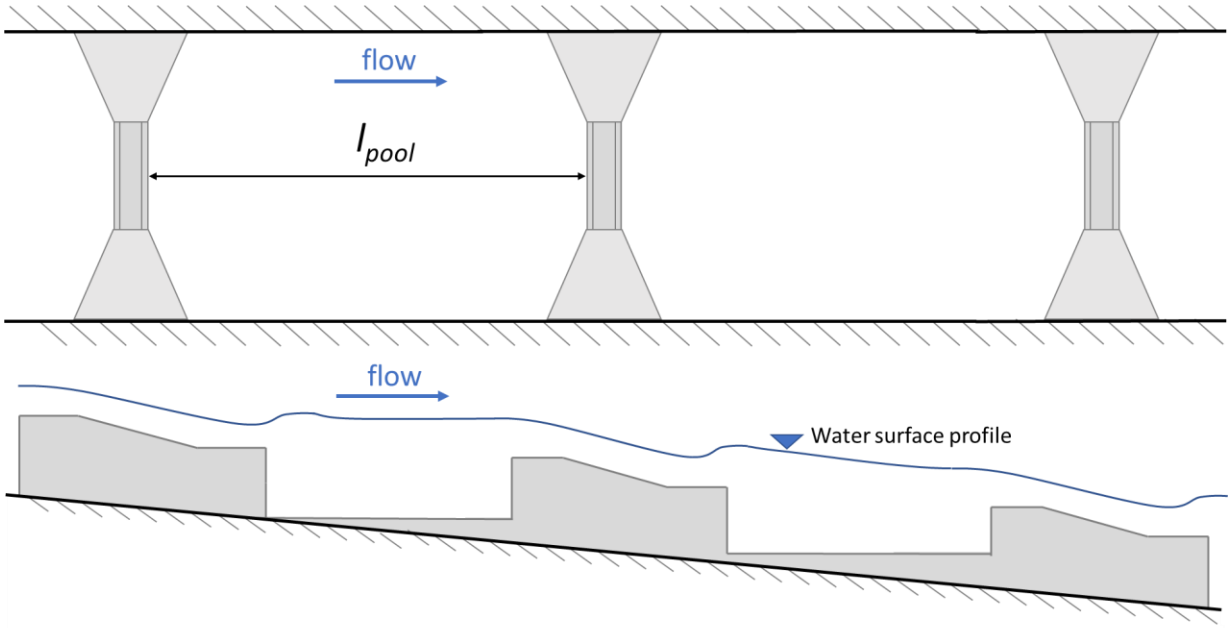

Figure B-2. Top view (top) and side view (bottom) of multiple drop structures in series (not to scale).

B.1 MAJOR ASSUMPTIONS

The recreation passage module design relies on several assumptions:

- The module is operated seasonally during user-specified recreation months.
- The minimum pool width must allow a canoe to fully rotate (~15 ft).
- Open canoes can handle a maximum drop of 1.3 ft per structure.
- Boaters need at least 4 ft of water depth (h_d) to recover in any pool if they capsize.

B.2 DESIGN FLOW

We first distinguish between recreation design flow and recreation module design flow. The former is the range of river discharge over which recreational craft are assumed to be using the module, and the latter is the actual flow to be passed through the module.

As a basis for setting recreation design flow limits, a flow duration curve is constructed using only mean daily discharge that occurs during desired recreation months (Figures B-3 and B-4). A minimum recreation design flow is selected as Q_{95} on the recreation flow duration curve (95% mean daily flow exceedance), and a maximum recreation design flow is selected as Q_{50} on the recreation flow duration curve (50% mean daily flow exceedance) as an upper limit on when recreation would likely be occuring—i.e., not in flood flows. The intent is to ensure the module is operational when boaters are present and to optimize the design to ensure flows are efficiently allocated to all modules.

Figure B-3. Mean daily discharge for a hypothetical location, with the start and end months of recreation identified.

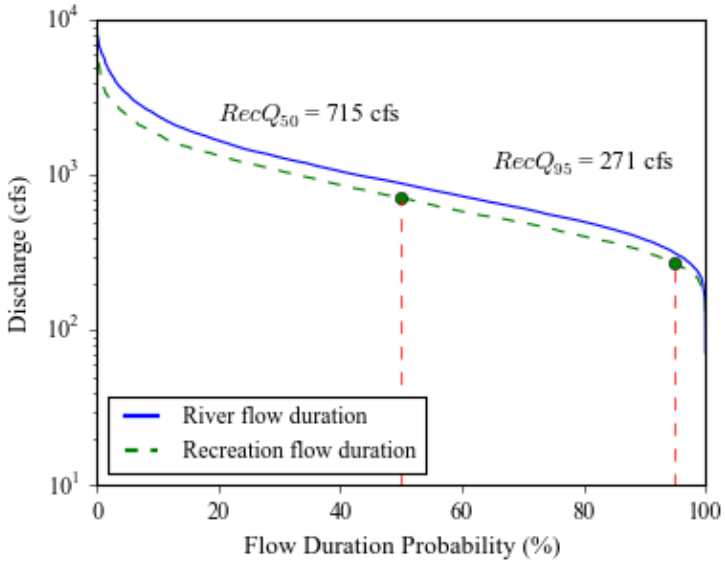

Figure B-4. Flow duration curve for all river flows and for flows that occur during a hypothetical recreation season of May through September.

Once the recreation flow limits are selected, the recreation module design flow is calculated as the stream-width–weighted percentage of recreation flow as

$$Q_{rec,min} = \frac{b_{pool}}{B_{stream}} RecQ_{95}, Q_{rec,max} = \frac{b_{pool}}{B_{stream}} RecQ_{50}\ , \tag{B-1}$$

where B_{stream} is the width of the stream at the design flow of the facility.

B.3 RECREATION MODULE SIZING PROCEDURE

A module sizing procedure is developed following the empirically derived relationships of Caisley, Bombardelli, and Garcia (1999). The most downstream drop in a sequence of drop structures is optimized first to ensure exit conditions are suitable for boaters at minimum and maximum tailwater depths. Upstream steps are added with a maximum height of 1.5 ft between steps until the invert elevation of the most upstream drop structure is 1.5 ft below the normal operating level of the modular facility. The sequence of calculations for drop *N* is summarized as follows.

1. Assign low and high tailwater depths.

Identify the low and high tailwater depth in the tailrace, $h_{d,low,N}$ and $h_{d,,high,N}$, respectively, associated with the low and high recreation design flow.

2. Estimate first upstream drop structure height.

Choose an upstream drop height, $h_{s,N}$, that is submerged below the mean tailwater depth by at least 0.4 ft.

3. Compute downstream drop structure height.

Compute the downstream height of the drop structure, $h_{a,N} = h_{s,N} - 1.3$, where 1.3 ft is the maximum feasible drop height based on physical scale modeling.

4. Compute dimensionless flow.

Compute dimensionless minimum and maximum flow limits, $Q_{dim,min,N}$ and $Q_{dim,max,N}$:, using the minimum and maximum recreation module design flows,

$$Q_{dim,min,N} = \frac{Q_{rec,min}}{\sqrt{g{h_{s,N}}^5}}, Q_{dim,max,N} = \frac{Q_{rec,max}}{\sqrt{g{h_{s,N}}^5}}. \quad \text{(B-2)}$$

5. Compute tailwater depth limits of acceptable hydraulic jump behavior.

For a given drop height and dimensionless flow, the tailwater depth can be predicted using classic hydraulic jump equations. The most desirable hydraulic jump for recreation passage is one that remains in an undular regime, with waves that propagate downstream rather than recirculate as potentially dangerous rollers. To ensure the drop structure sustains an undular regime, a bound on acceptable low and high tailwater depths for low and high flows is enforced. The lowest acceptable tailwater depth for minimum and maximum design flows is defined as

$$h_{d,low,min,N} = h_{s,N}\left(0.2136Q_{dim,min,N} - 0.0109\right) + h_{a,N}, \quad \text{(B-3)}$$

and

$$h_{d,low,max,N} = h_{s,N}\left(0.2136Q_{dim,max,N} - 0.0109\right) + h_{a,N}. \quad \text{(B-4)}$$

The highest acceptable tailwater depth for minimum and maximum design flows is defined as

$$h_{d,high,min,N} = h_{s,N}\left(0.2559Q_{dim,min,N} + 0.2269\right) + h_{a,N}\,, \tag{B-5}$$

and

$$h_{d,high,max,N} = h_{s,N}\left(0.2559Q_{dim,max,N} + 0.2269\right) + h_{a,N}\,. \tag{B-6}$$

6. Optimize drop height for acceptable hydraulic jump behavior.

The drop structure will sustain an undular regime across all design flows if the lowest and highest modeled tailwater depths are kept within the limits of the inequalities:

$$h_{d,low,min,N} < h_{d,low,N} < h_{d,high,min,N}\,. \tag{B-7}$$

$$h_{d,low,max,N} < h_{d,high,N} < h_{d,high,max,N}\,. \tag{B-8}$$

If the low and high tailwater depths are within the specified bounds, proceed to step 7. If not, an optimization algorithm is used to estimate a value of $h_{s,N}$ allowable within the constraints of B-7 and B-8.

7. Compute head over upstream drop height.

The head over the upstream step depends on the ratio of tailwater depth to upstream drop height. If $1.2 < h_{d,low,N}/h_{s,N} < 1.4$, the flow regime is considered a submerged hydraulic jump and the following equations are used:

$$H_{s,low,N} = h_{s,N}\left(\frac{Q_{dim,min,N}}{0.55 * b_{drop}/h_{s,N}}\right)^{-1.15}\,. \tag{B-9}$$

$$H_{s,high,N} = h_{s,N}\left(\frac{Q_{dim,max,N}}{0.55 * b_{drop}/h_{s,N}}\right)^{-1.15}\,. \tag{B-10}$$

If $h_{d,low,N}/h_{s,N} < 1.2$, the flow regime is considered an unsubmerged hydraulic jump and the following equations are used:

$$H_{s,low,N} = h_{s,N}\left(\frac{Q_{dim,min,N}}{0.59 * b_{drop}/h_{s,N}}\right)^{-1.5}\,. \tag{B-11}$$

$$H_{s,high,N} = h_{s,N}\left(\frac{Q_{dim,max,N}}{0.59 * b_{drop}/h_{s,N}}\right)^{-1.5}\,. \tag{B-12}$$

If neither condition is met, the upstream drop height is assumed to be too low, creating a submerged hydraulic jump across the recreation passage module design flow range. In this case, $h_{s,N}$, is incrementally raised and the sizing procedure is resumed at step 3.

8. Assign low and high tailwater depths for next upstream drop.

The new upstream drop, N+1, is assigned a low and high tailwater depth based on variables from the downstream drop:

$$h_{d,low,N+1} = h_{s,N} + H_{s,low,N}\,, \tag{B-13}$$

$$h_{d,high,N+1} = h_{s,N} + H_{s,high,N}\,. \tag{B-14}$$

9. Check to determine whether more drops are needed.

Once the flow depth above the upstream drop height is known, a check is performed to see whether additional drops are required. If $h_{d,low,N+1}$ is less than the desired invert of the recreation passage module, specified as 1.5 ft below normal operating level, a new drop is added. To simplify the sizing procedure, the next upstream drop height $h_{s,N}$ is estimated to be 1.5 ft above the downstream drop and the sizing procedure starts again from step 4. Additional steps are added until $h_{d,low,N+1}$ is equal to or greater than the desired invert of the recreation passage module. Then the calculation sequence is complete.

B.4 RESULTS AND DISCUSSION

By incorporating the preceding steps into a generalized computer model, the variable inputs from Table B-1 can be optimized and assessed for a variety of potential site conditions. Figure B-5 provides an example of a recreation passage module profile for a structure height of 23 ft; drop structure width of 15 ft; minimum and maximum design flows of 29 and 72 cfs, respectively; and minimum and maximum tailwater depths of 8 and 9.4 ft, respectively. The model produces a recreation passage module design that consists of 10 steps over a total length of 250 ft with a mean slope of 0.084. The model outputs a graph of dimensionless depth as a function of dimensionless flow for each drop (Figure B-6), demonstrating how the height of each drop is constrained to produce an undular flow regime in the downstream pool over the range of design flows.

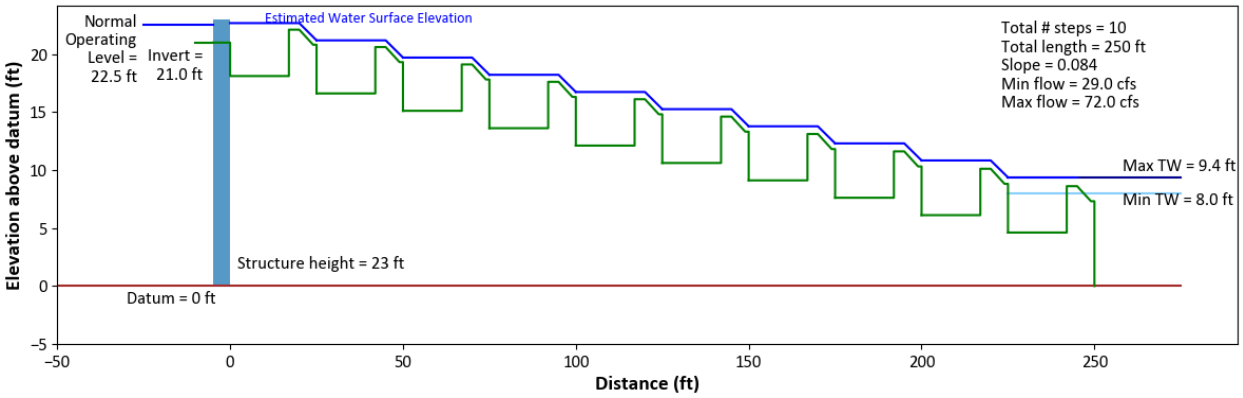

Figure B-5. Generalized tool output depicting optimal size and spacing of a recreation passage module.

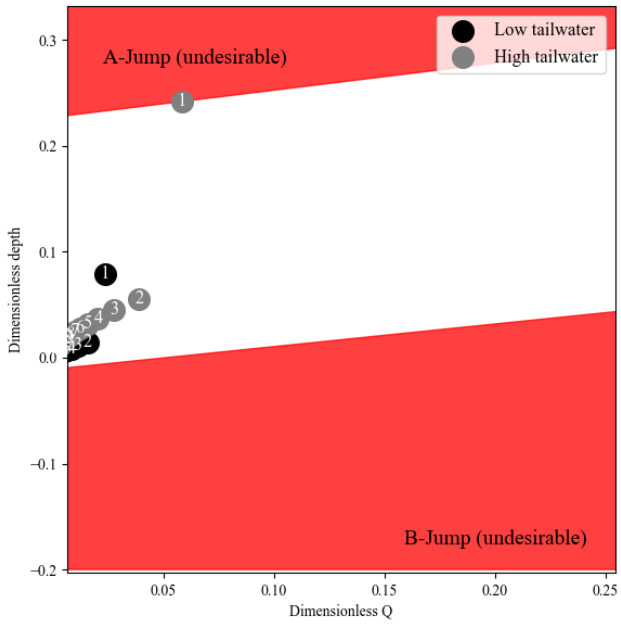

Figure B-6. Generalized tool output depicting dimensionless tailwater depth against dimensionless flow for a recreation passage module. Each marker represents a step, numbered from downstream to upstream. Regions of undesirable hydraulic jumps are outlined in red.

An assessment of several possible design parameters over a range of module design flows shows potential trade-offs in flow, size, and cost (Figure B-7). For the given structure height of 23 ft, a corresponding recreation passage module could vary in length from 210 to 300 ft depending on the width per drop and the minimum design flow (Figure B-7). As the minimum module design flow is increased, the total passage module length is reduced for a given drop width, a consequence of the increasing flow depth, increasing maximum viable drop structure height, and a wider range of tailwater depths for which undulating waves are predicted to occur. For a given minimum module design flow, the narrower the individual drop structures, the shorter the overall length of the structure. This arises from an increase in H_s with decreasing b_{drop}, a relationship that increases the tailwater depth at each structure, allowing for a larger step size, h_s, for each successive upstream drop structure.

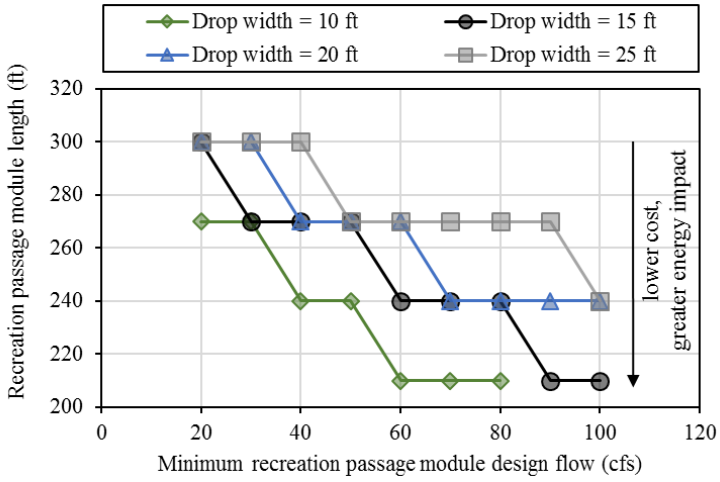

Figure B-7. Length of a recreation passage module as a function of minimum module design flow for various drop structure widths.

These design trade-offs present clear implications for energy generation and small hydro project development. A greater design flow allocated for recreation theoretically lowers the cost of a recreation passage module by decreasing the length, number of steps, and overall physical footprint of the design. This allocation comes at the expense of generation, as generation and recreation flows represent competing objectives that cannot be mutually satisfied.

B. 5 REFERENCE

Caisley, Marjorie E., Fabian A. Bombardelli, and Marcelo H. Garcia. 1999. *Hydraulic Model Study of a Canoe Chute for Low-Head Dams in Illinoi*s. Hydraulic Engineering Study 63, UILU-ENG-9-2012. Illinois Department of Water Resources.

APPENDIX C. REFERENCE SEDIMENT PASSAGE MODULE DESIGN

Generic sizing and operational criteria for a sediment passage module are developed using a vertical lift sluice gate as a reference module. Sediment trapping behind a small hydraulic structure can be minimized by timing the operation of sluice gates to pass the higher sediment concentrations present in flood flows (Figure C-1) (Brune 1953). Thus, we establish operational rules based on flow thresholds, which are used as surrogates for sediment transport. Once a volumetric discharge is exceeded, the gate is raised to ensure that sediment entrained into the flow is transported downstream through the lower depths of the facility. The technique is suggested by Morris and Fan (1998) for smaller reservoirs or dams, where discharging incoming sediment during high flows with heavy sediment concentrations can effectively route sediment without necessarily reducing water levels. They also suggest this method will increase the grain size of the material transported, with the amount and grain size of mobilized material controlled by gate operational rule curves. Furthermore, the annual flood pulse is considered a driver of river basin productivity, transporting the bulk of annual sediment and nutrient loads (Wild et al. 2016). Sediment sluicing through gates has recently been accepted by stakeholders as an adequate sediment management approach at a few new, small run-of-river hydropower facilities (Calligan Creek, Hancock, Gartina Falls) (FERC 2012; FERC 2014a, 2014b).

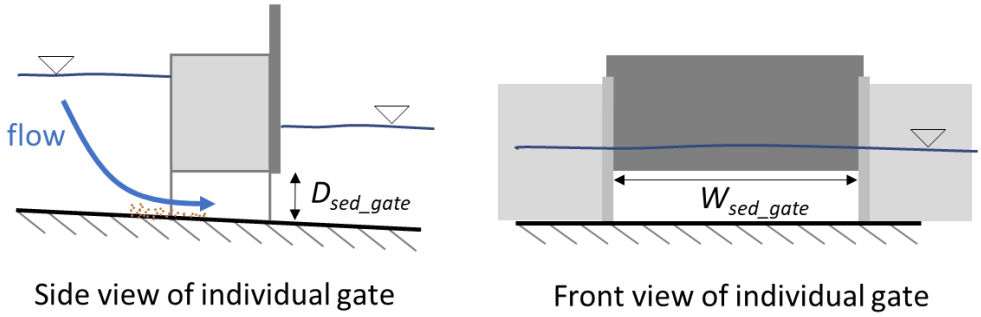

Figure C-1. Side view (left) and front view (right) of single vertical lift sluice gate as a reference sediment passage module.

C.1 ESTIMATING CONDITIONS FOR SEDIMENT MOVEMENT

Sediment passage modules should be designed considering all sources of sediment that contribute to fluxes at the site. The fluxes are integrated net contributions of eroded material from hill slopes and floodplains, as well as from channel beds and banks. Incoming terrestrial soil, typically finer material, is transported by the stream mostly as suspended load; whereas instream, coarser sediment may be transported as bed load or suspended load depending on flow conditions (Papanicolaou and Abban, 2016). A full balance of sediment inflows and outflows at the dam can be achieved only when both fine and coarse fractions are transported successfully beyond the dam. Approaches for determining instream contributions to sediment fluxes must consider processes specific to the stream type, e.g. sand-bed (fine) vs. gravel-bed (coarse) streams, and the presence or absence/influence of large-scale roughness features such as bed forms or boulders. We adopt an approach herein that considers these two factors.

Stage-discharge relations are beneficial for estimating sediment transport, as they offer a practical way of determining when and how much sediment is being entrained. The depth of flow for a given discharge and set of site characteristics is determined by the total flow resistance at the site. This flow resistance may be divided into two components: grain resistance, caused by surface drag on the bed particles, and form resistance, caused by a pressure difference between the stoss and lee sides of bed forms (e.g. ripples and dunes) in sand-bed rivers or large-scale roughness elements (such as boulders) in gravel-bed rivers (Chang 1998; Rickenmann and Recking 2011). Since the shear stress applied on the bed is directly

proportional to the flow resistance, it may also be partitioned into grain and form shear stresses (Einstein and Barbarossa 1952). The grain shear stress acting on sediment particles is responsible for entrainment in sand-bed rivers (Einstein and Barbarossa 1952). Similarly, in gravel-bed rivers, the portion of the shear stress directly applied on particles is responsible for their entrainment. Hence, for estimating sediment transport rates at a given flow discharge, it is important to know the fraction of the total shear stress that acts on the sediment particles. With a known stage-discharge relationship, this fraction of the total shear stress acting on the sediment particles can be related to the flow depth, which is more readily measured in the field. This relationship can then be used to establish a practical sediment rating curve (based on the flow depth) at the site that accounts for the influence of bed forms and large-scale roughness elements. We take this approach in the case study because a stage-discharge relationship is available. For sites where stage-discharge relations are not available, however, one can be developed using either the Brownlie (1983) method for fine beds, or the Rickenmann and Recking (2011) method for coarse beds. These methods are also described in the following sections.

Our overall approach uses the probability of sediment entrainment into the flow to estimate conditions for sediment movement in a stream, following the general method outlined in Elhakeem, Papanicolaou, and Tsakiris (2017). The flow condition at which sediment particles of given characteristics just start moving is known as the "condition of incipient motion of particles." Incipient motion of particles is probabilistic in nature (Choi and Kwak 2000; Papanicolaou et al. 2002). It depends primarily on the turbulence characteristics of flow in association with the location of a specific particle relative to the surrounding particles of various sizes and orientations, as well as on prevalent bed patterns. Two of the most widely used approaches to determine the incipient motion of a particular grain size relate it to either the flow velocity or the tractive force acting on it. Based on studies linking the characteristics of turbulent episodes with the initial entrainment of sediment, Papanicolaou et al. (2002) developed a stochastic incipient model that incorporates in its formulation the probability density function of the bed shear stress to account for the effects of both flow turbulence and bed surface irregularity on sediment entrainment. Recently, Elhakeem et al. (2017) enhanced the model to incorporate the collective effects of relative roughness, volumetric fraction, and relative position of sediment particles within the active layer. The model was validated for both fine and coarse sediment and is particularly suited to streams with pronounced bed irregularity. Practically, the model relates the probability of entrainment of a sediment particle to the shear stress acting on it. Hence, if the shear stress acting on the particle at a given flow condition is known, the probability that it will be entrained can be determined. In terms of net sediment flux, the probability of entrainment can be interpreted as the fraction of available sediment that will be mobilized at a given flow condition. Thus, the flow depth at the SMH site can be related to the shear stress acting on the sediment particles, and it is possible to relate the flow depth to the probability of entrainment. This relationship can then be used to design the sediment passage module and set operating rules (Figure C-2).

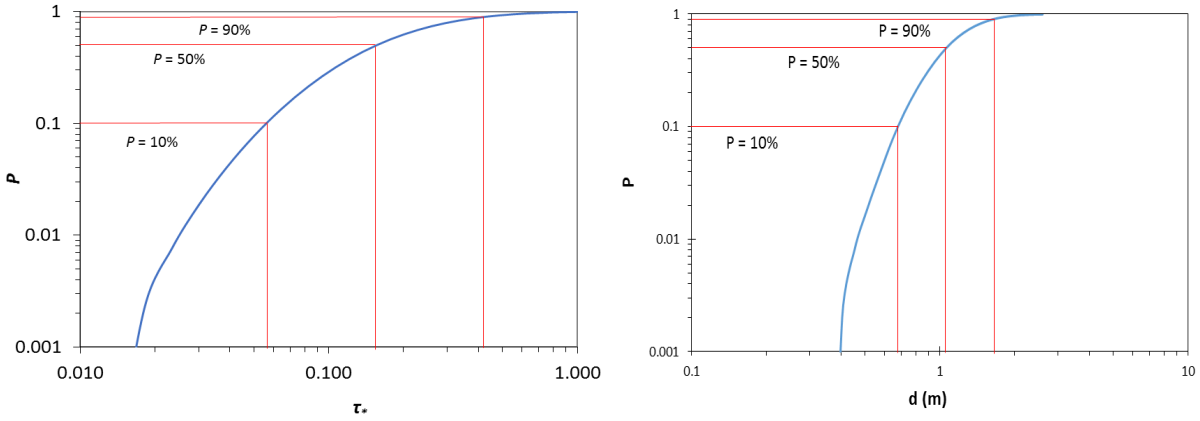

Figure C-2. Sample probability of entrainment-shear stress (left) and probability of entrainment-flow depth curves (right).

This approach relies on a series of variables and user-defined inputs based on site conditions (Table C-1). Based on the median particle diameter, d_{50}, the site is considered either a fine (sand) bed if d_{50} <2 mm, or a coarse (gravel) bed if d_{50} >2 mm. Though the procedure for estimating probability of sediment movement varies between fine and coarse beds, the general steps involved for each size are as follows:

- Estimate critical shear stress, τ_{*c}.
- Estimate maximum shear stress, τ_{*max}.
- Solve the probability formula for a range of $\tau_{*c} < \tau_{*} < \tau_{*max}$.
- Compute flow and depth for each probability and τ_{*}.

Table C-1. Sediment passage module input design variables.

Variable	Value	Units	Description
g	9.81	m/s^2	Gravitational acceleration
S_e	variable	[-]	Energy slope (assumed to be reach slope under steady-state conditions)
γ_w	1,000 g	N/m^3	Specific weight of water
γ_s	2,650 g	N/m^3	Specific weight of sediment
d_{50}	variable	m	Sediment size for which 50% of the material is finer
υ	1.31E-6	m^2/s	Kinematic viscosity at 10°C

C.2 ESTIMATE CRITICAL SHEAR STRESS ACTING ON A GRAIN

The critical shear stress acting on a grain, τ_{*c}, sets the lower boundary for shear stress, below which the probability of sediment entrainment is 0 (P = 0, no sediment is entrained in the flow). A value for τ_{*c} can be supplied in one of two ways. It can be calculated using equations from Elhakeem et al. (2017), or it can be supplied using an alternative method.

Fine

First, the particle Reynolds number is computed as

$$R_p = \frac{d_{50}}{\nu}\left(\left(\frac{\gamma_s}{\gamma_w} - 1\right) g d_{50}\right)^{0.5} . \quad \text{(C-1)}$$

Then critical shear stress is computed using R_p in the Brownlie (1983) formula as

$$\tau_{*c} = 0.22{R_p}^{-0.6} + 0.06 * 10^{-7.7{R_p}^{-0.6}} . \quad \text{(C-2)}$$

Coarse

The relationships outlined in Elhakeem et al. (2017) are used to estimate critical shear stress for coarse beds. The final equation used is

$$\tau_{*c} = \frac{cosS_e}{0.75(r_m C_D + C_L)f^2}, \quad \text{(C-3)}$$

where C_D and C_L are the drag and lift coefficients, respectively, and r_m is the ratio of the moment arms of the drag force to the lift force. For coarse beds $C_D = 0.4$ and $C_L = 0.12$. The remaining variables are computed using

$$f = 2.5 \ln(\beta R_r + 7.5) \text{ , and} \tag{C-4}$$

$$r_m = [3(R_r + 1)^2 - 4]^{0.5} , \tag{C-5}$$

where R_r is the relative roughness equal to d_s/d_b, the diameter of the entrainable particles divided by the diameter of the bed material; and β reflects the particle-flow interaction accounting for the effects of packing density and particle protrusion. For coarse beds, $\beta = 30y/d_s = 15$ (y = $d_s/2$) and $R_r = 1.5$.

C.3 ESTIMATE MAXIMUM BED SHEAR STRESS ACTING ON A GRAIN

The next value needed is the maximum bed shear stress acting on a grain, τ_{*max}. This value is used to set the upper boundary of shear stress, above which the probability of sediment entrainment is equal to 1 (P = 1, all sediment is entrained into the flow).

Three variables are needed to solve for τ_{*max}:

- n, number of particles describing the thickness of the active layer ($2 \le n \le 10$)
- C, volumetric fraction of sediment particles within the active layer ($0.1 \le C \le 0.74$)
- R_r, relative roughness, or the ratio of mobile particles to bed particles ($R_r \ge 0.22$)

Based on guidance from Elhakeem et al. (2017), we assume values for fine (n = 5, C = 0.6, R_r = 1) and coarse (n = 3, C = 0.4, R_r = 1.5) streams. These are used to estimate the maximum bed shear stress using

$$\tau_{*max} = nCa((R_r + 1)^2 - 1.333)^{-0.5} , \tag{C-6}$$

where the constant a, which has a range of $0.8 \le a \le 1.4$, is 0.94 for both sand and gravel.

C.4 COMPUTE THE PROBABILITY OF SEDIMENT ENTRAINMENT FOR A RANGE OF BED SHEAR STRESS

To simplify the analysis, a transformation of the log-normal distribution of the critical and maximum shear stresses to a Gaussian distribution is carried out. Defining $X = \ln \tau_*$, $X_c = \ln \tau_{*c}$, $X_m = \ln \tau_{*max}$, $\bar{X}$ = 1/2 $\ln(\tau_{*c}\tau_{*max})$, and σ_x = 1/6 $\ln(\tau_{*max}/\tau_{*c})$, we compute $m = (X - \bar{X})/\sigma_x$ and $m_c = (X_c - \bar{X})/\sigma_x$ for the range of $\tau_{*c} < \tau_* < \tau_{*max}$.

With the preceding variables accounted for, it is possible to use the Elhakeem et al. (2017) relationship to estimate the probability of sediment entrainment as

$$P = [1 + exp(-0.07056m^3 - 1.5976m)]^{-1} - [1 + \exp(-0.07056m_c^3 - 1.5976m_c)]^{-1} . \tag{C-7}$$

An example for fine beds will be used to illuminate the results. The variables outlined in Eqs. (C-1–C-6) are computed in Table C-2, and the probability of entrainment is plotted as function of shear stress in Figure C-3.

Table C-2. Example variables and calculations for estimating sediment entrainment probability of fine beds.

Variable	Value
d_{50}	1 mm
S	0.001
R_p	97.1
n	5
C	0.6
Rr	1
a	0.94
τ_{*c}	0.014
τ_{*max}	1.727

τ^*	X	m	P
τ_{*c} = 0.014	–4.26	–3.00	0.000
0.018	–4.01	–2.68	0.002
0.023	–3.75	–2.37	0.008
0.030	–3.50	–2.05	0.019
0.039	–3.25	–1.74	0.040
0.050	–2.99	–1.42	0.077
0.064	–2.74	–1.11	0.133
0.083	–2.49	–0.79	0.214
0.107	–2.24	–0.47	0.316
0.138	–1.98	–0.16	0.436
0.177	–1.73	0.16	0.562
0.228	–1.48	0.47	0.681
0.294	–1.22	0.79	0.784
0.379	–0.97	1.11	0.864
0.488	–0.72	1.42	0.921
0.628	–0.47	1.74	0.957
0.808	–0.21	2.05	0.979
1.041	0.04	2.37	0.990
τ_{*max} = 1.341	0.29	2.68	0.995

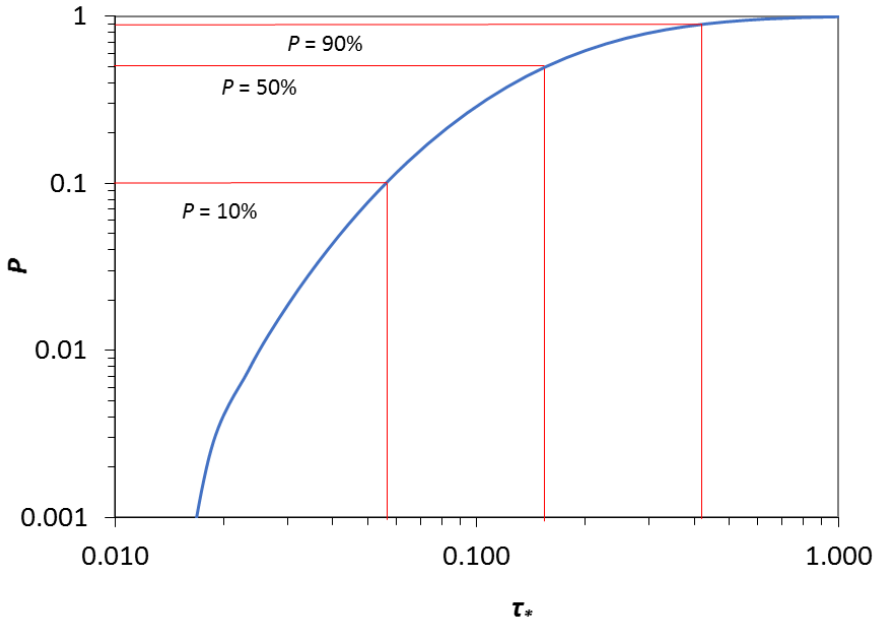

Figure C-3. Probability of sediment entrainment as a function of dimensionless shear stress acting on the grain.

C.5 LINKING SEDIMENT ENTRAINMENT PROBABILITIES TO FLOW PARAMETERS

Note that τ_* from Figure C-3 is the shear stress acting on the grain, and what is needed is the total shear stress acting on the bed, τ_{*P}. Using the range of potential shear stresses acting on the grain estimated in Section C.3 the depth of flow associated with each probability can be estimated using the following procedure.

Fine

The grain shear stress, τ_*, is used to calculate the portion of the depth of flow that relates to grain roughness, d', using the equation

$$d' = \frac{\tau_*(\gamma_s - \gamma)d_{50}}{\gamma S}. \tag{C-8}$$

The flow velocity, *U*, can then be found using this depth with the following relation

$$U = \sqrt{gd'S}\left(6 + 2.5\ln\frac{d'}{2.5d_{50}}\right). \tag{C-9}$$

Assuming the tailwater rating curve is available for a site, the flow discharge, *Q*, and flow depth, *d*, can then be calculated, given that $Q = UBd$, where *B* is the river width in feet. As an example, a generic tailwater rating curve may take the form of $d = bQ^k$, where *b* and *k* are regional specific coefficients, *Q* is discharge in cfs, and *d* is river depth in feet. The rating curve can be modified in the following manner to solve for flow depth

$$d = b(UBd)^k, \tag{C-10}$$

$$d = [b(UB)^k]^{1/(1-k)}. \tag{C-11}$$

Note this approach assumes that the rating curve accounts for the presence of bed forms.

To demonstrate this procedure, the values given in Table C-1, a τ_* of 0.177 (a probability of 0.56 from Table C-2), and a river width of 65 ft are used to calculate *d* and *Q*:

$$d' = \frac{0.177\left(2650\,{}^{N}/_{m^3} - 1000\,{}^{N}/_{m^3}\right)1mm}{1000\,{}^{N}/_{m^3}\,(0.001)} = 292.05mm = 0.958\,ft,$$

$$U = \sqrt{9.81\,{}^{m}/_{s^2} \times 0.292\,m \times 0.001}\left(6 + 2.5\ln\frac{0.292m}{2.5 \times 0.001m}\right) = 0.958\,{}^{m}/_{s} = 3.14\,{}^{ft}/_{s}.$$

Using typical coefficient values for fine bed streams of $b = 0.26$ and $k = 0.4$, the depth and flow associated with a 0.56 entrainment probability are:

$$d = \left[0.26\left(3.14\,{}^{ft}/_{s} \times 65\,ft\right)^{0.4}\right]^{1/(1-0.4)} = 3.7\,ft,$$
$$Q = 3.14\,{}^{ft}/_{s} \times 65\,ft \times 3.7\,ft = 756\,{}^{ft^3}/_{s} = 21\,{}^{m^3}/_{s}.$$

Coarse

For coarse sediment, Eq. (C-8) is again used to solve for d'.

The dimensionless unit discharge, q^{**}, in the stream, corresponding to conditions when the base level roughness contributes the portion d' to the total flow depth, is determined using Eqs. (C-12 and C-13):

$$q^{**} = (d' \times 3.20/d_{84})^{1/0.60} . \quad \text{(C-12)}$$

This value can be used to solve for the unit discharge, q, using the equation

$$q = q^{**}\sqrt{gSd_{84}^3} . \quad \text{(C-13)}$$

The cross-section flow discharge, Q, can be calculated by multiplying q by the river width. A rating curve can be used to determine the flow depth if one is available. *If one is not available*, Eq. (C-14) may be used for the velocity to determine the flow depth given $d = qU$:

$$\frac{U}{\sqrt{gSd_{84}}} = 1.5471q^{**0.7062}\left[1 + \left(\frac{q^{**}}{10.31}\right)^{0.6317}\right]^{-0.4930} . \quad \text{(C-14)}$$

An example of the above procedure is outlined below for a river with a d_{50} of 25 mm, a d_{84} of 50.9 mm, a width of 30 m, and a slope of 0.003.

Equation C-8 yields a d' value of 0.67 m (2.2 ft). The q^{**} is then calculated as

$$q^{**} = (0.67m \times 3.20/0.0509m)^{1/0.60} = 509 .$$

Next, q is solved for

$$q = 509\sqrt{9.81\,{}^{m}/_{s^2} \times 0.003 \times (0.0509m)^3} = 1.0\,{}^{m^2}/_{s} .$$

The discharge is then calculated

$$Q = 1.0\,{}^{m^2}/_{s} \times 30.0\,m = 30\,{}^{m^3}/_{s} .$$

Finally, velocity and flow depth are calculated as

$$U = 1.5471 \times 509^{0.7062}\left[1 + \left(\frac{509}{10.31}\right)^{0.6317}\right]^{-0.4930} \times \sqrt{9.81 \times 0.003 \times 0.0509} = 1.4\,\frac{m}{s},$$

$$d = 1.0 \times 1.4 \; = 1.39\,m = \; 4.5ft$$

The relationship between sediment entrainment probability and discharge for a range of d is computed by completing the procedure outlined above, substituting the range of τ_* from Table C-2 into Eq.(C-8) to produce a range of *d'*, *d*, and *Q*. The result is shown in Figure C-4.

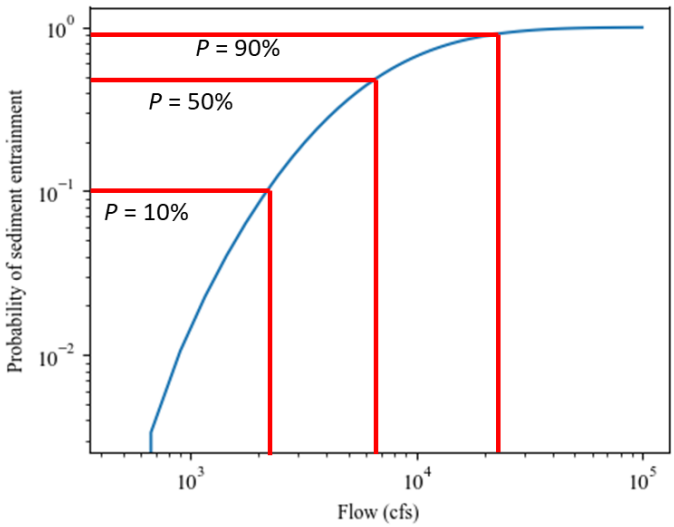

Figure C-4. Relationship between probability of sediment entrainment and discharge.

With the preceding equations, the user can estimate the probability of sediment entrainment at a site and set sediment operational rules and passage sizing accordingly.

C.6 SPECIFY SEDIMENT PASSAGE MODULE SIZE AND OPERATIONAL RULES

The operational rules for opening the sediment passage module are linked to the probability of sediment entrainment under a given flow and depth in an undeveloped stream. That is, once a critical depth associated with a predetermined probability of sediment entrainment is exceeded, it is assumed that the target sediment size is moving, and the gate should be opened to ensure sediment continuity across the facility. The appropriate probability of entrainment for a given site will be a user input, but we set the threshold at 50% for the following example.

Using the procedure outlined above, or using the probability discharge curve shown in Figure C-3, the critical flow, $Q_{crit,sed}$, associated with P = 50% is determined. It is assumed the sluice gate acts as a submerged rectangular orifice when discharging flow downstream. Thus, the equation for submerged orifice flow is used to size the gate:

$$Q_{sed} = C_{sed\_gate} D_{sed\_gate} W_{sed\_gate} \sqrt{2gH}\,, \tag{C-15}$$

where C_{sed_gate} = 0.61 (when Eq. [C-11] is computed using SI units), D_{sed_gate} is the largest vertical opening of the sediment gate in ft, W_{sed_gate} is the largest horizontal opening of the sediment gate in ft, H is the gross head in feet for a given flow. Balancing the recommendation that bottom outlets be located as deep as possible and be as wide as possible (Morris and Fan 1988) with the need to develop standardized and feasible sediment management solutions, we set a target for the sediment passage module itself to pass 20% of the critical flow discharge that is not being passed through other modules, and a maximum gate opening of 75% of the invert of the height of the facility above the channel bottom. We also establish a standard sediment passage module width in increments of 8 ft – that is, W_{sed_gate} is increased in increments of 8 ft until the equation the right-hand side of Eq. (C-15) is greater than $0.25*Q_{crit,sed}$.

As an example, given a $Q_{crit,sed}$ of 10,000 cfs, a facility with an invert of 13 ft, and a gross head of 8 ft, the design procedure proceeds as follows. The target sediment passage module design flow is set at $0.20*Q_{crit,sed}$ = 2,000 cfs. An initial sediment passage module width is specified as W_{sed_gate} = 8 ft and the

maximum opening is set as D_{sed_gate} = 0.75×12 ft = 9.75 ft. The right-hand side of Eq. (C-15) is computed as

$$C_{sed\_gate} D_{sed\_gate} W_{sed\_gate} \sqrt{2gH} = 0.61 * 9.75 * 8 * \sqrt{2 * 32.2 * 8} = 1{,}080 \text{ cfs.}$$

The estimated sediment passage module design flow of 1,080 cfs is less than the desired 2,000 cfs, and thus another sediment passage module is needed. The calculation is repeated using a wider W_{sed_gate}

$$C_{sed\_gate} D_{sed\_gate} W_{sed\_gate} \sqrt{2gH} = 0.61 * 9.75 * 16 * \sqrt{2 * 32.2 * 8} = 2{,}159 \text{ cfs.}$$

This value is greater than 0.20×$Q_{crit,sed}$, and thus the major dimensions are considered established. The module will operate under a design flow of $0.61 \times 9.75 \times 8 \times \sqrt{2gH}$ whenever the stream flow is greater than $Q_{crit,sed}$.

C.7 DISCUSSION

Once the sluice gate has been sized and a set of rules has been established, operation of the sediment passage module can be expected to create a cycle of some sediment trapping/deposition and entrainment behind the dam (Pearson and Pizzuto 2015). Simulations of sediment trapping/deposition and entrainment based on dam operation may be needed to determine the effectiveness of the design, as well as the potential impacts that these operations may have on the transport and storage of sediment-associated contaminants in a river system (Bosch 2008). Sediment transported by rivers and streams can be contaminated with toxic compounds such as heavy metals, polychlorinated biphenyls (PCBs), and excess nutrients such as nitrogen and phosphorus (Wetzel, Wahrendorf, and von der Ohe 2013). Assessment of the effects of sediment accumulation on living organisms, on increased contamination through settling and accumulation, and on scour of contaminated sediment may be performed using models such as EFDC and ECOMSED. A systems dynamics framework that integrates these water quality models (contaminated sediment processes) with appropriate watershed models (watershed inputs to site) and an SMH module simulation package (holistic dam operations) should be used for a complete evaluation of the SMH design.

C.8 REFERENCES

Bosch, N. 2008. The influence of impoundments on riverine nutrient transport: An evaluation using the Soil and Water Assessment Tool. *Journal of Hydrology* 355(1–4), 131–147.

Brownlie, W. R. 1983. "Flow depth in sand-bed channels." *J. Hydraul. Div. ASCE* 109(7), 959–990.

Brune, Gunnar M. 1953. "Trap efficiency of reservoirs." *Eos, Transactions American Geophysical Union* 34(3), 407–418. https://doi.org/10.1029/TR034i003p00407

Choi, S. U., and S. Kwak. 2000. "Probabilistic analysis of incipient motion of sediment particles." *Proceedings of the 8th International Symposium on Stochastic Hydraulics*, Beijing, China, July 25–28, 2000, pp. 317–324.

Einstein, H. A., and N. Barbarossa. 1952. "River channel roughness," *Transactions ASCE* 117, 1121–1146.

Elhakeem, Mohamed, A. N. Thanos Papanicolaou, and Achilleas G. Tsakiris. 2017. "A probabilistic model for sediment entrainment: The role of bed irregularity." *International Journal of Sediment Research* 32(2), 137–48.

FERC (Federal Energy Regulatory Commission). 2012. *Environmental Assessment for Hydropower License: Gartina Falls Hydropower Project*. FERC Online eLibrary. https://elibrary.ferc.gov/idmws/file_list.asp?document_id=14072983

FERC (Federal Energy Regulatory Commission). 2014. *Environmental Assessment for Original Hydropower License: Calligan Creek Hydroelectric Project*. FERC Online eLibrary. https://elibrary.ferc.gov/idmws/file_list.asp?document_id=14279488

FERC (Federal Energy Regulatory Commission). 2014. *Draft Environmental Assessment for Original Hydropower License: Hancock Creek Hydroelectric Project*. FERC Online eLibrary. https://elibrary.ferc.gov/idmws/file_list.asp?document_id=14279495.

Morris, Gregory L., and Jiahua Fan. 1998. *Reservoir Sedimentation Handbook: Design and Management of Dams, Reservoirs, and Watersheds for Sustainable Use*. McGraw Hill Professional.

Papanicolaou, A. N., P. Diplas, N. Evaggelopoulos, and S. Fotopoulos (2002), "A stochastic incipient motion criterion for spheres under various packing conditions," *Journal of Hydraulic Engineering*, 128(4), 369–380.

Papanicolaou, A. N. and B. Abban (2016), "Channel Erosion and Sediment Transport. " Chapter 65 in *Handbook of Applied Hydrology*, 2nd Edition. Ed. V.P. Singh. McGraw Hill. ISBN:9780071835107.

Pearson, A. J. and J. Pizzuto. 2015. "Bedload transport over run-of-river dams, Delaware, U.S.A." *Geomorphology*, 248, 382–395.

Rickenmann, D., and A. Recking. 2011. "Evaluation of flow resistance in gravel-bed rivers through a large field data set." *Water Resour. Res.* 47, W07538. doi:10.1029/2010WR009793

Wetzel, M. A., D. S. Wahrendorf, and P. C. von der Ohe (2012), "Sediment pollution in the Elbe estuary and its potential toxicity at different trophic levels." *Science of the Total Environment* 449(C), 199–207.

APPENDIX D. REFERENCE GENERATION MODULE DESIGN

The reference generation modules are designed assuming an axial flow Kaplan-style turbine as the reference module. These turbines are common at low-head sites (ESHA 2004; Kössler 2018), and attempts at standard designs have been made in the past (see, e.g., Pugh 1979). For modeling purposes, we assume the turbine-generator unit is a single module and self-contained within a structure that has an intake, trash rack or screen, and outlet with a draft tube. Because we are focused purely on a systems approach that defines flow through the generation module and overall footprint, we use a conservative approach to estimate only the basic dimensions and operating characteristics of a generation module using the design variables outlined in Table D-1.

Table D-1. Generation module input design variables.

Variable	Value	Units	Description
H_{plant}	variable	ft	Plant design head
Q_{plant}	variable	cfs	Plant design flow
$N_{turbines}$	variable		Number of generation modules

D.1 PLANT DESIGN FLOW AND HEAD

The user specifies a plant design flow, Q_{plant}, based on the flow exceedance curve of the site. A suggested value is between Q_{40} and Q_{80}. The plant design head, H_{plant}, is assumed to be equivalent to 95% of the gross head at the site (assuming minor intake losses).

D.2 TURBINE DIMENSIONS

In the following sections, all units are in metric units. The user specifies the desired number of turbines, $N_{turbines}$. The individual desired turbine design flow, $Q_{turbine}$, is specified as the plant design flow divided by the number of turbines, or $Q_{plant}/N_{turbines}$.

A viable turbine diameter is estimated using installation data from Kössler (2018), which reports the runner diameter, head, rotational speed, and turbine output for a set of 126 axial flow Kaplan units installed throughout the world. Using these data and assuming a peak efficiency of 90%, $Q_{turbine}$ is estimated for all references. A regression of turbine diameter as a function of $Q_{turbine}$ shows a strong correlation (Figure D-1) that follows the relationship

$$D_T = 0.5\, Q_{turbine}{}^{0.457}, \tag{D-1}$$

where D_T is runner diameter in meters.

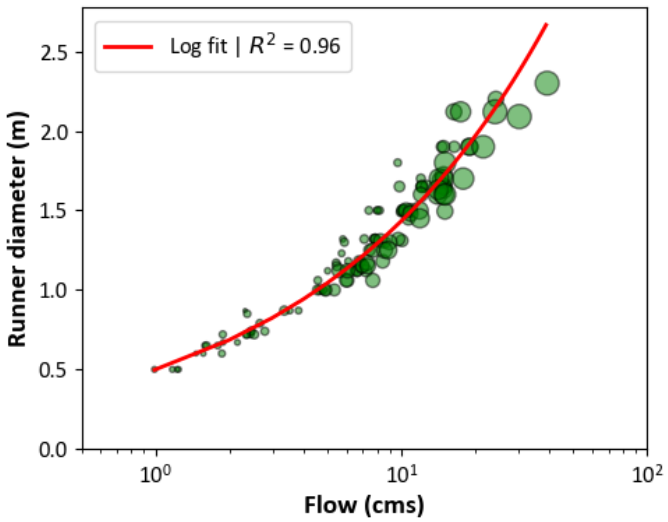

Figure D-1. Runner diameter as a function of flow.
Markers are sized by installed capacity.

Next, turbine rotational speed is estimated using the same data set as

$$n_T = 375\, {D_T}^{-1.02}\,, \tag{D-2}$$

where n_T is turbine rotational speed in rpm. The predictive relationship is shown in Figure D-2.

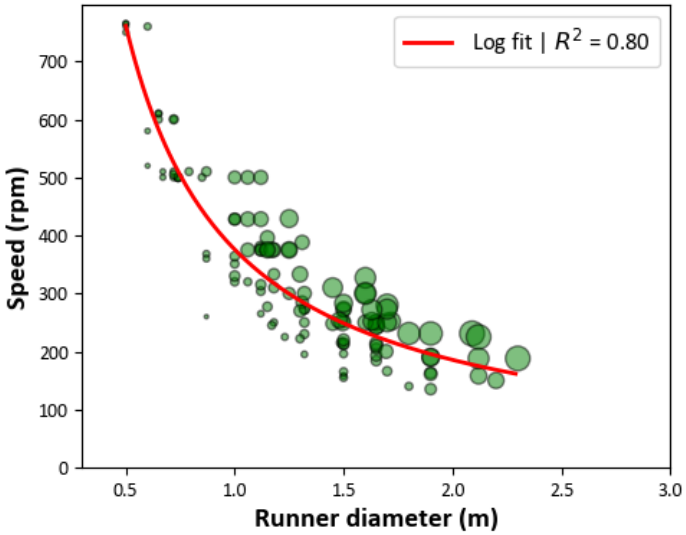

Figure D-2. Turbine rotational speed as a function of runner diameter.
Markers are sized by installed capacity.

D.3 TURBINE AND PLANT PERFORMANCE

Using an empirical relationship for axial flow turbines established in Gordon (2001), we estimate a generic turbine efficiency curve for an axial flow unit. The peak turbine efficiency is estimated as

$$\varepsilon_{peak} = A - \Delta\varepsilon_{N_q} + \Delta\varepsilon_{size}\,, \tag{D-3}$$

where A = 0.904 for axial flow runners, and

$$\Delta\varepsilon_{N_q} = \left[\left(\frac{N_q - C}{D}\right)^2\right]^Z, \tag{D-4}$$

where for axial flow runners C = 162, D = 533, and Z = 0.979,

$$N_q = \frac{{n_T Q_{turbine}}^{0.5}}{{H_{plant}}^{0.75}}\,, \tag{D-5}$$

$$\Delta\varepsilon_{size} = \left(1 - A + \Delta\varepsilon_{N_q}\right)\left(1 - 0.789{D_T}^{-0.2}\right). \tag{D-6}$$

Next, the ratio of peak flow to rated flow is computed as

$$Q_{peak} = Q_{rated} 1.9{N_q}^{-0.2}\,. \tag{D-7}$$

The snl (speed no load) flow, the point at which the runner is rotating at synchronous speed and ready to be placed online, is estimated as

$$Q_{snl} = Q_{rated}\left(\frac{N_q}{20000}\right)^{0.5}. \tag{D-8}$$

The complete efficiency curve is developed using the prior equations in two parts. At flows of less than Q_{peak}, the change from peak efficiency is computed as

$$\Delta\varepsilon_{peak} = \varepsilon_{peak}\left(1 - \frac{Q_{snl}}{Q_{peak}}\right)^{-k}\left(1 - \frac{Q}{Q_{peak}}\right)^{k}, \tag{D-9}$$

where the exponent k = 7.2 for new turbines. For flows greater than Q_{peak}, the change from peak efficiency is computed as

$$\Delta\varepsilon_{peak} = \left(\frac{Q}{Q_{peak}} - 1\right)^{1.5}. \tag{D-10}$$

A dimensionless turbine efficiency curve computed using the preceding steps is show in Figure D-3.

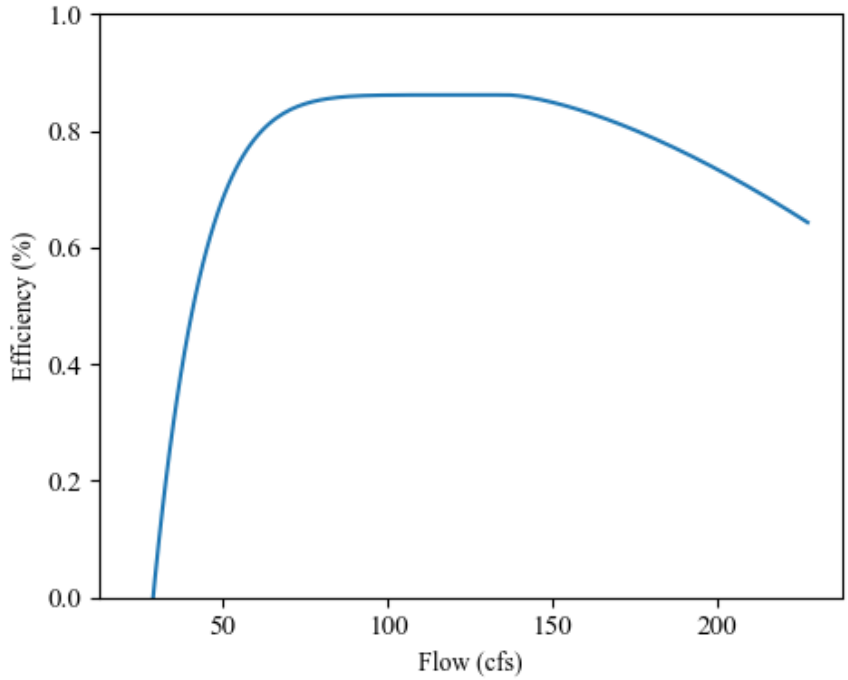

Figure D-3. Efficiency curve for a reference generation module.

To estimate overall plant efficiency, we develop an algorithm to compute the best-efficiency point of multiple turbines when they are in operation. A generic plant efficiency curve is shown in Figure D-4 for four generation modules. For a given generation flow discharge, we assume an optimal dispatch of generation modules to produce the optimum plant efficiency.

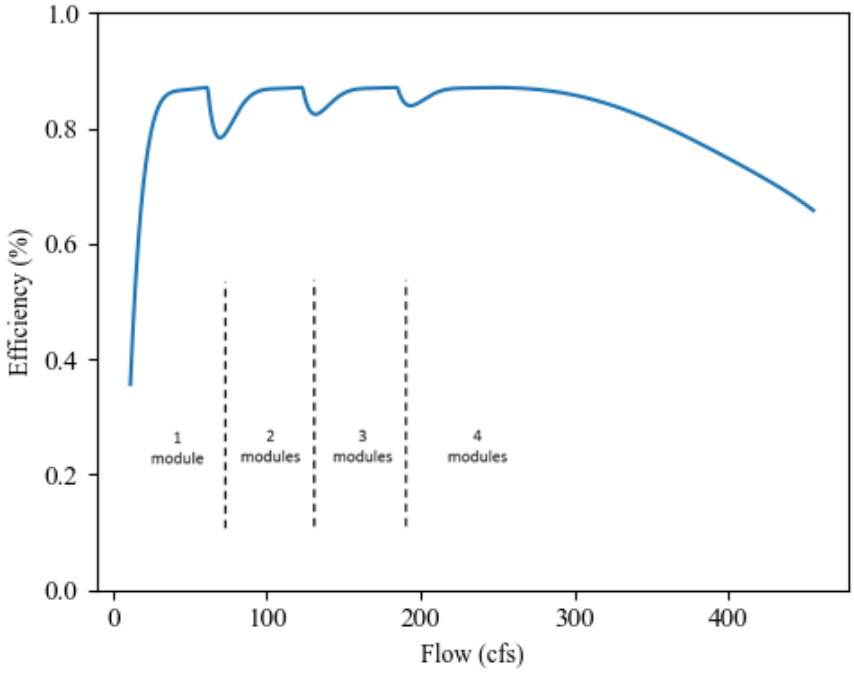

Figure D-4. Plant efficiency curve for four reference generation modules.

D.4 FOOTPRINT OF GENERATION MODULE(S)

We assume the generation module contains all equipment and systems necessary to produce power within a single functional unit, including the intake, turbine, generator, draft tube, and all equipment and systems necessary for handling electromechanical equipment. As a first-order estimate of a module footprint, we assume a generation module length of $7D_T$ and width of $3D_T$. We assume the outlet of the generation module must be submerged D_T below normal tailwater depth, computed as the depth observed at a flow exceedance of Q_{95}%, and that a depth of D_T must exist below the turbine to ensure the flow can expand through the draft tube into the tailrace (Figure D-5).

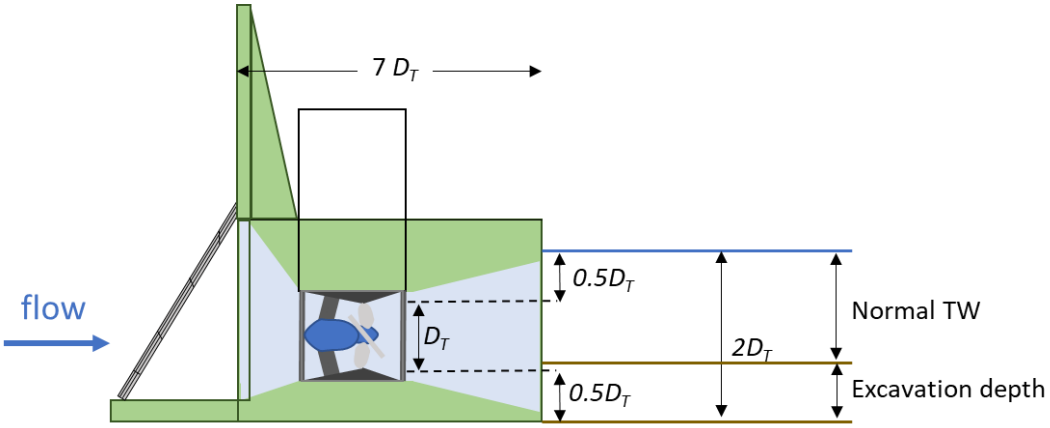

Figure D-5. Concept sketch of a generation module with major dimensions.

D.5 REFERENCES

European Small Hydropower Association (ESHA). 2004. Guide on How to Develop a Small Hydropower Plant. https://energiatalgud.ee/img_auth.php/a/ab/Guide_on_How_to_Develop_a_Small_Hydropower_Plant.pdf

Gordon, J. L. "Hydraulic turbine efficiency." Canadian Journal of Civil Engineering 28.2 (2001): 238-253.

Kössler, 2018. http://www.koessler.com/en/

Pugh, C. 1979. Standardized intakes and outlets for low-head hydropower developments. Bureau of Reclamation , DOE-79-01.

APPENDIX E. REFERENCE WATER PASSAGE MODULE DESIGN

To control water levels and meet water passage requirements at a low-head in-stream structure, various gated structures may be used. One such structure often used for flow in open channels is an overshot gate, which is described in Chapter 7 of USBR (2001) and in Wahlin and Replogle (1994). An overshot gate acts as a dynamic weir structure and can be raised or lowered using various types of mechanical equipment (e.g., a winched chain or an inflatable bladder). The advantage of this structure is its ability to finely control water surface elevations across a range of flow conditions, ensuring the inverts of all passage modules and the intakes of generation modules are sufficiently submerged. Figure E-45 includes an example illustration of an overshot gate, in which p is the height from the channel bottom to the crest of the gate, h_1 is the head on the gate, H is the length of the gate, θ is the gate angle against the channel bottom, d_{tw} is the tailwater depth, and h_2 is the submergence of the gate.

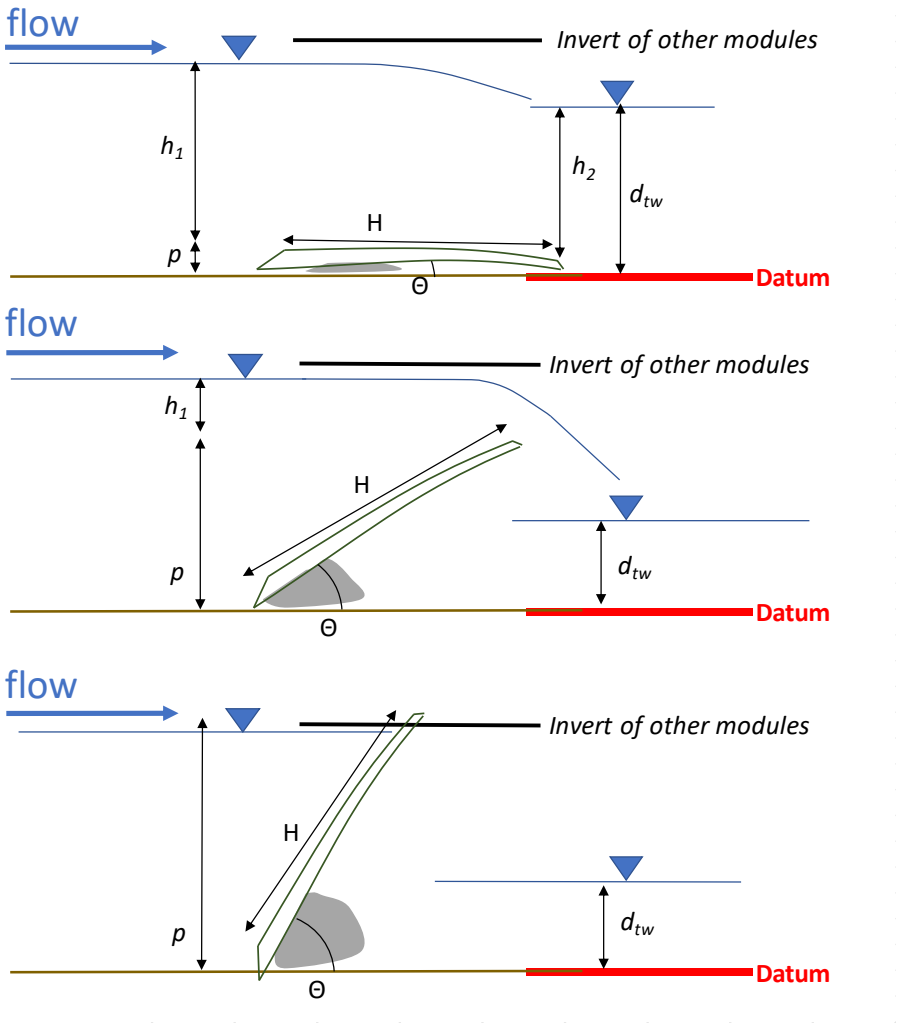

Figure E-45. Sectional view of an overshot gate with a deflated bladder (top), partially inflated bladder (middle), and inflated bladder (bottom).

Flow over an overshot gate is estimated using the equation

$$Q = C_a C_e C_{df} L_e h_e^{1.5} , \quad \text{(E-1)}$$

where Q = flow discharge in cfs, C_a = correction factor for angle of the gate, C_e = effective discharge coefficient for a vertical weir, C_e = drowned flow reduction coefficient, L_e = effective crest length, h_e = effective measurement head. To size the water passage module as an overshot gate, we seek to establish an effective length L_e that can pass the input values of Q and h_e given the computed values of coefficients and correction factors. The list of required input design variables is referenced in Table E-1.

Table E-1. Water passage module input design variables.

Variable	Value	Units	Description
Q_{10yr}	variable	ft^3/s	Maximum design flow for a site (10-year flood)
d_{tw10yr}	variable	ft	Tailwater depth at maximum design flow (10-year flood)
$WSE_{hw,10yr}$	variable	ft	Desired water surface elevation of headwater, above datum, at maximum design flow (10-year flood)
B_{river}	variable	ft	River width
$B_{wpm,i}$	variable	ft	Initial width of water passage module section

E.1 MAJOR ASSUMPTIONS

The spill module design relies on several assumptions:

- The entire water passage module section consists of individually controlled overshot gates of a standard width.
- To maintain a semi-constant upstream water surface elevation, gates are lowered uniformly when inflow exceeds the cumulative outflow through other modules, to a minimum of p =0.5 ft.
- The effects of entrance contraction and the distribution of the velocity approach are considered negligible.
- The water passage module section is designed to pass a 10-year flood flow without overtopping the invert height of the facility. Flows greater than the 10-year flood flow will pass through the water passage modules and over the facility under the assumption the facility is designed to be overtopped safely by flows from the 10-year flood to the 100-year flood.
- Velocity over the modules is not a limiting design factory.

E.2 DESIGN PROCEDURE

For the purposes of this study, the water passage modules are designed to pass a 10-year flood, which is consistent with New York State's service spillway design flood requirement for low-hazard dams with heights of less than 40 ft, as specified in *Guidelines for Design of Dam* (NYSDEC 1989). The 10-year flood flow, Q, is estimated by fitting USGS annual peak streamflow gage measurements to a log-Pearson Type III frequency distribution using USGS PeakFQ software[14]. An example frequency distribution fit is provided in Figure E-2.

[14] https://water.usgs.gov/software/PeakFQ/

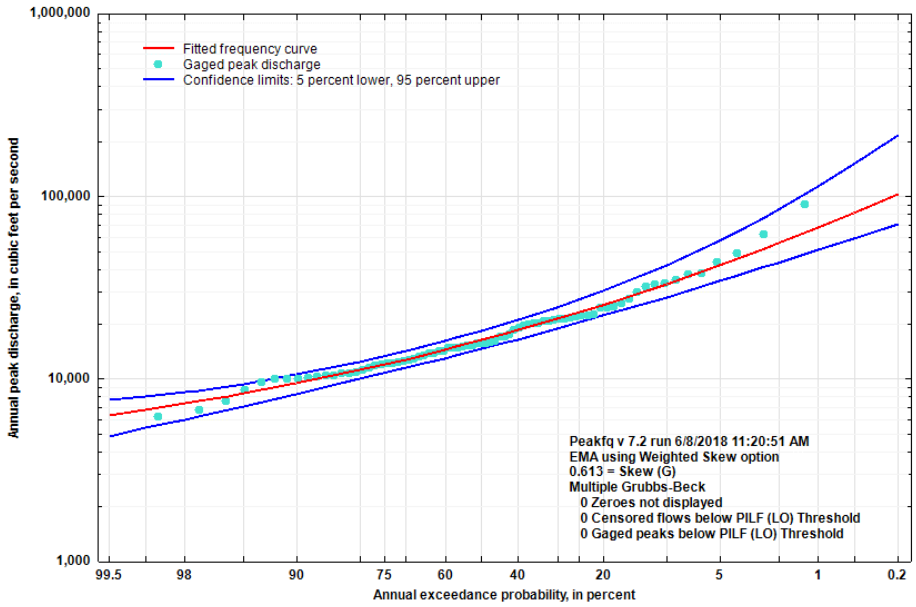

Figure E-2. Example log-Pearson Type III frequency distribution produced with PeakFQ.

Assuming all water passage modules are in the down position, and assuming the facility will overtop when flow is above the 10-year flood, the maximum effective head is estimated as the distance between all modules in the down position with p = 0.5 ft, and the invert elevation of the facility.

Values of C_a provided in USBR (2001) were determined empirically from laboratory tests using the data shown in Figure E, with the following formula providing a reasonable approximation:

$$C_a = 1.0333 + 0.003848\theta - 0.000045\theta^2 \,, \tag{E-2}$$

where θ = gate angle (from horizontal).

Values of C_e are estimated using the Kindsvater-Carter method:

$$C_e = C_1(h_1/p) + C_2 \,, \tag{E-3}$$

where C_1 = effective coefficient of discharge, h_1 = head on the weir, p = height of crest above approach invert, and C_2 = equation constant. Values of C_1 and C_2 vary based on the ratio of the weir crest length (L) to the average approach channel width (B). Example values for C_1 and C_2 are provided in USBR (2001), while values of C_e can be determined using Figure E-4. For calculation purposes, it is assumed $p = H \sin\theta$.

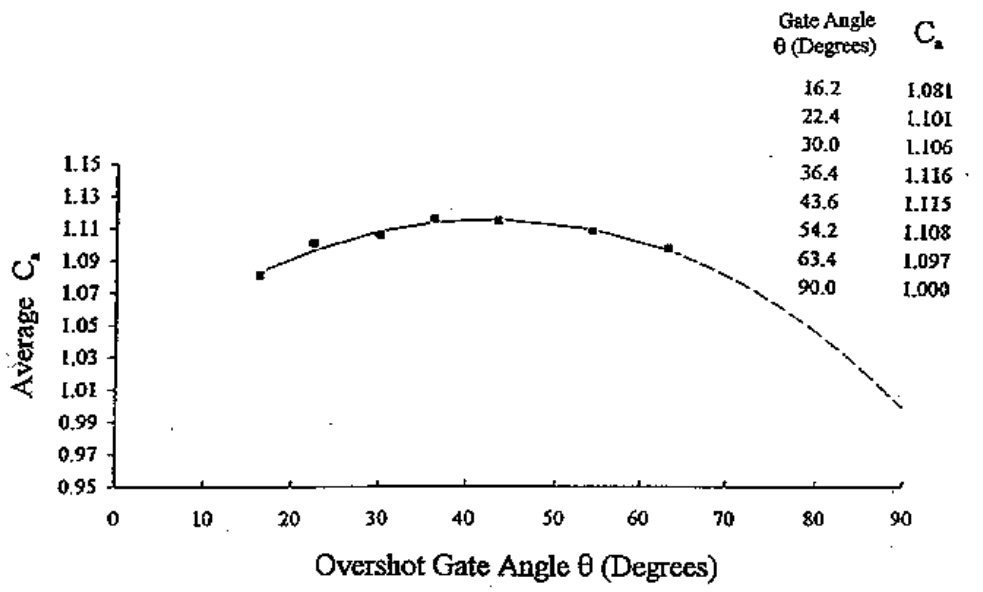

Figure E-3. Correction factor for gate angle. (USBR 2001)

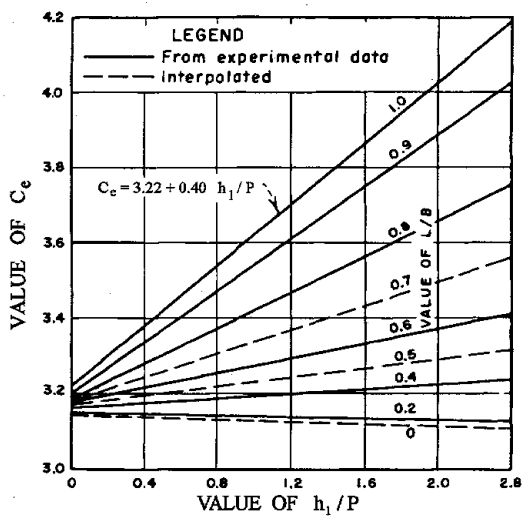

Figure E-4. Effective coefficient of discharge for a vertical weir. (USBR 2001)

When the gate is submerged, which is assumed to be possible given the range of flow conditions across which the gate will operate (Figure E-5), the flow discharge estimate must include a drowned flow reduction factor, C_{df}. Values of C_{df} are estimated using the equation established in Wahlin and Replogle (1994) as

$$C_{df} = A\left[1 - \left(\frac{h_2}{h_1}\right)^{1.5}\right]^n, \tag{E-4}$$

where $h_2 = d_{tw} - p$ and

$$n = 0.1525 + 0.006077\theta - 0.000045\theta^2 \ . \quad \text{(E-5)}$$

$$A = -0.0013\theta + 1.0663 \ for \ \theta < 60^o \ .$$
$$A = 1.0 \ for \ \theta > 60^o \ . \quad \text{(E-6)}$$

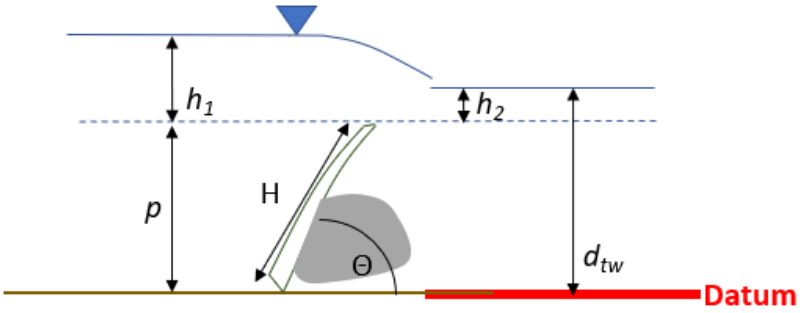

Figure E-5. Sectional view of a submerged overshot gate.

For a given effective head, tailwater input, and desired design flow, the effective length of a water passage module section is estimated using Eqs. (E-1 though E-6). The effective length is compared against the width of stream that does not contain modules, i.e., the total stream width minus the width of the generation, sediment passage, recreation passage, and aquatic species passage modules. If this width is greater than the effective length of the water passage modules, the design procedure continue. If not, the design is flagged as not being capable of passing the 10-year flood. To encourage standardization, water passage modules are assumed to be available in standard lengths of 12 ft, and thus the model output for all water passage modules is rounded up to the nearest 12 ft interval.

E.3 EXAMPLE AND DISCUSSION

Assuming a site with a 10-year flood flow of 15,000 cfs, a desired water surface elevation of 10 ft above datum during flood conditions, a river width of 150 ft, an initial water passage module section width of 48 ft, and a tailwater depth of 6 ft at the 10-year flood, the effectiveness of a water passage module design is evaluated as follows.

- Gate height H is estimated as $1.25 \times h_1 = 1.25 \times 10 = 12.5$ ft.
- Minimum gate angle of $\theta = 3$, corresponding to $p = H \sin \theta = 0.65$ ft.
- Effective head $h_1 = 10$ ft – 0.65 ft = 9.35 ft.
- L/B = 0.32.
- $C_a = 1.044$.
- $C_e = 3.25$.
- $C_{df} = 0.96$.
- $L_e = 48$ ft.

The flow over water passage modules in these conditions is

$$Q = C_a C_e C_{df} L_e h_e^{1.5} = 1.044 * 3.25 * 0.96 * 48 * 9.35^{1.5} = 4{,}485 \ cfs$$

In this case, the design flow is less than the 10-year flood flow, the design is not within the allowable parameters for the model, and the effective length is increased 12 ft to 60 ft. The following variables are changed in the design computation:

- L/B = 0.4
- C_e = 3.54
- L_e = 60 ft

And the new flow estimate is

$$Q = C_a C_e C_{df} L_e h_e^{1.5} = 1.044 * 3.54 \times 0.96 \times 60 \times 9.35^{1.5} = 6{,}093\ cfs\ .$$

Again, this length is not sufficient to pass the design flood. The effective length must be increased in two more lengths of 12 ft before a feasible design is established:

$$Q = C_a C_e C_{df} L_e h_e^{1.5} = 1.044 * 4.43 \times 0.96 \times 84 \times 9.35^{1.5} = 10{,}682\ cfs\ .$$

An example of the concept design and variables is shown in Figure E-6.

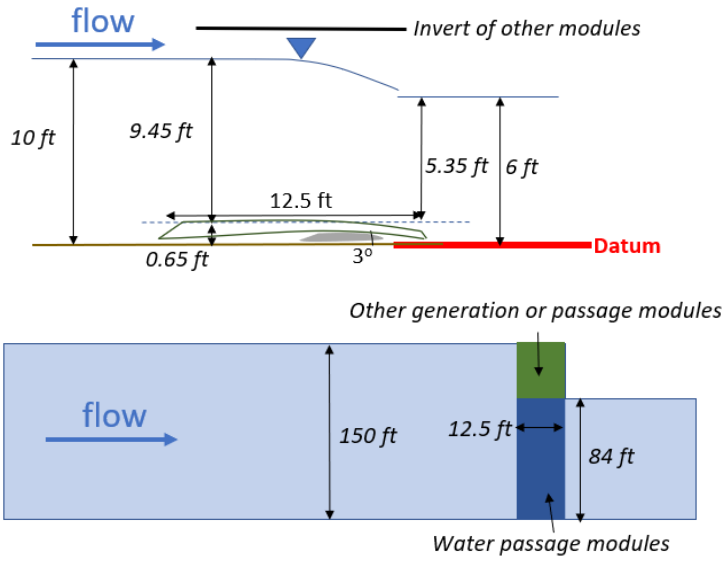

Figure E-6. Sectional view of an example water passage module (top) and top view of a water passage module array (bottom).

E.4 REFERENCES

NYSDEC (New York State Department of Environmental Conservation). 1989. *Guidelines for Design of Dams*. Division of Water, Albany, New York.

USBR (US Bureau of Reclamation). 2001. *Water Measurement Manual*. US Bureau of Reclamation, Washington DC, 317.

Wahlin, B. T., and J. A. Replogle. 1994. *Flow Measurement Using an Overshot Gate*. UMA Engineering for the Bureau of Reclamation, US Department of Interior.

APPENDIX F. REFERENCE FOUNDATION MODULE DESIGN

The foundation module is essential to the overall performance of a modular hydropower facility, as it provides a stable platform that enables itself and other modules to maintain their location, orientation, and stability. Although the Department of Energy Water Power Technologies Office awarded two companies with federal funds to develop rapidly deployable hydropower civil works technologies[15], proven modular foundation technologies have not been successfully deployed.

F.1 MAJOR ASSUMPTIONS

The foundation module design relies on several assumptions:

- Foundation can be segmented into overbank and center foundation modules.
- Special retaining structures are not assumed at the left or right abutments/river banks.
- The reference site has outcropping of bedrock, though no geotechnical investigation program has been conducted to confirm actual site conditions.
- The foundation modules will be supported on sound bedrock with some undulation across the river channel.
- Loose soil, gravel and cobbles on the top of the bedrock can be removed using conventional excavation techniques without using of cofferdams and dewatering.
- The center foundation modules are continuous from bank to bank.
- Overbank modules are of uniform length (upstream-to-downstream).
- Overbank module height is based on plant design head.
- Center foundation module length may vary across the stream according to upper generation or passage modules and may require an apron (extra foundation length upstream or downstream of the superstructure).
- Excavation volume is approximated based on available cross-sectional data and bathymetry (or assumed flow depth) and selected excavation depth.

F.2 FOUNDATION GEOMETRY

As envisioned for this study, the foundation module is simplified into a center foundation module segment and overbank segments. The center foundation module would offer structural support and connection to the generation and passage modules that connect above it. The overbank modules would (if the design calls for it) impound flow across the stream or river segment to a design elevation and prevent adverse flow conditions from affecting the banks.

The foundation modules need to interface with the streambed and may require up to several feet of excavation, depending on site conditions and module design. To estimate the module geometry, knowledge of the stream and overbank cross section is important. Figure F-1 provides an example elevation profile for a modular facility. As shown, a cross section (shown in blue) is used as a reference to inform the foundation module dimensions. For this particular example, only land elevations are provided. Ideally, a bathymetric profile and geotechnical evaluation would be available to inform the foundation module excavation and geometry.

[15] https://www.energy.gov/eere/articles/energy-department-awards-65-million-advance-low-environmental-impact-hydropower

F.3 FOUNDATION VOLUME

In lieu of more detailed data, a first-order approximation for the foundation module volume is provided by assuming the center foundation module stretches across the width of the normal water surface elevation (approximately 160 ft wide in the example illustrated) and into the bank on either side to support overbank modules, and requires an excavation of 5 ft. The abutment (non-overflow) foundation modules are sized to meet the plant design head specification, with a bottom elevation gradually sloping upward in concert with the cross-sectional profile.

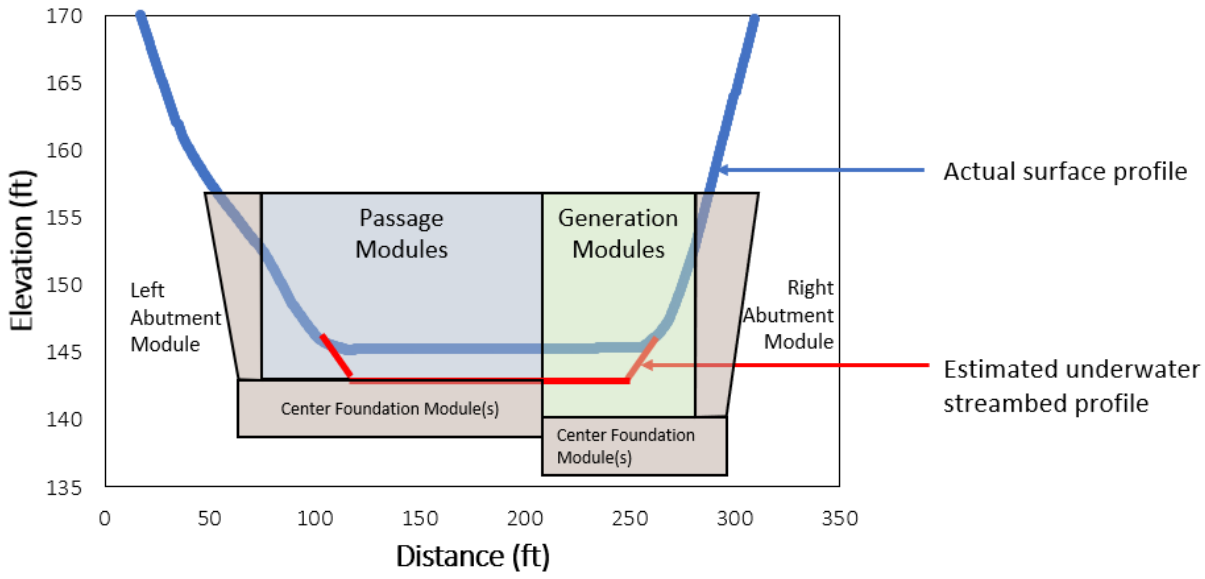

Figure F-1. Example elevation profile for a modular facility.

Using this reference design, the foundation module volumetric requirements can be roughly approximated. For the example illustrated:

- The left abutment module would require approximately
  - 157.5 ft^3/ft-length of material
- The center foundation module would require approximately
  - 850 ft^3/ft-length of material
  - 850 ft^3/ft-length of excavation
- The right abutment module would require approximately
  - 213.8 ft^3/ft-length of material

As shown in Figure 33, individual generation and passage modules may require vastly different upstream-to-downstream lengths to accomplish the module-specific functional requirements. Thus, approximating the volumetric requirements as a volume "per-ft-length" allows for customization. The approach described assumes overbank modules of uniform length across the river. In practice, the design may call for a trapezoidal shape or some other geometry.